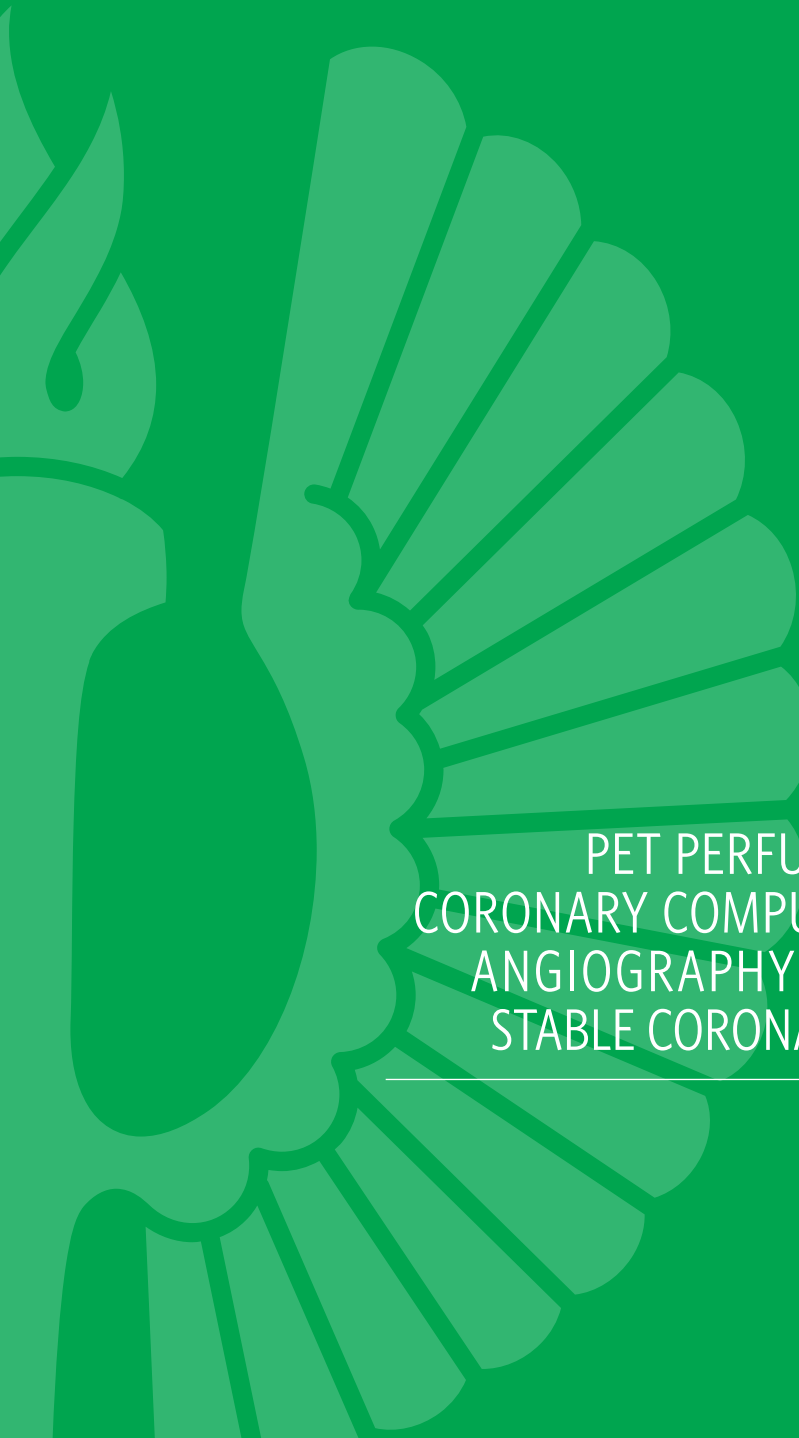




Turun yliopisto
University of Turku



COMBINED USE OF
PET PERFUSION IMAGING AND
CORONARY COMPUTED TOMOGRAPHY
ANGIOGRAPHY IN EVALUATION OF
STABLE CORONARY ARTERY DISEASE

Teemu Maaniitty



Turun yliopisto
University of Turku

COMBINED USE OF PET PERFUSION IMAGING AND CORONARY COMPUTED TOMOGRAPHY ANGIOGRAPHY IN EVALUATION OF STABLE CORONARY ARTERY DISEASE

Teemu Maaniitty

University of Turku

Faculty of Medicine

Department of Clinical Physiology and Nuclear Medicine

Doctoral Programme in Clinical Research

Turku PET Centre

Supervised by

Professor Juhani Knuuti, MD, PhD

Turku PET Centre

University of Turku

Turku, Finland

Associate professor Antti Saraste, MD, PhD

Department of Cardiology, Turku PET Centre

University of Turku

Turku, Finland

Reviewed by

Professor Jari Laukkanen, MD, PhD

Department of Medicine

University of Eastern Finland

Kuopio, Finland

Central Finland Health Care District

Jyväskylä, Finland

Professor Riemer H.J.A. Slart, MD, PhD

Medical Imaging Center, Department of

Nuclear Medicine & Molecular Imaging

University of Groningen,

University Medical Center Groningen

Groningen, the Netherlands

Opponent

Docent Antti Loimaala, MD, PhD

Clinical Physiology and Nuclear Medicine

Helsinki University Hospital

Helsinki, Finland

The originality of this thesis has been checked in accordance with the University of Turku quality assurance system using the Turnitin OriginalityCheck service.

ISBN 978-951-29-7245-6 (PRINT)

ISBN 978-951-29-7246-3 (PDF)

ISSN 0355-9483 (Print)

ISSN 2343-3213 (Online)

Painosalama Oy - Turku, Finland 2018

To Rebekka,

ABSTRACT

Teemu Maaniitty

Combined use of PET perfusion imaging and coronary computed tomography angiography in evaluation of stable coronary artery disease.

University of Turku, Faculty of Medicine, Department of Clinical Physiology and Nuclear Medicine, Doctoral Programme in Clinical Research, Turku PET Centre, Turku, Finland

Annales universitatis turkuensis, Series D, Turku, 2018

Coronary computed tomography angiography (CTA) enables non-invasive detection of coronary atherosclerotic plaques. In turn, myocardial perfusion imaging (MPI) using positron emission tomography (PET) allows non-invasive measurement of myocardial blood flow. Hybrid imaging refers to combining data from two different imaging modalities. Anatomical information from CTA and functional information from MPI are potentially complementary in evaluation of coronary artery disease (CAD). However, the clinical benefit and optimal use of cardiac hybrid imaging are unclear.

We investigated the selective combined use coronary CTA and PET MPI in evaluation of stable symptomatic patients with suspected CAD. Patients first underwent coronary CTA to detect coronary stenoses, and those patients who presented with a suspected obstructive stenosis on CTA also underwent PET MPI to study the hemodynamic significance of the stenosis. We found that obstructive CAD could be ruled out by coronary CTA alone in about half of the patients, associated with an excellent prognosis. Instead, reduced myocardial PET perfusion was associated with an impaired outcome.

Renal injury is a potential complication of iodine contrast agents. We found a low incidence of persistent renal dysfunction after coronary CTA in stable patients with suspected CAD. We also studied an integrated risk score derived from CTA findings, and found this score to predict future adverse events in patients with suspected CAD. Finally, we assessed hybrid PET/CTA findings in symptomatic patients with previous coronary artery bypass grafting. The integrative assessment allowed the evaluation of myocardial perfusion defects and their co-localization with the supplying coronary arteries or bypass grafts.

Keywords: computed tomography, contrast media, coronary artery disease, multimodal imaging, positron emission tomography, prognosis

TIIVISTELMÄ

Teemu Maaniitty

PET-perfuusiokuvantamisen ja sepelvaltimoiden tietokonetomografian yhteiskäyttö vakaaoireisen sepelvaltimotaudin arvioinnissa.

Turun yliopisto, Lääketieteellinen tiedekunta, Kliininen fysiologia ja isotooppilääketiede, Turun kliininen tohtoriohjelma, Turun PET-keskus, Turku, Suomi

Turun yliopiston julkaisuja, Sarja D, Turku, 2018

Sepelvaltimoiden tietokonetomografialla (TT) voidaan havaita sepelvaltimoiden ateroskleroottiset plakit kajoamattomasti. Positroniemissiotomografia (PET) puolestaan mahdollistaa sydänlihaksen verenvirtauksen eli perfuusion mittaamisen. Hybridi- eli yhdistelmäkuvantamisella tarkoitetaan kahdella eri kuvantamismenetelmällä saadun tiedon yhdistämistä. TT-tutkimuksen antama tieto sepelvaltimoiden anatomiasta ja PET-kuvantamisen tarjoama toiminnallinen tieto voivat täydentää toisiaan sepelvaltimotaudin arvioinnissa. On kuitenkin epäselvää, mikä on sydämen yhdistelmäkuvantamisen kliininen hyöty ja paras tapa soveltaa sitä käytännössä.

Tutkimme sepelvaltimoiden TT-kuvantamisen ja sydänlihaksen PET-perfuusiokuvantamisen valikoitua yhteiskäyttöä vakaaoireisilla potilailla, joilla epäiltiin sepelvaltimotautia. Potilaille tehtiin ensin sepelvaltimoiden TT-tutkimus sepelvaltimoahtaumien havaitsemiseksi, ja mikäli TT-tutkimuksessa todettiin epäily merkittävästä sepelvaltimoahtaumasta, tehtiin lisäksi PET-perfuusiokuvaus ahtauman merkittävyyden tarkemmaksi arvioimiseksi. Havaitsimme, että noin puolella potilaista ahtauttava sepelvaltimotauti voitiin poissulkea pelkän TT-tutkimuksen perusteella, ja näillä potilailla ennuste oli erinomainen. Sen sijaan alentunut sydänlihasperfuusio PET-tutkimuksessa oli yhteydessä heikentyneeseen ennusteeseen.

Munuaisvaurio on mahdollinen jodivarjoaineiden käytön haittavaikutus. Havaitsimme, että pysyvä munuaisten toimintahäiriö oli harvinainen vakaaoireisilla potilailla, joille tehtiin sepelvaltimoiden TT-tutkimus epäillyn sepelvaltimotaudin vuoksi. Tutkimme myös sepelvaltimoiden TT-löydöksistä johdettua riskipisteytystä ja havaitsimme sen ennustavan tulevia haittatapahtumia potilailla, joilla epäiltiin sepelvaltimotautia. Lopuksi analysoimme PET/TT-kuvantamislöydöksiä oireisilla potilailla, joille oli aiemmin tehty sepelvaltimoiden ohitusleikkaus. Yhdistelmäkuvantamisella voitiin arvioida sydänlihaksen perfuusiopuutoksia ja paikantaa ne suhteessa yksilölliseen sepelvaltimoiden ja ohitteiden kulkuun.

Avainsanat: ennuste, multimodaalinen kuvantaminen, positroniemissiotomografia, sepelvaltimotauti, tietokonetomografia, varjoaineet

TABLE OF CONTENTS

ABSTRACT	4
TIIVISTELMÄ	5
ABBREVIATIONS	10
LIST OF ORIGINAL PUBLICATIONS	11
1 INTRODUCTION	13
2 REVIEW OF LITERATURE	14
2.1 Coronary artery disease	14
2.1.1 Pathophysiology and clinical manifestations of coronary artery disease	14
2.1.2 Diagnostic strategies in stable coronary artery disease	15
2.1.3 Prognosis and risk stratification in stable coronary artery disease ..	16
2.1.4 Treatment of stable coronary artery disease	17
2.2 Coronary computed tomography angiography	19
2.2.1 Principles and limitations of coronary computed tomography angiography	19
2.2.2 Coronary computed tomography angiography in detection of coronary artery disease	22
2.2.3 Coronary CTA in risk stratification of coronary artery disease	24
2.2.4 Contrast-induced nephropathy	28
2.3 Myocardial perfusion imaging	30
2.3.1 Principles of myocardial perfusion imaging	30
2.3.2 Techniques for assessing myocardial perfusion	32
2.3.3 Diagnostic accuracy of myocardial perfusion imaging in coronary artery disease	34
2.3.4 Myocardial perfusion imaging in risk stratification	36
2.4 Hybrid imaging in coronary artery disease	37
2.4.1 Rationale, benefits, and weaknesses of hybrid imaging in coronary artery disease	37
2.4.2 Diagnostic performance of hybrid imaging in suspected coronary artery disease	38
2.4.3 Prognostic value of hybrid imaging findings in coronary artery disease	39
2.4.4 Patient management after hybrid imaging of coronary artery disease	41
2.4.5 Different approaches to hybrid imaging of coronary artery disease ..	41
2.5 Evaluation of patients with prior coronary artery disease	44

2.5.1	Testing strategies for symptomatic patients with prior known coronary artery disease	44
2.5.2	Coronary computed tomography angiography in patients with prior coronary artery disease	44
2.5.3	Myocardial perfusion imaging and hybrid imaging in patients with prior coronary artery disease.....	45
3	AIMS OF THE STUDY	47
4	MATERIALS AND METHODS	48
4.1	General characteristics of Turku cardiac CTA registry	48
4.2	Prognostic value of coronary CTA with selective PET perfusion imaging (Study I): Materials and methods.....	49
4.2.1	Study design and patient population in Study I	49
4.2.2	Data acquisition and analysis in Study I.....	50
4.2.3	Statistical methods in Study I	51
4.3	Persistent renal dysfunction after coronary computed tomography angiography (Study II): Materials and methods.....	52
4.3.1	Study design and patient population in Study II.....	52
4.3.2	Data acquisition and analysis in Study II.....	52
4.3.3	Statistical methods in Study II	53
4.4	Coronary computed tomography angiography -derived risk score in predicting cardiac events (Study III): Materials and methods	54
4.4.1	Study design and patient population in Study III	54
4.4.2	Data acquisition and analysis in Study III	54
4.4.3	Statistical methods in Study III.....	57
4.5	Hybrid PET/CTA imaging in patients with previous coronary artery bypass grafting (Study IV): Materials and methods	57
4.5.1	Study design and patient population in Study IV	57
4.5.2	Data acquisition and analysis in Study IV	57
4.5.3	Statistical methods in Study IV	59
5	RESULTS.....	60
5.1	Prognostic value of coronary CTA with selective PET perfusion imaging (Study I): Results.....	60
5.1.1	General patient characteristics and imaging findings in Study I	60
5.1.2	Prognosis in patients undergoing coronary CTA with selective PET perfusion imaging	62
5.2	Persistent renal dysfunction after coronary computed tomography angiography (Study II): Results	64
5.2.1	General patient characteristics in Study II.....	64
5.2.2	Changes in creatinine concentration and renal function after contrast agent exposure	64

5.2.3	Patients having an increase in plasma creatinine concentration after contrast agent exposure.....	66
5.3	Coronary computed tomography angiography -derived risk score in predicting cardiac events (Study III): Results	66
5.3.1	General patient characteristics in Study III.....	66
5.3.2	Association of quantitative coronary CTA characteristics with future adverse events	67
5.3.3	Prognostic value of coronary CTA -derived risk score	67
5.4	Hybrid PET/CTA imaging in patients with previous coronary artery bypass grafting (Study IV): Results	68
5.4.1	General patient characteristics in Study IV	68
5.4.2	Coronary CTA, PET perfusion, and hybrid imaging findings in Study IV	69
5.4.3	CTA characteristics of unprotected and non-evaluable coronary territories	70
6	DISCUSSION.....	73
6.1	Prognostic value of coronary CTA with selective PET perfusion imaging: Discussion	73
6.2	Persistent renal dysfunction after coronary computed tomography angiography: Discussion	74
6.3	Coronary computed tomography angiography -derived risk score in predicting cardiac events: Discussion	76
6.4	Hybrid PET/CTA imaging in patients with previous coronary artery bypass grafting: Discussion.....	77
6.5	Future study directions on coronary CTA and PET MPI.....	79
7	CONCLUSIONS	81
	ACKNOWLEDGEMENTS	82
	REFERENCES.....	85
	ORIGINAL PUBLICATIONS.....	103

ABBREVIATIONS

AE	Adverse event
CABG	Coronary artery bypass graft
CAC	Coronary artery calcium
CAD	Coronary artery disease
CFR	Coronary flow reserve
CI	Confidence interval
CIN	Contrast-induced nephropathy
CMD	Coronary microvascular dysfunction
CT	Computed tomography
CTA	Computed tomography angiography
CT-LeSc	Computed tomography -adapted Leaman score
ECG	Electrocardiography
eGFR	Estimated glomerular filtration rate
FFR	Fractional flow reserve
HR	Hazard ratio
ICA	Invasive coronary angiography
LAD	Left anterior descending
LCX	Left circumflex artery
LITA	Left internal thoracic artery
LM	Left main artery
LV	Left ventricle/ventricular
LVEF	Left ventricular ejection fraction
MACE	Major adverse cardiac event
MBF	Myocardial blood flow
MFR	Myocardial flow reserve
MI	Myocardial infarction
MPI	Myocardial perfusion imaging
NPV	Negative predictive value
OMT	Optimal medical therapy
PCI	Percutaneous coronary intervention
PDA	Posterior descending artery
PET	Positron emission tomography
PPV	Positive predictive value
PTP	Pre-test probability
RCA	Right coronary artery
SD	Standard deviation
SPECT	Single photon emission computed tomography
UAP	Unstable angina pectoris
UCT	Unprotected coronary territory

LIST OF ORIGINAL PUBLICATIONS

This thesis is based on the following original scientific publications (referred in the text by I–IV):

- I** **Maaniitty T**, Stenström I, Bax JJ, Uusitalo V, Ukkonen H, Kajander S, Mäki M, Saraste A, Knuuti J. Prognostic Value of Coronary CT Angiography With Selective PET Perfusion Imaging in Coronary Artery Disease. *JACC Cardiovasc Imaging* 2017;10:1361–70.
- II** **Maaniitty T**, Stenström I, Uusitalo V, Ukkonen H, Kajander S, Bax JJ, Saraste A, Knuuti J. Incidence of persistent renal dysfunction after contrast enhanced coronary CT angiography in patients with suspected coronary artery disease. *Int J Cardiovasc Imaging* 2016;32:1567–75.
- III** Uusitalo V, Kamperidis V, de Graaf MA, **Maaniitty T**, Stenström I, Broersen A, Dijkstra J, Scholte AJ, Saraste A, Bax JJ, Knuuti J. Coronary computed tomography angiography derived risk score in predicting cardiac events. *J Cardiovasc Comput Tomogr* 2017;11:274–280.
- IV** **Maaniitty T**, Jaakkola S, Saraste A, Knuuti J. Hybrid PET/CT imaging in evaluation of symptomatic patients with previous coronary artery bypass grafting. [Manuscript].

The original publications have been reproduced with the permission of the copyright holders.

1 INTRODUCTION

Atherosclerosis is a disease process in which a plaque or plaques develop into the innermost layer of an artery, called *intima*. Coronary artery disease (CAD) is an atherosclerotic disease affecting coronary arteries that are supplying heart muscle, or *myocardium*, with blood. Myocardial *ischemia* denotes for insufficient myocardial blood flow, or *perfusion*, in relation to the demand of the heart muscle. The growth of a coronary plaque may result in gradual narrowing, or *stenosis*, of the arterial lumen, finally compromising the myocardial blood flow. A stenosis that is sufficiently severe to cause myocardial ischemia is termed *hemodynamically significant*. Stable obstructive CAD is characterized by a relatively slow growth of a coronary plaque, first causing myocardial ischemia and related symptoms such as chest pain during stress when the myocardial demand of oxygen and nutrients is high. Instead, unstable manifestations of CAD are characterized by a more rapid and unexpected obstruction of a coronary artery due to plaque rupture or erosion, potentially inducing cardiac arrhythmias, permanent myocardial injury, or even death. Cardiovascular diseases are the leading cause of death globally. Therefore, the challenge is to estimate patients' risk for future adverse cardiac events, and to provide the most aggressive therapies to patients with the highest risk, aiming to prevent those harmful events.

Non-invasive imaging modalities provide versatile information on CAD, allowing the detection of obstructive CAD as well as the estimation of a risk for future adverse events. Coronary computed tomography angiography (CTA) is a non-invasive anatomic imaging modality allowing the detection of atherosclerotic plaques in coronary arteries. A strength of coronary CTA is the ability to exclude obstructive CAD with high certainty, while it is suboptimal for the assessment of the hemodynamic significance of a detected coronary artery stenosis, i.e. whether the stenosis causes myocardial ischemia (Meijboom, Meijs, et al. 2008). A normal coronary CTA scan is associated with an excellent outcome, while other CTA parameters such as the extent and severity of coronary atherosclerosis are associated with an increasing risk for adverse events (Min et al. 2011). In turn, myocardial perfusion imaging (MPI) is a well-established non-invasive approach for detection of impaired myocardial perfusion caused by obstructive CAD. Positron emission tomography (PET) MPI allows non-invasive quantification of myocardial blood flow (MBF) in absolute terms (Knuuti et al. 2009). The presence, extent, and severity of MPI abnormalities are known to predict the outcome (Dorbala et al. 2013). The results of non-invasive imaging studies are used to guide patient management, and non-invasive modalities are generally utilized as gatekeepers to invasive studies, i.e. cardiac catheterization.

Hybrid imaging refers to combining or fusing data provided by different imaging modalities (Kaufmann 2009). Often this means integration of anatomical and functional data that are complementary. For example, hybrid imaging combining coronary CTA and PET MPI allows detection of a coronary stenosis and evaluation of its hemodynamic significance (Kajander et al. 2010).

This thesis focuses on the use of coronary CTA, PET MPI, and their combination in real-life patients with suspected or known stable obstructive CAD.

2 REVIEW OF LITERATURE

2.1 Coronary artery disease

2.1.1 *Pathophysiology and clinical manifestations of coronary artery disease*

Coronary artery disease (CAD) is an atherosclerotic disease of coronary arteries supplying heart muscle that may eventually result in myocardial ischemia or infarction. According to the World Health Organization (WHO), cardiovascular diseases (CVD) are the leading cause of death globally, with an estimated 17.7 million cardiovascular deaths in 2015, of which 7.4 million being due to coronary disease (WHO Media Centre, <http://www.who.int/mediacentre/factsheets/fs317/en/>; accessed on 30th July 2017). In Europe, CVD are estimated to cause 3.9 million annual deaths, 45% of all deaths in Europe (European Society of Cardiology Press Office, <https://www.escardio.org/The-ESC/Press-Office/Fact-sheets/About-Cardiovascular-Disease-in-Europe>; accessed on 30th July 2017). In Finland, CVD caused 37% of all deaths in 2015, and one in five deaths was due to CAD. However, the age-standardized mortality from CVD and CAD has been continuously falling in Finland over the recent decades (Official Statistics of Finland, http://www.stat.fi/til/ksyyt/2015/ksyyt_2015_2016-12-30_kat_002_en.html; accessed on 30th July 2017).

Traditional risk factors for CAD include age, gender, smoking, hypertension, diabetes, high serum low-density lipoprotein (LDL) cholesterol level, low serum high-density lipoprotein (HDL) cholesterol level, and family history of premature CAD (Castelli et al. 1986; Myers et al. 1990; Anderson et al. 1991). In addition, other less established or currently unknown factors may contribute to the development of CAD.

The relatively slow progression of coronary artery atherosclerosis, usually during many years or decades, is a key process in the development of obstructive CAD. The process of atherosclerosis starts early in life, and endothelial dysfunction, accumulation of LDL cholesterol into arterial intima, and vascular wall inflammation are thought to be pivotal in this process (Juonala et al. 2004; Nakashima et al. 2007). Gradually some of the fatty streaks in the vessel wall may develop into atherosclerotic plaques and also become calcified.

An epicardial coronary stenosis, when sufficiently severe, may cause myocardial ischemia. This is called stable obstructive CAD. In addition to epicardial coronary stenoses, microvascular dysfunction or coronary artery spasm may induce myocardial ischemia in stable CAD (Montalescot et al. 2013). Symptoms of stable obstructive CAD may include e.g. chest pain or shortness of breath, and the myocardial ischemia and symptoms first appear during exercise or other stress situations when the myocardial oxygen demand is high.

In addition to the stable manifestations, CAD may also present as an acute coronary syndrome (ACS). A rupture or erosion of a coronary atherosclerotic plaque, whether obstructive or non-obstructive, may subsequently result in intravascular thrombosis and impair the coronary blood flow (Libby 2013). The unstable manifestations of CAD include e.g. unstable angina pectoris (UAP), acute myocardial infarction (MI), arrhythmias, and sudden cardiac death. Actually, acute myocardial infarction or sudden cardiac death is the first manifestation of CAD in a significant proportion of the patients (Maurovich-Horvat et al. 2014).

2.1.2 Diagnostic strategies in stable coronary artery disease

According to the current international guidelines, the diagnostic strategy in symptomatic patients with suspected stable CAD is determined by the estimated pre-test probability (PTP) of obstructive CAD in each patient (Fihn et al. 2012; Montalescot et al. 2013). The PTP of obstructive CAD can be estimated based on age, gender, and symptoms (Genders et al. 2011). For patients having a low PTP (<15%), other causes than obstructive CAD should be investigated for their symptoms (Montalescot et al. 2013). For most patients with an intermediate PTP (15–85%), non-invasive modalities including stress testing and coronary CTA should be used for diagnostic purposes. In patients having a high PTP (>85%), the diagnosis of obstructive CAD can be clinically established, as further testing would not improve the diagnostic accuracy; however, testing may be appropriate to assess the risk for future adverse events (Montalescot et al. 2013).

The reduction in coronary artery blood flow, for example due to an epicardial coronary artery stenosis, leads to hypoperfusion of myocardium, and therefore, an imbalance between the myocardial oxygen supply and demand (Renker et al. 2015). With the worsening degree of myocardial ischemia, a following sequence of abnormalities, called *myocardial ischemic cascade*, may progressively occur: myocardial metabolic abnormalities, diastolic dysfunction, systolic dysfunction, electrocardiographic abnormalities, and finally clinical symptoms (Figure 1) (Renker et al. 2015). Different stress testing modalities focus on different stages in the ischemic cascade, accounting for their relative differences in sensitivities and specificities for detection of obstructive CAD. For example, myocardial perfusion imaging (MPI) is a highly sensitive method as it is detecting hypoperfusion, the first stage in ischemic cascade, while wall-motion imaging is more specific as it is detecting ventricular dysfunction which is a later stage in the ischemic cascade (Schinkel et al. 2003). Conversely, non-invasive and invasive angiographical methods are not detecting ischemia but focus on the anatomic coronary lesions, providing a different approach to the detection of obstructive CAD.

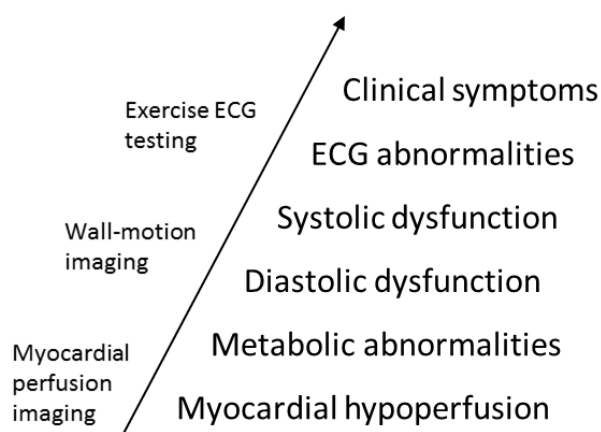


Figure 1 The sequence of events typically occurring during myocardial ischemia, called myocardial ischemic cascade. Different imaging modalities detect different stages in the ischemic cascade. ECG = electrocardiography.

2.1.3 Prognosis and risk stratification in stable coronary artery disease

Data derived from clinical trials suggest annual rates of 1.2–2.4% for all-cause mortality, 0.6–1.4% for cardiac mortality, and 0.6–2.7% for non-fatal myocardial infarction in stable CAD (Montalescot et al. 2013). Endothelial dysfunction and coronary microvascular dysfunction (CMD) are early manifestations of coronary atherosclerosis and CAD, and are associated with an increased risk of adverse events (Juonala et al. 2004; Kitta et al. 2009; Jespersen et al. 2012). Among patients with established CAD, prognosis varies considerably between individuals based on clinical and demographic factors, coronary anatomy, ischemia, and left ventricular (LV) function (Montalescot et al. 2013). Traditional cardiovascular risk factors are related to an increased risk for adverse events also in patients with established CAD (Hjemdahl et al. 2006). The extent, severity, and proximal location of coronary stenoses, as well as the extent of myocardial ischemia, are associated with adverse outcome in stable CAD (Min et al. 2007, 2011; Hachamovitch et al. 1998). Reduced LV function is a strong and independent predictor of unfavorable survival (Emond et al. 1994). Maximum exercise capacity, which is at least partly related to the LV function, can be objectively measured and is a marker of prognosis (Ashley, Myers, and Froelicher 2000).

The diagnosis of stable CAD should be followed by the risk stratification for future adverse events (Fihn et al. 2012; Montalescot et al. 2013). The aim of this process is to identify low-risk patients, in whom invasive procedures can be avoided without compromising patient safety, and high-risk patients, who may need aggressive treatment. As reduced LV function is a strong and independent predictor of adverse prognosis, the European guidelines recommends resting echocardiography

in all patients with suspected stable CAD, whereas the American guidelines suggest more selective application of resting echocardiography (Fihn et al. 2012; Montalescot et al. 2013). Non-invasive measures of myocardial ischemia (e.g. exercise electrocardiography (ECG), MPI) and angiographical CAD (usually by coronary CTA) are associated with outcome, and in most patients with intermediate PTP of obstructive CAD this information is already achieved in the process of establishing the diagnosis. In patients with a high PTP (>85%) the diagnosis of obstructive CAD can be clinically constituted, but additional non-invasive testing may be performed for risk stratification purposes if the patient is a candidate for revascularization in case of high risk (Montalescot et al. 2013). Invasive angiography is seldom needed for risk stratification, but instead, should be selectively applied in those patients having an intermediate or high risk based on non-invasive testing.

2.1.4 Treatment of stable coronary artery disease

The management of stable CAD has two main targets: to relieve symptoms and to improve prognosis. Lifestyle modifications and control of cardiovascular risk factors have favorable effects on prognosis and, accompanied with adequate patient education, should be provided to all patients with CAD. Coronary revascularization should be seen as complementary to optimal pharmacological therapy in CAD.

Pharmacological therapy of obstructive CAD should include an antithrombotic drug (e.g. low-dose aspirin) and a statin, both of which have well-documented roles in preventing adverse events (Berger, Brown, and Becker 2008; Baigent et al. 2010). In addition to reduction of serum low density lipoprotein cholesterol level, statins may act by other mechanisms such as via favorable effects on endothelial function, vascular inflammation, and stability of atherosclerotic plaques (Koh 2000; Oesterle, Laufs, and Liao 2017). Angiotensin converting enzyme (ACE) inhibitors are beneficial for outcome and should be considered in patients who have stable CAD co-existing with LV dysfunction, hypertension, diabetes mellitus, or chronic kidney disease (Montalescot et al. 2013; Ponikowski et al. 2016). Short- and long-acting nitrates relieve ischemic symptoms via arterial and venous vasodilatation. Beta blockers and calcium channel blockers are anti-ischemic and effective in reducing symptoms of CAD (Frishman et al. 1999; Heidenreich et al. 1999). Moreover, beta blockers also have prognostic benefit in the presence of reduced left ventricular ejection fraction (LVEF \leq 40%) (Thompson 2013).

Targeting revascularization procedures in stable coronary artery disease

Coronary revascularization has an established role in acute coronary syndromes for improving patient prognosis (Boersma 2006; Fox et al. 2010). In stable CAD, the prognostic benefit obtained by elective coronary revascularization is more controversial, and its utilization should be more carefully judged (Boden et al. 2007; Simoons and Windecker 2010). According to the current

guidelines, optimal medical therapy (OMT) is the first-line treatment in stable CAD, and revascularization may be indicated to relieve persistent symptoms that are unresponsive to medical therapy and/or to improve survival in patients with high event risk (Windecker et al. 2014; Fihn et al. 2014; NICE Guidance: “Stable angina: management”; <http://www.nice.org.uk/guidance/cg126>; accessed on 28th Dec 2017). The choice of revascularization strategy between percutaneous coronary intervention (PCI) or coronary artery bypass graft (CABG) surgery depends on multiple factors such as complexity and severity of CAD, patient comorbidities and preferences, surgical risk, and local expertise (Deb et al. 2013). CABG is preferred to PCI in patients with multivessel CAD, especially in those with diabetes (Fihn et al. 2014).

For performing revascularization in stable CAD, there should be an evidence of ischemia, either by non-invasive MPI or invasive fractional flow reserve (FFR) measurement (Windecker et al. 2014; Fihn et al. 2014). It has been shown that only about half of anatomically obstructive coronary lesions (i.e. $\geq 50\%$ diameter stenosis) are really hemodynamically significant, i.e. causing myocardial ischemia (Meijboom, Van Mieghem, et al. 2008). Hachamovitch et al. retrospectively studied the prognostic benefit of revascularization in 10,627 patients with no prior CAD undergoing stress single photon emission computed tomography (SPECT) MPI (Hachamovitch et al. 2003). Using multivariable Cox proportional hazards model for predicting cardiac death, the investigators found that revascularization was associated with a survival benefit in patients with moderate to severe ischemia ($>10\%$ of myocardium) during ~ 2 -year follow-up, while medical therapy was superior to revascularization in patients with no or only mild myocardial ischemia ($<10\%$ of myocardium). In a subsequent study with longer follow-up time (mean 8.7 years), patients with prior CAD were also included (Hachamovitch et al. 2011). In this study, survival benefit by early revascularization was present in patients with significant ischemia and no prior myocardial infarction, while no such benefit was found in patients with a prior infarction.

FFR measurement is an invasive method to study the functional significance of a coronary artery stenosis. FFR is defined as the ratio of maximum coronary flow in the presence of a stenosis to normal maximum flow in the absence of a stenosis, and is calculated based on invasive measurements of intravascular pressure during pharmacological vasodilatation (Pijls et al. 1995). In the prospective randomized DEFER trial ($n=325$), patients with hemodynamically non-significant coronary stenosis (i.e. $FFR > 0.75$) were randomly assigned to deferral or performance of PCI (Bech et al. 2001). At 2 and 5 years of follow-up, adverse event rates were similar in the both groups, indicating the safety of the deferral of revascularization of hemodynamically non-significant lesions (Bech et al. 2001; Pijls et al. 2007). Interestingly, in a 15-year follow-up study of this cohort, the mortality was similar between the groups, but the rate of myocardial infarction was about 5-fold in those undergone PCI of a non-significant stenosis compared to those with the initial deferral of PCI (Zimmermann et al. 2015).

In the prospective COURAGE trial, 2,287 patients with CAD and evidence of myocardial ischemia were randomized to OMT with PCI or to OMT alone (Boden et al. 2007). After 4.6 years of

follow-up, no differences were observed between the treatment groups in the rates of death, myocardial infarction, or other major cardiovascular events. PCI provided small incremental benefits in terms of symptoms, exercise capacity, and quality of life, but these benefits were attenuated after two years (Weintraub et al. 2008). A total of 314 patients in the COURAGE trial participated in the nuclear cardiology substudy with a follow-up MPI scan at 6 to 18 months after randomization (Shaw et al. 2008). Greater reduction in ischemic myocardium was observed in patients with OMT+PCI compared to OMT alone, and significant (i.e. $\geq 5\%$) reduction in ischemic myocardium was more frequently achieved with OMT+PCI, especially in patients with moderate to severe ($\geq 10\%$) ischemia prior to treatment. Moreover, the significant reduction in ischemic myocardium was associated with a lower risk of death or myocardial infarction in an unadjusted analysis.

The FAME trial demonstrated a lower combined rate of death or myocardial infarction at 1 year after FFR-guided PCI compared to angiography-guided PCI in patients with multivessel CAD (Tonino et al. 2009). In the subsequent FAME 2 trial, patients with at least one functionally significant stenosis (i.e. $\text{FFR} \leq 0.80$) were randomized to medical therapy with FFR-guided PCI or to medical therapy alone (De Bruyne et al. 2012). However, the recruitment was prematurely halted after enrollment of 1,220 patients, because of a significant difference in the primary endpoint (composite of death, myocardial infarction, or urgent revascularization) between PCI group and medical therapy group (4.3% vs. 12.7%, respectively), which was driven by a difference in the rates of urgent revascularization. No significant differences were found in the rates of death and myocardial infarction even at 2 years of follow-up (De Bruyne et al. 2014). A meta-analysis by Johnson et al. demonstrated a continuous relationship between decreasing FFR and worsening outcome (Johnson et al. 2014). Revascularization was associated with a survival advantage over medical therapy if the FFR value was low, while medical therapy was superior in the presence of preserved FFR, thereby representing some analogy with the study by Hachamovitch et al. utilizing SPECT MPI (Hachamovitch et al. 2003).

An ongoing ISCHEMIA trial, in which patients with suspected stable CAD and at least moderate ischemia on stress imaging are randomized to either invasive or conservative strategy, will hopefully clarify the rather controversial role of revascularization in stable CAD (Phillips et al. 2013).

2.2 Coronary computed tomography angiography

2.2.1 Principles and limitations of coronary computed tomography angiography

Computed tomography angiography (CTA) is a non-invasive modality for anatomical imaging of blood vessels utilizing X-ray computed tomography (CT) and intravenously administered iodine contrast media. High spatial and temporal resolutions have allowed anatomical imaging of coronary arteries using CTA. The scanners currently used for coronary CTA are usually multi-detector

computed tomography (MDCT) scanners with at least 64 and up to 320 rows of detectors, in contrast to the preceding helical CT scanners.

The use of intravenous iodine contrast agents allows visualization of coronary artery lumen and measurement of the degree of luminal stenosis using coronary CTA. Epicardial coronary arteries with the luminal diameter of at least 1.5 mm are generally considered evaluable by coronary CTA, and short-acting nitrates are usually given before CTA for coronary vasodilation to improve image quality (Leipsic et al. 2014; Takx et al. 2015). In contrast to invasive coronary angiography (ICA), coronary CTA allows not only the visualization of coronary artery lumen but also the coronary artery plaques themselves, making it possible to evaluate the location, size, eccentricity, and composition of a plaque, and also assess coronary artery remodeling.

Coronary CTA is prone to several types of image artifacts. The movement of the imaging target (i.e. coronary arteries) should be minimized during a CTA scan to optimize the image quality and reduce motion-related artifacts. A coronary CTA scan with a 64-row scanner usually takes only 10–15 seconds, allowing the respiratory movement to be eliminated with adequate breath-holding. Due to the continuous contraction and relaxation of heart, coronary CTA study is performed using ECG-gating, allowing CT images to be reconstructed and evaluated at different temporal phases of cardiac cycle. At present, prospective ECG-triggering is routinely used with coronary CTA, meaning that the scanning is performed during predefined phases of the cardiac cycle, usually at the end-diastolic phase when the contractile movement of the heart is minimized. The use of prospective ECG-triggering significantly reduces radiation dose to a patient, compared to retrospective ECG-gating. Regular heart rate is a requirement for using prospective ECG-triggering, and therefore, prospectively triggered coronary CTA has not been applicable to patients with heart rate irregularities such as atrial fibrillation. However, improvement in CT scanner technology, such as 320-row and dual source scanners, and development in image acquisition strategies are promising to allow prospectively ECG-gated coronary CTA also in patients with atrial fibrillation (Kondo et al. 2013). Not only regular but the heart rate must also be low enough to prevent artefacts due to motion of epicardial coronary arteries. Heart rate lower than 60 beats per minute (bpm) is the target and, if necessary, intravenous or per-oral beta blockers are usually administered to achieve this.

Artifacts due to coronary artery calcification, including *blooming* and *beam-hardening* artifacts, are frequently encountered with coronary CTA and partly explain the relatively low specificity of this imaging modality (C.-C. Chen et al. 2011). Blooming artifacts are related to partial-volume averaging effects and make a calcified plaque to appear larger than it actually is, potentially resulting in overestimation of stenosis severity or even totally preventing the assessment of vessel lumen (Leipsic et al. 2014). A beam-hardening artifact can appear as a dark area in image in the proximity of calcification and can be erroneously interpreted as a non-calcified plaque component. Other types of coronary CTA artifacts include those due to misalignment, implanted metal, reduced signal-to-noise ratio, and low contrast intensity. To avoid artifacts and improve image quality, special attention must be paid to patient selection and preparation (e.g. breath holding

capability, obesity, rate and regularity of heart rhythm). Due to the increasing risk of artifacts and reducing specificity, it may be adequate to refrain from performing coronary CTA in patients showing abundant coronary calcification on a calcium scoring scan (Fihn et al. 2012; Montalescot et al. 2013; Abbara et al. 2016). In addition to the factors impacting image quality, safety aspects such as patient's renal function and possible prior adverse reactions to contrast agents must be considered.

Table 1 An overview of estimated effective radiation doses for different imaging modalities. The doses are estimated based on previous literature. The actual effective radiation dose to the patient is dependent on many factors such as the hardware, software, imaging protocols, and patient characteristics. For example, stress-only imaging with ^{15}O -water PET is associated with ~1 mSv effective dose, while the dose from rest–stress imaging is about two-fold. Moreover, the radiation dose can be reduced by using high-sensitivity detector camera systems (e.g. cadmium–zinc–telluride SPECT, IQ-SPECT, or digital PET).

Imaging modality	Typical effective radiation dose	(Reference)
Helical coronary CTA	19 mSv	(Einstein 2008; Kajander et al. 2009)
Prospectively-triggered coronary CTA	4–8 mSv	(Einstein 2008; Kajander et al. 2009; Hausleiter et al. 2012; Marwan et al. 2017)
Coronary calcium scoring CT scan	1–2 mSv	(Einstein 2008; Leipsic et al. 2014)
Invasive coronary angiography	7 mSv	(Einstein 2008)
Thallium-201 SPECT MPI	17 mSv	(Einstein 2008)
Technetium-99m SPECT MPI	4–10 mSv	(Einstein 2008; Slomka et al. 2012)
Rubidium-82 PET MPI	1–4 mSv	(Slomka et al. 2012)
^{13}N -ammonia PET MPI	1–2 mSv	(Slomka et al. 2012)
^{15}O -water PET MPI	1–2 mSv	(Kajander et al. 2009)
^{18}F -flurpiridaz PET MPI	5–6 mSv	(Berman et al. 2013)
Echocardiographic techniques	0 mSv	(Einstein 2008)
Magnetic resonance techniques	0 mSv	(Einstein 2008)

CT = computed tomography; CTA = computed tomography angiography; MPI = myocardial perfusion imaging; PET = positron emission tomography; SPECT = single photon emission computed tomography.

Typical effective radiation doses for different cardiac imaging modalities are shown in Table 1. Radiation safety has been a concern associated with coronary CTA, and relatively high effective radiation dose estimates around 19 mSv were reported for conventional helical CTA scanning techniques (Einstein 2008). However, advances in technology have gradually led to reduced radiation doses, and as low as 2 mSv mean effective doses have been reported with the recent CTA technology (Kajander et al. 2009; Bischoff et al. 2010; Hausleiter et al. 2010, 2012; Deseive et al. 2015). For comparison, the average annual radiation dose is 3.2 mSv per person in Finland

(STUK - Radiation and Nuclear Safety Authority in Finland, <http://www.stuk.fi/web/en/topics/emergencies/examples-of-radiation-doses-and-external-dose-rates>; accessed on 24th Jan 2018).

2.2.2 Coronary computed tomography angiography in detection of coronary artery disease

Although coronary CTA is a relatively novel method for cardiac imaging, it is currently widely used for detection or exclusion of stable obstructive CAD. In addition, it has been investigated for exclusion of coronary etiology in patients presenting with acute chest pain on emergency department.

Detection or exclusion of stable obstructive CAD with coronary CTA is based on the anatomical assessment of the degree of luminal stenosis in a coronary artery. Most of the previous studies have applied a cut-off point 50% of diameter stenosis to define an obstructive stenosis on coronary CTA, and set the degree of stenosis on invasive angiography as a gold standard. These studies have reported sensitivities of 95–99% and specificities of 64–83% for coronary CTA to detect an anatomically significant $\geq 50\%$ stenosis on ICA (Budoff et al. 2008; Meijboom, Meijs, et al. 2008). The negative predictive value (NPV) of coronary CTA is high, i.e. a CTA scan showing normal coronary arteries or non-obstructive coronary atherosclerosis (diameter stenosis $< 50\%$) accurately excludes obstructive CAD, compared to ICA (Budoff et al. 2008; Meijboom, Meijs, et al. 2008). However, the positive predictive value (PPV) is generally lower, which is a key limitation of coronary CTA. The relatively low PPV is partially related to blooming artifacts caused by calcified coronary plaques, and an increasing amount of calcification has been shown to reduce the specificity of coronary CTA (C.-C. Chen et al. 2011).

The hemodynamic significance of a coronary stenosis is an important prognostic factor, and revascularization procedures should be targeted to hemodynamically significant lesions (Tonino et al. 2009). There is a non-linear relationship between the anatomical degree of a coronary stenosis, usually measured as luminal diameter reduction, and the hemodynamic consequences of the stenosis (Di Carli et al. 1995). It has been previously demonstrated that only about half of the coronary lesions with $\geq 50\%$ diameter reduction on ICA are actually hemodynamically significant based on FFR measurement (Meijboom, Van Mieghem, et al. 2008).

Due to the overestimation of stenosis severity by coronary CTA, and furthermore, the poor correlation between the anatomy and functional effects of a stenosis, coronary CTA is insufficient for assessing the hemodynamic significance of a stenosis $\geq 50\%$ in diameter, unless the stenosis is very tight (Uren et al. 1994; Di Carli et al. 1995; Sato et al. 2008). Meijboom et al. reported a specificity of 48% for visual coronary CTA analysis, using invasive FFR < 0.80 as reference for a hemodynamically significant stenosis (Meijboom, Van Mieghem, et al. 2008). In their study,

the PPV was low as only 49% of obstructive lesions on CTA were truly hemodynamically significant based on the FFR. Similarly, a recent meta-analysis reported a high 90% per-patient sensitivity but lower 39% specificity for coronary CTA as compared to invasive FFR (Danad et al. 2017). Di Carli et al. investigated the relationship between anatomical findings on coronary CTA and stress myocardial perfusion findings in 110 patients referred for hybrid PET/CT imaging for suspected CAD (Di Carli et al. 2007). In the patient-based analysis, they found that an increasing degree of luminal narrowing on CTA (<50%, 50–70%, and >70%) was associated with an increase in PPV for detecting ischemia on PET (29%, 44%, and 77%, respectively), with no significant change in NPV (92%, 91%, and 88%, respectively).

Owing to its high NPV, coronary CTA is an excellent modality for exclusion of obstructive CAD and has a high diagnostic accuracy in the target populations with a relatively low prevalence of obstructive CAD (Meijboom et al. 2007; Paech and Weston 2011). In contrast, the amount of coronary calcium and the number of stenoses with uncertain functional significance increase in parallel with the prevalence of obstructive CAD, which reduces the diagnostic accuracy of coronary CTA in patients with higher PTP of obstructive CAD. The increasing number of unclear CTA findings might lead to over-application of further invasive angiography. Accordingly, the 2013 guidelines on stable CAD by the European Society of Cardiology (ESC) state that coronary CTA should be considered in suitable symptomatic patients with a low intermediate (15–50%) PTP of obstructive CAD as an alternative to stress imaging or when exercise ECG or stress imaging is non-conclusive or contraindicated (Montalescot et al. 2013). If the result of coronary CTA is “unclear”, these guidelines suggest non-invasive ischemia testing using stress imaging (Montalescot et al. 2013). The 2012 American guidelines for the diagnosis and management of patients with stable ischemic heart disease state that coronary CTA may be considered for initial diagnosis of stable obstructive CAD in suitable patients with an intermediate PTP, and especially, coronary CTA is reasonable to perform in intermediate PTP patients unsuitable for stress testing or with inconclusive or contradictory prior test results (Fihn et al. 2012). The 2016 update on the guidelines for chest pain of recent onset by the National Institute for Health and Care Excellence (NICE) in the United Kingdom emphasizes the role of coronary CTA as a first-line diagnostic test in stable chest pain patients without previously confirmed CAD (NICE Guidance: “Chest pain of recent onset: assessment and diagnosis”; <http://www.nice.org.uk/guidance/cg95>; accessed on 27th Dec 2017). This update advises to offer coronary CTA in patients presenting with either typical or atypical anginal pain or with ST–T changes or Q-waves on resting ECG. Furthermore, these guidelines recommend further non-invasive functional imaging of myocardial ischemia if coronary CTA is non-diagnostic or demonstrates lesions with uncertain functional significance.

The optimal second-line testing modality after an inconclusive CTA result has not been established. In the recent Dan-NICAD trial 392 patients having a positive or non-evaluable coronary CTA result were randomized to MPI using either single photon emission computed tomography (SPECT) or cardiac magnetic resonance (Nissen et al. 2018). Both SPECT and cardiac magnetic resonance imaging showed good specificities (94% and 84%, respectively) but the sensitivities were surprisingly low (36% and 41%, respectively) as compared to ICA with FFR. In addition,

non-invasive CTA-derived FFR might be a choice to increase the specificity of coronary CTA without additional radiation exposure (Nørgaard et al. 2014).

2.2.3 Coronary CTA in risk stratification of coronary artery disease

Establishing the diagnosis of stable CAD is accompanied by the process of risk stratification for future adverse events. The aim of risk stratification in stable CAD is to identify high-risk patients who would likely benefit from revascularization in terms of prognosis, i.e. beyond relieving symptoms. The long-term prognosis in stable CAD is depending on many factors including clinical variables, left ventricular function, result of stress testing, and angiographically defined coronary anatomy (Montalescot et al. 2013). Many of these prognostic markers can be assessed with the same non-invasive modalities that are used for establishing the diagnosis of stable CAD, and therefore, prognostic information is already achieved along with the diagnostic testing in patients with an intermediate PTP of CAD. In contrast, ICA is rarely needed purely for risk stratification purposes.

Coronary CTA is used to detect coronary plaques, evaluate plaque morphology, and assess stenosis severity, and accordingly, coronary CTA has been shown to provide prognostic information on stable CAD (Min et al. 2011). The relation between coronary anatomy and prognosis may be partly attributable to the presence of plaque *per se* (a plaque causing an acute coronary syndrome if eroded or ruptured), and partly to the myocardial ischemia induced by a hemodynamically significant obstructive coronary stenosis. At present, the indication for using coronary CTA is establishing or excluding the diagnosis of CAD; however, prognostic information can be obtained at the same time and same costs. Due to the potential overestimation of CAD severity, a positive CTA finding may need further ischemia testing both in terms of diagnosis and risk stratification (Montalescot et al. 2013).

Several previous studies have shown that the CTA-defined presence, extent, and severity of coronary atherosclerosis are associated with an increased risk of future adverse events (Min et al. 2007, 2011; Ostrom et al. 2008; Gaemperli et al. 2008; Hadamitzky et al. 2009; Hadamitzky, Täubert, et al. 2013; Bamberg et al. 2011; Chow, Small, et al. 2011; Hulten et al. 2011; Hou et al. 2012; Bittencourt et al. 2014; Nakazato et al. 2014). An analysis of nearly 24,000 patients in the international multicenter CONFIRM registry demonstrated a dose–response relationship between coronary CTA findings and all-cause mortality: the hazard was continuously increasing for patients with non-obstructive, 1-vessel obstructive, 2-vessel obstructive, and 3-vessel or left main obstructive CAD (Min et al. 2011). Similarly, the prognostic value of the extent and severity of CAD on coronary CTA has been shown for different composite endpoints of adverse events, including all-cause or cardiovascular death, myocardial infarction, UAP requiring hospitalization, and/or coronary revascularization (Gaemperli et al. 2008; Hadamitzky et al. 2009; Hadamitzky, Täubert, et al. 2013; Bamberg et al. 2011; Hulten et al. 2011; Hou et al. 2012; Bittencourt et al. 2014; Nakazato et al. 2014). Particularly, the prognosis in patients with normal coronary arteries

(i.e. no detectable atherosclerosis on CTA) is very favorable (Hulten et al. 2011; Min et al. 2011; Hadamitzky, Täubert, et al. 2013; Nakazato et al. 2014), and the adverse event risk of these patients may be even lower than predicted by conventional cardiovascular risk factors (Hadamitzky et al. 2009). In contrast, certain CTA findings are considered as high-risk findings, including significant left main, proximal left anterior descending (LAD), or proximal three-vessel stenoses, analogously to ICA (Pundziute et al. 2007; Min et al. 2007; Montalescot et al. 2013).

The association between the presence, extent, and severity of CAD on coronary CTA and the impaired prognosis may be partly attributable to the myocardial ischemia induced by obstructive epicardial coronary artery stenoses. However, the presence and extent of coronary atherosclerotic plaques *per se* may impair the prognosis, even in the absence of stable myocardial ischemia, as the plaques may be vulnerable and eventually result in an acute coronary syndrome. Several studies have demonstrated the prognostic implications of non-obstructive atherosclerosis, especially when extensively distributed, and the adverse event rate in non-obstructive atherosclerosis has been found to be higher than in the absence of coronary atherosclerosis but lower than in obstructive CAD (Ostrom et al. 2008; Hulten et al. 2011; Bittencourt et al. 2014; Nakazato et al. 2014). Moreover, a hybrid imaging study by van Werkhoven et al. showed incremental prognostic value of coronary CTA findings over single photon emission computed tomography (SPECT) perfusion imaging (van Werkhoven et al. 2009). A study by Chow et al. on the CONFIRM registry showed that the severity of CAD by coronary CTA is an independent prognostic factor and provides incremental prognostic value over LVEF for predicting all-cause mortality (Chow, Small, et al. 2011).

Coronary plaque morphology can be assessed using coronary CTA, and that may potentially provide incremental prognostic information over CAD extent and stenosis severity. The coronary artery plaques are generally categorized into calcified, non-calcified, and partially calcified, or mixed-type, plaques based on their composition. Non-calcified or partially calcified plaques may represent vulnerable thin-cap fibroatheromas, and their presence seem to pose an increased risk for subsequent adverse events (Gaemperli et al. 2008; van Werkhoven et al. 2009; Bamberg et al. 2011; Hou et al. 2012). Other morphological CTA characteristics that may be related to plaque vulnerability and future adverse events include the large volume of a plaque and the presence of low-CT-attenuation plaques, positive vessel remodeling, spotty calcification, and a napkin-ring sign (Motoyama et al. 2009; Maurovich-Horvat et al. 2014; Otsuka et al. 2014).

Coronary risk scores

A typical report of coronary CTA findings should describe the location and severity of coronary stenosis using standardized segmentation model, such as a model with 18 segments proposed by the Society of Cardiovascular Computed Tomography (SCCT), and preferably also include plaque composition, stenosis length, and vessel remodeling (Leipsic et al. 2014). Several different scores have been derived from anatomical coronary findings, both invasive and non-invasive, with an aim to integrate and express individual CAD burden in a single number (Leaman et al. 1981; Agatston et al. 1990; Sianos et al. 2005; Hadamitzky, Achenbach, et al. 2013; de Araújo

Gonçaves et al. 2013; de Graaf et al. 2014). A risk score that is based on the individual coronary atherosclerotic burden would probably give a better estimate of future cardiovascular risk than do the scores that are based on conventional cardiovascular risk factors, such as the SCORE and Framingham risk scores (Conroy et al. 2003; D'Agostino et al. 2008).

Leaman and colleagues developed a coronary score considering the degree of luminal stenosis on ICA and having a weight factor for every coronary artery segment. The weight factor is based on the typical blood flow to LV myocardium through a specific arterial segment and patients with right or left dominant coronary tree have different weight factors (Leaman et al. 1981). In this scoring system patients without obstructive CAD get a score of zero, while the greater degrees of obstructive CAD on ICA results in a corresponding increase in the Leaman coronary score. Another scoring system for invasive angiographic findings is the SYNTAX Score, which is used for assessing the complexity of CAD and thereby guiding the treatment decision between CABG and PCI (Sianos et al. 2005). There is ongoing research on applying the SYNTAX Score for non-invasive imaging using coronary CTA (Cavalcante et al. 2017).

Coronary artery calcium (CAC) scoring is a non-invasive system for detection and quantifying coronary artery calcium. CAC scoring is based on non-contrast enhanced, low-radiation dose CT, with a few different scoring methods available (e.g. Agatston score, mass score, and volume score) (Agatston et al. 1990). The amount of coronary artery calcium correlates roughly to the severity of atherosclerosis in the coronary arteries and patient prognosis (O'Rourke et al. 2000; Shaw et al. 2003). In asymptomatic individuals CAC scoring provides incremental prognostic information over traditional cardiovascular risk factors, and may be considered in certain asymptomatic adults for improved cardiovascular risk assessment (Shaw et al. 2003; Montalescot et al. 2013; Goff et al. 2014; Hecht et al. 2017). CAC scoring does not consider the degree of luminal stenosis and fails to detect non-calcified plaque components, and therefore, is not recommended by the guidelines for detection or ruling out of obstructive CAD in symptomatic patients with intermediate PTP (Fihn et al. 2012; Montalescot et al. 2013). Still, a CAC scoring scan is commonly performed in conjunction with coronary CTA, although the evidence of the incremental benefits of CAC scoring over coronary CTA seems to be sparse (Hecht et al. 2017). For example, the CAC scan may be helpful in optimizing CTA image coverage and adjusting X-ray tube voltage. As the radiation dose from coronary CTA has been decreasing, the relative contribution of an additional CAC scan to the total radiation dose might increase (Alluri et al. 2015). Some guidelines suggest not to proceed with coronary CTA in the presence of abundant calcification on the CAC scoring scan (e.g. Agatston score >400) due to the decreased specificity of CTA in these patients (Montalescot et al. 2013), while the others state that such approaches have not been adequately studied and the decision to proceed with coronary CTA should be left to the discretion of a physician (Abbara et al. 2016). Importantly, anatomical detection of coronary calcification using CAC scoring seems to provide incremental prognostic information over SPECT MPI findings in symptomatic patients with suspected CAD (Engbers et al. 2016).

Hadamitzky and colleagues, using the large CONFIRM registry, modeled an optimized prognostic score combining three significant predictors for subsequent all-cause mortality: NCEP ATP III clinical risk score, the number of proximal segments with stenosis $>50\%$ on coronary CTA, and the number of proximal segments with either calcified or mixed plaques (Hadamitzky, Achenbach, et al. 2013). They found this score to provide incremental prognostic value over clinical risk factors, and approximately one-third of the patients could be reclassified with this score regarding the mortality risk. The presence of proximal manifestation of CAD on coronary CTA carried a risk increment comparable with smoking or a 5-year increase in age.

Recently, the coronary score originally proposed by Leaman et al. has been adapted to non-invasive coronary CTA, taking into account not only plaque location and stenosis severity but also plaque composition (de Araújo Gonçalves et al. 2013). In this score, lesions/segments with non-calcified or mixed plaques have higher weight factors compared to predominantly calcified lesions (1.5 vs. 1.0). The CTA-adapted Leaman score (CT-LeSc) also considers non-obstructive plaques in the quantification of total coronary atherosclerotic burden, in contrast to the original score by Leaman et al. There are different weight factors for non-obstructive ($<50\%$ stenosis) and obstructive ($\geq 50\%$) plaques (0.615 and 1.0, respectively). The total score of an individual patient is the sum of the scores of all evaluable coronary segments. Mushtaq et al. demonstrated the prognostic value of CT-LeSc in predicting cardiac death and nonfatal acute coronary syndromes; they found that patients with non-obstructive atherosclerosis but high CT-LeSc had survival similar to patients with obstructive CAD on CTA with high CT-LeSc, but slightly lower survival than patients with obstructive CAD with low CT-LeSc (Mushtaq et al. 2015).

De Graaf et al. introduced a risk score that is based on quantitative coronary CTA (QCT) (de Graaf et al. 2014). The investigators used their automated QCT software, which had been previously cross-correlated with intravascular ultrasound virtual histology (IVUS-VH), for quantitative assessment of the location, severity, and composition of CAD (de Graaf et al. 2013). Based on the quantitative parameters derived from automated QCT analysis, different coronary artery segments were scored using weight factors derived from the previous literature, as detailed in the paper. The scoring system integrated the location of a segment (same weight factors as in the Leaman score), stenosis severity (factors 1 and 1.4, for $<50\%$ and $\geq 50\%$ stenosis, respectively), and plaque type (factors 1.2, 1.6, and 1.7, for calcified, partially calcified, and non-calcified, respectively). Finally, the individual segment scores were summed into a single per-patient risk score. The investigators then evaluated the feasibility of this risk score in 300 patients referred to coronary CTA for the evaluation of chest pain or dyspnea. They found that the risk score was independently associated with the composite endpoint of all-cause mortality, myocardial infarction, and revascularization, but concluded that the improvement of risk stratification owing to this score should be confirmed in larger studies (de Graaf et al. 2014).

2.2.4 Contrast-induced nephropathy

Contrast-induced nephropathy (CIN) is a potential side effect of iodine contrast agents used in contrast enhanced radiologic examinations. CIN is characterized by an acute kidney injury (AKI) with serum creatinine levels peaking at 3–5 days after the exposure to iodine contrast agent. Usually this increase is transient, and serum creatinine concentration is normalized into the baseline level within 1–3 weeks after the contrast exposure (McCullough and Sandberg 2003). Occasionally the decline in renal function may persist or even require renal replacement therapy (Kooiman et al. 2012).

The pathophysiologic mechanism of CIN is not fully understood. Hemodynamic changes in renal circulation and direct toxicity of contrast agent on renal tubular cells are thought to play central roles, together leading to acute tubular necrosis (Tumlin et al. 2006; Wong et al. 2012). The most important risk factor for CIN is a pre-existing chronic kidney disease, with the risk of CIN increasing in parallel with the degree of pre-existing renal dysfunction (Stacul et al. 2011). Diabetes mellitus, especially when associated with kidney disease, and congestive heart failure are also major patient-related risk factors for CIN (J. R. Brown, DeVries, et al. 2008; Stacul et al. 2011). The risk of CIN seems to be higher after intra-arterial administration of contrast media above the level of renal arteries than after intravenous administration (Stacul et al. 2011). The lower risk after intravenous administration may be related to smaller iodine concentration achieving the kidneys, smaller contrast agent doses, or lower prevalence of hemodynamically unstable patients. Multiple studies indicate that the risk of CIN after intravenous contrast administration starts to increase when the pre-procedural estimated glomerular filtration rate (eGFR) falls below 45 mL/min/1.73m² (Katzberg and Lamba 2009; Stacul et al. 2011). A more comprehensive list of established or potential risk factors for CIN is provided in Table 2. There is a clinical consensus that hydration reduces the risk of CIN, although randomized blinded trials have not been conducted (Stacul et al. 2011).

In the literature, CIN is usually defined as a relative $\geq 25\%$ or an absolute $\geq 44.2 \mu\text{mol/L}$ increase in serum creatinine concentration within three days following contrast agent exposure in the absence of another etiology for the increase (Morcos, Thomsen, and Webb 1999). Various diagnostic criteria have been suggested but none has been proven superior to others (Stacul et al. 2011).

Table 2 Established or potential risk factors for contrast induced nephropathy. Data is aggregated from J. R. Brown, DeVries, et al. 2008; Stacul et al. 2011; and Moos et al. 2013.

<i>Patient-related:</i>
Chronic kidney disease
Diabetes mellitus
Congestive heart failure
Advanced age
Recent myocardial infarction
Hemodynamic instability
Reduction of the renal oxygen supply (e.g. anemia)
Malignancy
Concomitant use of nephrotoxic drugs
<i>Procedure-related:</i>
Intra-arterial route of contrast administration
High osmolality of contrast agent
High dose of contrast agent administered
Multiple contrast enhanced studies within a short time period
Urgent or emergent priority of contrast enhanced examination
Reduction of renal blood supply during vascular procedures

The incidence of CIN has been varying among different studies. A high incidence of 15% has been reported in patients undergoing PCI (McCullough et al. 2006). Two large meta-analyses reported overall incidences of 5–6% after contrast enhanced CT using intravenous contrast agents (Kooiman et al. 2012; Moos et al. 2013). The incidence of persistent decline in renal function after CT was ~1%, and the risk for renal replacement therapy (dialysis) was 0.06%, according to the meta-analysis by Kooiman et al. (Kooiman et al. 2012). Katzberg and Lamba reviewed prospective studies on patients (n=1,075) with pre-existing renal dysfunction and thereby having an increased risk for CIN (Katzberg and Lamba 2009). They concluded that the incidence of CIN was 5.1% after contrast enhanced CT, and there was no acute need for dialysis or CIN-related mortality. One study reported a relatively low incidence of CIN (2.4%) after contrast enhanced CT in outpatients with mild baseline renal dysfunction (eGFR >45 mL/min/1.73m²), while inpatients and patients with more severe renal impairment at baseline had substantially higher rates (11–13%) of CIN (Weisbord et al. 2008). A few studies with relatively small patient cohorts have addressed CIN after coronary CTA and reported incidences between 0% and 10% (El-Hajjar et al. 2008; Yoshikawa et al. 2011; Pedersen et al. 2014; Li et al. 2015).

Assessing the frequency of CIN is complicated by normal physiological fluctuation of serum creatinine level (Katzberg and Newhouse 2010). A change between two measurements can be attributable to “regression to the mean” phenomenon. Furthermore, other factors such as a concurrent disease or medical therapy, rather than the contrast agent exposure, may cause changes in serum creatinine concentration. The current definitions of CIN focus only on those patients with increase in creatinine level that may lead to overestimation of CIN prevalence. Newhouse et al. demonstrated that a ≥25% change (i.e. increase or decrease) in serum creatinine concentration during five consecutive days occurred in over half of the 32,161 patients who did not receive

contrast agents (Newhouse et al. 2008). A $\geq 25\%$ increase in creatinine level, which is the usual definition of CIN, was observed in 27% of patients with normal baseline creatinine level in their study, reflecting the magnitude of “normal” variation in serum creatinine concentration. McDonald et al. retrospectively studied 53,439 patients who had undergone either intravenous contrast enhanced CT or unenhanced CT (R. J. McDonald et al. 2013). After propensity score adjustment due to a non-randomized study design, risk of meeting the CIN criteria was not different between contrast and non-contrast groups.

Previous studies have shown that increased serum creatinine concentration after contrast agent exposure is associated with increased mortality, but the causality of this association is unclear (Rihal et al. 2002; J. R. Brown, Malenka, et al. 2008). The association may be partially explained by confounding factors (e.g. cardiovascular disease) that predispose both to changes in serum creatinine concentration and to increased mortality. Thus, CIN may be, at least in part, rather a marker of elevated risk than the actual cause for mortality (Rudnick and Feldman 2008).

2.3 Myocardial perfusion imaging

2.3.1 Principles of myocardial perfusion imaging

Myocardial perfusion imaging (MPI) involves a group of different non-invasive techniques to assess myocardial perfusion, i.e. blood flow through the myocardium. Myocardial perfusion may be reduced in different disease settings, such as in the presence of an epicardial coronary artery stenosis limiting the blood flow to myocardium, or in the disease of coronary microvasculature. The reduction of myocardial perfusion is an early phenomenon in the ischemic cascade, making MPI a sensitive method for the detection of ischemic heart disease.

The main indication for MPI is the detection of obstructive CAD. Anatomical imaging of CAD, such as coronary CTA, is based on the detection of coronary artery narrowing that may result in reduced blood flow to the myocardium, and subsequently, myocardial ischemia. In contrast to anatomical imaging, MPI is functional imaging aiming to detect this reduction in blood flow, or perfusion, *per se*.

In a normal healthy person, myocardial perfusion is typically 3–4 times higher during physical exercise compared to rest, and the level of perfusion is mainly regulated by the coronary microvasculature (i.e. the small vessels diverging from epicardial coronary arteries). A mild epicardial coronary artery stenosis does not pose any significant hemodynamic effect. However, a stenosis of greater degree may lead to increased resistance for blood flow in the coronary artery. In a rest situation, the increased resistance can be compensated with the adaptation of coronary microvasculature, maintaining sufficient myocardial blood flow. However, myocardial perfusion during stress cannot be appropriately multiplied due to the coronary stenosis, leading to insufficient

blood flow in relation to the increased oxygen demand. This type of myocardial ischemia during stress may present as an exertional angina pectoris. The ratio of stress and rest perfusion, called coronary flow reserve (CFR) or myocardial flow reserve (MFR), is reduced in case of reversible or inducible myocardial ischemia, reflecting the insufficiently low perfusion during stress but usually normal perfusion during rest. However, rest perfusion may also be disturbed in the presence of very severe coronary stenosis. In contrast to reversible ischemia, a perfusion defect may be persistent due to a myocardial infarction scar, seen as a “fixed” perfusion defect both during stress and rest. This is the basis for rest-stress perfusion imaging, in which both rest and stress images are obtained with an aim to classify perfusion defects as reversible, and possibly suitable for revascularization, or fixed, reflecting scar tissue. Furthermore, stress-only and stress-first imaging protocols are increasingly used, with no need to perform rest imaging if there is no perfusion defect in stress images (Gowd, Heller, and Parker 2014).

In addition to a significant focal coronary artery stenosis, myocardial perfusion may also be impaired due to diffuse atherosclerosis of epicardial coronary arteries (De Bruyne et al. 2001). In turn, coronary microvascular dysfunction (CMD) refers to a situation in which functional and/or structural abnormalities in coronary microcirculation cause the reduction in myocardial perfusion (Crea, Camici, and Merz 2014). CMD may exist in the presence or absence of obstructive epicardial CAD, and may be related to cardiovascular risk factors, such as diabetes, or non-coronary cardiovascular disease, such as hypertrophic or dilated cardiomyopathy (Crea, Camici, and Merz 2014).

There are two main types of stress, i.e. physical and pharmacological, that can be used for stress MPI. Physical exercise is a preferred method in patients with adequate exercise capabilities and is well suitable for perfusion tracers with long half-life, such as technetium-99m (^{99m}Tc) -labeled tracers used for single photon emission computed tomography (SPECT) MPI. In this case, the intravenous tracer injection is given during peak physical exercise and scanning is performed after the exercise. However, this approach is not suitable for positron emission tomography (PET) perfusion tracers with relatively short half-lives, but the image data should be collected during the stress. Therefore, the stress is achieved by an intravenous administration of pharmacologic stress agents during the scan. Maximal myocardial blood flow (MBF) can be induced with vasodilator stress agents, including adenosine, regadenoson, and dipyridamole, that artificially increase myocardial perfusion via vasodilation of coronary circulation. Adenosine and regadenoson act by directly stimulating adenosine A_{2A} receptors, while dipyridamole inhibits the cellular reuptake of endogenously produced adenosine and indirectly acts as an adenosine agonist (Henzlova et al. 2016). The use of pharmacologic vasodilator stress requires adequate patient preparation; importantly, the consumption of methylxanthines, e.g. caffeine, should be discontinued for at least 12 hours prior to the imaging (Henzlova et al. 2016). There are several contraindications, for example related to bronchospastic lung disease and atrioventricular conduction block, that may prevent the use of vasodilator stress agents (Henzlova et al. 2016). In patients with limited exercise capabilities and contraindications to vasodilator stress agents, sympathomimetic dobutamine can be used to pharmacologically stimulate myocardial perfusion via increased metabolic demand

of the myocardium (Geleijnse et al. 2000). If needed, atropine may be administered in conjunction with dobutamine to further increase heart rate (Geleijnse et al. 2000).

2.3.2 Techniques for assessing myocardial perfusion

There are two nuclear imaging modalities, SPECT and PET, that are used for MPI. In addition, myocardial perfusion can be non-invasively assessed using computed tomography (CT), magnetic resonance imaging (MRI), and echocardiography.

Single photon emission computed tomography for myocardial perfusion imaging

SPECT MPI is a tomographic nuclear imaging modality allowing visualization of flow-dependent tracer distribution in the myocardium. Radioactive gamma ray-emitting tracers are used, including technetium-99m (^{99m}Tc) -labeled tracers sestamibi and tetrofosmin, and a potassium analog thallium-201 (^{201}Tl) (Henzlova et al. 2016). Three-dimensional images are reconstructed and analyzed in short axis, horizontal long axis, and vertical long axis planes, and optionally in a polar map (“a bull’s eye”). Currently, the analysis of SPECT perfusion images is usually relative, although there have also been attempts to develop SPECT quantification (Hsu et al. 2014). The relative analysis means that a myocardial region with the highest tracer uptake is assumed to be normally perfused and other myocardial areas are compared to this reference region. If the perfusion is globally reduced, that might be the case in three-vessel obstructive CAD, the relative image analysis may underestimate the extent of ischemia or lead to a false negative result, as the region with the highest tracer uptake is erroneously interpreted as normal. In addition to visual analysis, a semiquantitative approach with summed scores is commonly used. In this method, the myocardium is segmented using e.g. the 17-segment system proposed by the American Heart Association, and the individual myocardial segments are numerically graded based on their relative tracer uptake (Cerqueira et al. 2002). The segmental values are then summed, providing a *per-patient* summed score integrating both the severity and extent of myocardial perfusion defects. Three scores are commonly used: summed rest score (SRS; calculated on rest images, and reflecting fixed perfusion defects, i.e. scar), summed stress score (SSS; calculated on stress images, and reflecting total, i.e. both fixed and reversible, perfusion defects), and summed difference score (SDS; calculated as difference between stress and rest images, reflecting reversible perfusion defects, i.e. inducible ischemia). However, these scores are also based on relative differences in tracer uptake, and hence, not truly quantitative. ECG-gating is recommended for SPECT MPI, allowing the assessment of LV volume and ejection fraction (Henzlova et al. 2016). Increased amount of soft-tissue in obese patients may result in inferior quality of perfusion images and reduced diagnostic accuracy, especially due to frequent false positive findings and decreased specificity (Taqueti 2017). Accordingly, the use of attenuation correction (e.g. using CT) seems to increase the diagnostic accuracy of SPECT MPI (Huang et al. 2016).

Positron emission tomography for myocardial perfusion imaging

PET MPI is another tomographic nuclear imaging modality, in which positron-emitting tracers are used. The emitted positrons annihilate with electrons, producing two gamma photons moving in opposite directions, and these coincidental events are recorded with a PET scanner. PET MPI provides several advantages compared to SPECT, including better image quality, interpretative certainty, and diagnostic accuracy (Bateman et al. 2006; Mc Ardle et al. 2012). The spatial resolution of PET is better compared to that of SPECT (Bateman et al. 2006). In addition, the detection of coincident photons waives the need for using collimators, resulting in a higher sensitivity and/or a lower radiation dose with PET. Attenuation correction is routinely used with PET, and importantly, absolute quantification of myocardial blood flow (MBF) is feasible for PET MPI (Knuuti et al. 2009). More limited availability and higher costs of scanners and tracers can be considered as disadvantages of PET compared to SPECT (Montalescot et al. 2013).

There are a few tracers available for PET MPI with different profiles of advantages and disadvantages. Oxygen-15 (^{15}O) -labeled water molecule is metabolically inert and freely diffusible, and has a high extraction fraction of ~ 1 , meaning that the uptake rate into myocardium is in linear relationship to the MBF, that makes it an ideal tracer for absolute quantification of MBF (Knuuti et al. 2009). However, the retention of the tracer into myocardium is almost absent, and therefore, conventional visual image analysis is not feasible with ^{15}O -water (deKemp et al. 2016). Accordingly, the ECG-gated measurement of LV volume and function using ^{15}O -water PET is not currently in clinical use (Nordström et al. 2017). The half-life of oxygen-15 is about two minutes, and the production of this isotope requires an on-site cyclotron. With ^{15}O -water, a dynamic PET scan is started immediately after the tracer injection (Kajander et al. 2010). ^{15}O -water is not approved for clinical use by the Food and Drug Administration (FDA) of the United States.

Nitrogen-13 (^{13}N) -labeled ammonia also has a quite high extraction fraction over a wide range of flow values, and therefore, is well suitable for MBF quantification. In addition, the retention fraction is relatively high compared to other perfusion tracers, allowing visual perfusion image analysis and ECG-gated assessment of LV volumes and ejection fraction at rest and during pharmacologic stress (deKemp et al. 2016). The half-life of nitrogen-13 isotope is relatively short 10 minutes, and its production also requires an on-site cyclotron.

Rubidium-82 (^{82}Rb) is a widely-used generator-produced PET perfusion tracer, not requiring an on-site cyclotron. The extraction fraction of ^{82}Rb is low and further reduces with increasing MBF, resulting in underestimation of myocardial perfusion at high flow values (Saraste et al. 2012). The underestimated flow values must be corrected with mathematical models that also multiply the noise in MBF estimates. In turn, the washout rate for ^{82}Rb is slow, leading to relatively high retention of the tracer into myocardium and good quality of visual perfusion images (deKemp et al. 2016). Moreover, the ECG-gated assessment of LV volumes and function is feasible at rest and during pharmacologic stress.

A novel fluorine-18 (^{18}F) -labeled PET perfusion tracer ^{18}F -flurpiridaz, currently undergoing the Phase 3 trial, has shown higher image quality and interpretative certainty compared to SPECT MPI (Berman et al. 2013). Furthermore, a high and flow-independent extraction fraction has been demonstrated in an animal model, and absolute quantitation of MBF in humans seems to be feasible with flurpiridaz (Huisman et al. 2008; Packard et al. 2014). A key advantage of ^{18}F -labeled PET perfusion tracers would be their relatively long half-life of 110 minutes, allowing these agents to be distributed to distant study sites without need for an on-site cyclotron.

When interpreting the results of any MPI study, the characteristics of different tracers must be considered. Furthermore, unequal cut-off values may be needed when using different tracers for absolute quantification of MBF (Knuuti et al. 2009).

Radiation dose from myocardial perfusion imaging

Radiation dose to a patient significantly varies between different modalities, tracers, and protocols (Table 1). SPECT MPI with thallium-201 is associated with a high average effective dose around 20 mSv (Einstein 2008). A rest-stress SPECT MPI study using $^{99\text{m}}\text{Tc}$ -labeled tracers tetrofosmin or sestamibi is associated with lower effective dose, typically 5–10 mSv, and this can be further reduced by using stress-only protocols (Einstein 2008; Slomka et al. 2012). The effective patient doses for rest-stress PET MPI are generally lower, typically less than 4 mSv including an attenuation correction scan (Slomka et al. 2012). An estimated effective dose of 3.7 mSv has been suggested for rest-stress rubidium-82 MPI with a standard two-dimensional PET scanner, and can be potentially reduced with a three-dimensional scanner (Senthamizhchelvan et al. 2010). An effective dose of 2.2 mSv has been estimated for ^{13}N -ammonia PET MPI (Di Carli and Murthy 2011). For ^{15}O -water PET MPI, an effective dose of 1 mSv has been reported for a single tracer injection (Kajander et al. 2009). For ^{18}F -flurpiridaz, the mean effective patient dose from rest-stress MPI protocols has been estimated to be approximately 5–6 mSv (Berman et al. 2013).

2.3.3 Diagnostic accuracy of myocardial perfusion imaging in coronary artery disease

As previously reviewed, the anatomical degree of a coronary stenosis only partially reflects the hemodynamic effects of the given stenosis. MPI provides estimates on the myocardial perfusion, which is affected not only by the epicardial coronary arteries but also by the resistance of coronary microcirculation and the hemodynamic status of a patient. Stress testing for myocardial ischemia is indicated for diagnostic testing in symptomatic patients with suspected obstructive CAD and an intermediate PTP (Fihn et al. 2012; Montalescot et al. 2013).

Different studies have revealed sensitivities of 73–92% and specificities of 63–87% for stress SPECT MPI in detection of obstructive CAD (Montalescot et al. 2013). SPECT stress testing has significantly higher sensitivity compared to conventional exercise ECG testing without imaging,

as the reduction of myocardial perfusion precedes the occurrence of ECG changes in the ischemic cascade (Montalescot et al. 2013). For patients with left bundle branch block (LBBB), ^{99m}Tc SPECT MPI using adenosine or dipyridamole seems to be more accurate than using physical exercise, as false positive septal perfusion defects are less often encountered (Higgins et al. 2006).

PET MPI provides several advantages over SPECT, including better spatial image resolution and possibility for absolute quantification of MBF, and as might be expected, the diagnostic accuracy of PET MPI has been shown to be higher than that of SPECT (Bateman et al. 2006; Mc Ardle et al. 2012; Parker et al. 2012). In a meta-analysis, Jaarsma et al. reported a pooled sensitivity of 84% and a specificity of 81% for PET MPI in detection of obstructive CAD, mainly including studies using rubidium-82 tracer (Jaarsma et al. 2012). In another meta-analysis, Mc Ardle et al. reported a sensitivity of 90% and a specificity of 88% for ^{82}Rb PET MPI (Mc Ardle et al. 2012). Quantitative ^{82}Rb PET measures have been shown to correlate with the angiographic severity of a coronary artery stenosis (Anagnostopoulos et al. 2008; Yoshinaga et al. 2011).

Kajander et al. reported high per-patient sensitivity 95%, specificity 91%, and accuracy 92% of ^{15}O -water PET MPI for detection of obstructive CAD, using absolute quantification of stress MBF and a gold standard of ICA, with FFR when feasible (Kajander et al. 2011). As previously explained, real visual analysis of tracer retention in the myocardium is not feasible with ^{15}O -water. However, in the study by Kajander et al. the quantitative perfusion data were also assessed on a relative scale, and a higher diagnostic accuracy was achieved using absolute scale compared to the relative analysis (sensitivity 74%, specificity 73%, and accuracy 73%). Similarly, studies using ^{13}N -ammonia PET have consistently shown an improved accuracy and especially a higher sensitivity of quantitative flow measures, either stress MBF or MFR, compared to relative MPI analysis in detection of obstructive CAD (Muzik et al. 1998; Hajjiri et al. 2009; Fiechter et al. 2012; J. M. Lee et al. 2016). The extent of ischemia may be underestimated in relative analysis as the area with the highest perfusion is assumed to be normal, which might not be the case in multivessel obstructive CAD. On the other hand, coronary microvascular dysfunction (CMD) may cause low absolute MBF values in the absence of significant epicardial coronary artery stenoses.

In the study by Kajander et al. absolute MBF <2.5 mL/g/min during adenosine stress was considered abnormally low, and this cut-off value was based on an earlier receiver operating characteristic (ROC) analysis by the same investigators (Kajander et al. 2010). Later, Danad et al. studied 330 patients with suspected CAD who underwent both quantitative ^{15}O -water PET MPI and ICA, with FFR when feasible (Danad, Uusitalo, et al. 2014). The diagnostic performance of stress MBF and myocardial flow reserve (MFR; the ratio of stress MBF and rest MBF) were separately analyzed. The investigators found a slightly lower optimal cut-off value of 2.3 mL/g/min for stress MBF, yielding a per-patient sensitivity of 89%, specificity of 84%, and accuracy of 86% in detection of flow-limiting CAD. An optimal cut-off value 2.5 for MFR was identified, resulting in an inferior diagnostic performance of MFR (a per-patient sensitivity 86%, specificity 72%, and accuracy 78%) compared to stress MBF. This finding suggests that a single quantitative PET scan

during vasodilator stress is sufficient for diagnosis of CAD, with no need to routinely measure rest MBF.

In a substudy of the EVINCI study population, MPI studies were classified as normal or abnormal based on segmental MBF/MFR values alone, i.e. without visual analysis and without considering global or territorial flow values (Berti et al. 2016). A high NPV of segmental PET measures was observed while the PPV was lower, verifying the role of quantitative PET for excluding obstructive CAD but suggesting that minor perfusion defects may not always imply the presence of significant epicardial CAD.

2.3.4 Myocardial perfusion imaging in risk stratification

The prognostic value of MPI, either using SPECT and PET, has been shown in multiple studies, in which the extent and severity of ischemia were associated with the risk of future adverse events (Ladenheim et al. 1986; K. Brown 1991; Hachamovitch et al. 1998; Shaw and Iskandrian 2004; Herzog et al. 2009; Murthy et al. 2011; Dorbala et al. 2013). The current ESC guidelines state that after establishing the diagnosis of CAD patients should undergo stress testing for event risk stratification, if they are candidates for coronary revascularization in case of high risk (Montalescot et al. 2013). However, in most patients the information for risk stratification will already be achieved as a part of their diagnostic testing.

Hachamovitch et al. demonstrated the prognostic value of myocardial perfusion findings using dual-isotope (^{201}Tl and $^{99\text{m}}\text{Tc}$ -sestamibi) rest-stress SPECT MPI (Hachamovitch et al. 1998). Normal MPI finding was associated with a low rate of adverse cardiac events (combined rate <1% per year for cardiac death or myocardial infarction), while an increasing degree of perfusion abnormalities was associated with a corresponding increase in the adverse event rate. Similar findings have been reported in numerous other studies using SPECT MPI, as was extensively reviewed in 2004 by Shaw and Iskandrian, who summarized that the literature-based median annual rate of major adverse cardiac events (MACE) was 0.6% in patients with normal or low-risk SPECT perfusion findings and 5.9% in the setting of high-risk findings (Shaw and Iskandrian 2004).

Dorbala et al. investigated the prognostic value of ^{82}Rb rest-stress PET MPI findings and their potential for risk reclassification over clinical variables in a large cohort of 7,061 patients (Dorbala et al. 2013). The adjusted risk for cardiac death increased with each 10% of abnormal myocardium at stress, and the addition of percent myocardium ischemic and percent myocardium scarred to a risk model with clinical factors resulted in correct reclassification in ~12% of patients, regarding the risk for cardiac death. Moreover, gated PET-measured LVEF reserve (i.e. LVEF during pharmacologic stress minus LVEF at rest) seems to provide incremental prognostic value over perfusion findings (Dorbala et al. 2009).

Herzog et al. studied the incremental prognostic value of coronary flow reserve (CFR; the ratio of stress MBF and rest MBF) in 256 patients using quantitative ^{13}N -ammonia PET (Herzog et al. 2009). The scans were analyzed semiquantitatively using summed stress scores (SSS) and quantitatively using global CFR. In patients with “relative” perfusion defects, reduced CFR (<2.0) was incrementally predictive of MACE and cardiac death during the whole follow-up period (mean 5.5 years). Conversely, in patients with visually normal perfusion, abnormal CFR predicted outcome only for the first 3 years of follow-up. Murthy et al. studied 2,783 patients using quantitative rest-stress ^{82}Rb PET, with a median follow-up of 1.4 years (Murthy et al. 2011). Severely reduced (<1.5) and intermediate (1.5–2.0) global CFR were associated with 5.6 and 3.4 -fold risk of cardiac death, respectively, compared to preserved CFR (>2.0), after adjustment for semiquantitative measures of myocardial ischemia, LV function, and clinical variables. Furthermore, CFR allowed correct risk reclassification. Patients with preserved CFR had favorable prognosis ($<0.5\%$ annual rate of cardiac mortality), while lower CFR identified higher-risk patients at every level of semiquantitative perfusion abnormalities, also in patients with visually normal PET scans.

In a study by Taqueti et al. 329 patients underwent both ICA and quantitative PET MPI using ^{82}Rb or ^{13}N -ammonia (Taqueti et al. 2015). The extent and severity of angiographic CAD were assessed using CAD prognostic index, and global CFR was measured using PET. In an adjusted analysis, patients with low CFR, independently of angiographic index, had a high risk for MACE similarly to patients with high angiographic scores, while patients with preserved CFR and low angiographic index had the most favorable outcome. The authors and editorialists suggested that diffuse atherosclerosis may, in part, be responsible for the increased risk of cardiovascular events (Gould and Johnson 2015; Taqueti et al. 2015).

2.4 Hybrid imaging in coronary artery disease

2.4.1 *Rationale, benefits, and weaknesses of hybrid imaging in coronary artery disease*

Hybrid imaging is defined as combining or fusing two datasets from different imaging modalities in a way that both modalities equally contribute to image information (Kaufmann 2009). The rationale is to obtain different types of information (e.g. on anatomy and function) using different imaging modalities and interpret these data together. In detection of CAD, hybrid imaging most commonly refers to a combination of coronary CTA and myocardial perfusion imaging by SPECT or PET, but other combinations and modalities, such as magnetic resonance imaging, are also possible (van Werkhoven et al. 2010). The most recent guidelines by ESC and EACTS on myocardial revascularization state that hybrid imaging “should be considered” for diagnostic testing in stable symptomatic patients with an intermediate PTP of obstructive CAD (Windecker et al. 2014).

Cardiac hybrid imaging combining coronary CTA and MPI provides several potential advantages over a single imaging modality in detection of obstructive CAD (Saraste and Knuuti 2012). Assessment of myocardial perfusion clarifies the hemodynamic significance of an anatomic coronary artery stenosis. In addition, MPI will be helpful when there are artifacts or abundant calcifications on coronary CTA that hamper reliable evaluation of the degree of stenosis. On the other hand, coronary CTA may increase the diagnostic confidence when interpreting equivocal perfusion defects on MPI. Anatomic data by CTA allows assignment of a perfusion defect to a certain vessel or branch region, taking into account an inter-individual variability in the coronary tree anatomy. Moreover, it has been shown that the fusion of CTA and MPI into a single image increases the diagnostic accuracy in detection of obstructive CAD and allows better localization of a stenosis, compared to side-by-side analysis of CTA and MPI, or MPI analysis alone (Santana et al. 2009). Reduced myocardial perfusion on quantitative PET in the absence of obstructive CAD on CTA may suggest the presence of coronary microvascular dysfunction (CMD). In turn, extensive obstructive lesions on CTA in the presence “normal” perfusion by qualitative SPECT MPI may arouse a suspicion of 3-vessel obstructive CAD causing balanced myocardial ischemia and a false negative SPECT finding. Finally, non-obstructive atherosclerosis can be detected using coronary CTA. Potential disadvantages of hybrid imaging could be related to an increased radiation exposure, costs, time consumption, and patient inconvenience, and an additional exposure to pharmacologic agents, such as contrast or stressor agents. However, when evaluating the potential advantages and disadvantages of cardiac hybrid imaging, effects of the hybrid imaging on downstream resource utilization should be also considered. For example, coronary CTA, although having an excellent NPV in exclusion of obstructive CAD, may lead to unnecessary invasive procedures unless the hemodynamic significance of a coronary stenosis is confirmed by MPI (Hulten et al. 2013).

2.4.2 Diagnostic performance of hybrid imaging in suspected coronary artery disease

Hybrid imaging using SPECT MPI and coronary CTA has a higher diagnostic accuracy in detection of obstructive CAD than does coronary CTA alone, and this is mainly related to improvements in specificity and PPV (Rispler et al. 2007; Sato et al. 2010; Gaemperli, Bengel, and Kaufmann 2011; Schaap et al. 2014). These findings are consistent with the known high sensitivity but relatively low specificity of coronary CTA. Similarly, studies have shown the feasibility and diagnostic accuracy of hybrid imaging combining PET MPI and coronary CTA (Namdar et al. 2005; Groves et al. 2009; Kajander et al. 2010; Danad et al. 2013).

Di Carli et al. studied 110 patients with hybrid PET/CTA and found that only about half of anatomically obstructive stenoses on coronary CTA were associated with ischemia on stress ^{82}Rb -PET MPI, while half of normal PET studies showed some atherosclerotic changes on CTA (Di Carli et al. 2007). The investigators suggested the potential complimentary roles of CTA and MPI

in evaluation of patients with suspected CAD. In a study by Kajander et al. 107 patients underwent quantitative ^{15}O -water PET/CTA hybrid imaging and ICA, with FFR measurement when feasible (Kajander et al. 2010). The per-patient sensitivity to detect an invasively defined flow-limiting coronary stenosis was equally high (95%) for coronary CTA alone, PET MPI alone, and their combination. In turn, the per-patient specificity was improved by using hybrid PET/CTA (100%), compared to either CTA alone (87%) or PET MPI alone (91%). Perfusion imaging allows the assessment of the hemodynamic significance of a coronary stenosis, while anatomic imaging with CTA permits the evaluation whether a perfusion defect is assigned to a significant epicardial coronary stenosis or rather related to coronary microvascular dysfunction. Similarly, a study by Danad et al. demonstrated the improved diagnostic accuracy of hybrid ^{15}O -water PET/CTA compared to either modality alone, and additionally, showed superiority of quantitative hyperemic MBF over CFR (Danad et al. 2013).

In the “hybrid imaging substudy” of the multicenter EVINCI study population, 252 patients underwent coronary CTA, SPECT or PET MPI, and quantitative ICA, preferably with FFR measurement of intermediate lesions (Liga et al. 2016). The study revealed that in 18% of patients a perfusion defect on MPI was reclassified from a standardized coronary territory (AHA 17-segment model) to another vessel territory if perfusion images were fused with CTA (Cerqueira et al. 2002). The segment reclassification occurred almost exclusively in segments belonging to standardized left circumflex artery (LCX) or right coronary artery (RCA) territories. A positive matched hybrid imaging finding (i.e. a perfusion defect in a stenotic vessel area) was found in 24% of patients with PPV of 87%, whereas significant CAD was excluded based on normal hybrid imaging finding (i.e. both MPI and CTA negative) in 41% of patients with NPV of 88%. Similar discrepancies between standardized and actual coronary territories were reported by Javadi et al., emphasizing the role of considering individual coronary anatomy when interpreting perfusion defects (Javadi et al. 2010). However, in a hybrid ^{15}O -water PET/CTA study of 44 subjects by Thomassen et al., true CTA-defined coronary territories deviated from standardized territories in about half of patients, but only in one patient this resulted in a change from a false positive to a true negative finding in the particular coronary territory (Thomassen et al. 2015).

2.4.3 Prognostic value of hybrid imaging findings in coronary artery disease

As previously reviewed in this thesis, the extent and severity of both coronary anatomical lesions and myocardial perfusion abnormalities are related to an increasing risk of adverse events in stable CAD. The agreement between anatomy and perfusion is imperfect, and therefore, the integration of anatomic and functional imaging modalities could potentially provide incremental information not only for diagnosis but also on patient outcome (Valenta et al. 2013; H. Lee et al. 2016). A few studies have evaluated the prognostic implications of hybrid imaging findings in CAD (Schenker et al. 2008; van Werkhoven et al. 2009; Pazhenkottil, Nkoulou, Ghadri, Herzog, Buechel, et al. 2011; Ghadri et al. 2013).

Schenker et al. investigated the interrelation of coronary artery calcification and ^{82}Rb PET myocardial perfusion in 695 patients with an intermediate PTP of obstructive CAD (Schenker et al. 2008). They found that among patients with normal PET perfusion, the annual rate of death or myocardial infarction (MI) was lower in patients with CAC score of zero compared to those with CAC score of ≥ 1000 (2.6% versus 12.3%, respectively). Similarly, among patients with ischemia on PET MPI, the annual event rate was lower in those with CAC score of zero compared to CAC score ≥ 1000 (8.2% versus 22.1%, respectively). In turn, Ghadri et al. investigated 462 patients and found that a matched finding of CAC and SPECT MPI (i.e. a stress perfusion defect with CAC score ≥ 1 in the supplying coronary artery) was an independent predictor of adverse cardiac events (Ghadri et al. 2013).

Van Werkhoven et al. studied the prognostic value of hybrid coronary CTA and SPECT MPI findings in 517 patients, and found a low 1.0% annual event rate in patients with none or only mild CAD ($< 50\%$ CTA stenosis) and normal SPECT perfusion (van Werkhoven et al. 2009). The presence of either abnormal perfusion or a significant $\geq 50\%$ stenosis was associated with moderately increased event rates (3.7% and 3.8%, respectively), while the highest annual event rate (9.0%) was found in patients with both abnormal perfusion and a significant stenosis. Likewise, Pazhenkottil et al. studied event risk stratification using hybrid coronary CTA and stress-rest SPECT MPI in 335 patients (Pazhenkottil, Nkoulou, Ghadri, Herzog, Buechel, et al. 2011). Patients with a reversible SPECT perfusion defect in the territory supplied by a significantly ($\geq 50\%$) stenosed coronary artery had the highest annual rate of death or MI (6.0%), while “unmatched” combinations of pathological CTA and/or SPECT findings were associated with a moderately increased risk (2.8%). Patients with no significant stenosis and no perfusion defect had the most favorable prognosis with an annual event rate of 1.3%.

In a recent study by Chen et al., 379 patients were followed-up for 2 years, with a majority of end-point events being revascularizations (M. Y. Chen et al. 2017). The investigators concluded that the non-invasive combination of coronary CTA and CT-based MPI enables event risk stratification similarly to that provided by a combination of ICA and SPECT MPI.

As with other forms of obstructive CAD, coronary CTA has shown a high sensitivity of 95% but a lower specificity of 83% in detection of “high-risk” forms of CAD, i.e. left main and/or three-vessel obstructive CAD (Dharampal et al. 2013). Wall-motion imaging seems to have a higher sensitivity than SPECT MPI in detection of left main and/or three-vessel obstructive CAD (Lima et al. 2003; Mahajan et al. 2010). The lower sensitivity of MPI is probably due to the underestimation of global or balanced myocardial ischemia, but might be potentially improved by the absolute quantification of MBF using PET. A hybrid imaging finding showing anatomical left main and/or three-vessel obstructive disease and coexisting extensive myocardial ischemia should raise a suspicion of high-risk CAD.

2.4.4 Patient management after hybrid imaging of coronary artery disease

For being cost-effective, non-invasive cardiac imaging findings should affect downstream resource utilization without compromising patient safety. Ideally, non-invasive imaging findings would not only impact the decision to proceed to further invasive diagnostic procedures, but they would also guide the therapeutic interventions (Saraste and Knuuti 2012). For example, the extent of diffuse CAD on coronary CTA or the extent of perfusion abnormalities on MPI might impact the choice between PCI or CABG as the revascularization strategy – extensive diffuse CAD and/or extensive ischemia potentially favoring CABG (Gould and Johnson 2015). In symptomatic patients with suspected CAD, coronary CTA leads to a more appropriate use of ICA and to favorable alterations in the use of preventive therapies (Williams et al. 2016). A few studies have addressed the patient management after hybrid imaging of CAD (Pazhenkottil, Nkoulou, Ghadri, Herzog, Küest, et al. 2011; Schaap et al. 2013; Danad, Rajmakers, et al. 2014; Liga et al. 2016).

Pazhenkottil et al. assessed the referral to early revascularization after cardiac SPECT/CTA hybrid imaging in 318 consecutive patients with suspected or known CAD, and found revascularization rates of 41%, 11%, and 0% for patients with matched pathologic, unmatched pathologic, and normal hybrid imaging findings, respectively (Pazhenkottil, Nkoulou, Ghadri, Herzog, Küest, et al. 2011). In a substudy of the EVINCI population, 252 patients who had undergone both hybrid MPI/CTA imaging (MPI with either SPECT or PET) and ICA were included (Liga et al. 2016). The investigators reported early revascularization rates of 70%, 36%, and 10% for matched, mismatched, and normal hybrid imaging findings, respectively. Danad et al. studied the downstream referral to early ICA and revascularization after hybrid ¹⁵O-water PET/CTA imaging (Danad, Rajmakers, et al. 2014). Among patients with normal or non-obstructive CTA findings, 9% had abnormal MPI, 5% underwent ICA, and none underwent revascularization. In turn, among patients with equivocal or obstructive CTA finding, an abnormal MPI result was associated with increased rates of ICA and revascularization.

In a study by Schaap et al. 107 patients with suspected CAD underwent both hybrid SPECT/CTA imaging and ICA (Schaap et al. 2013). Treatment decisions on the necessity of revascularization were first made based on hybrid SPECT/CTA findings, and second, based on SPECT and ICA findings, resulting in a high agreement between these two different strategies (92%). However, the agreement between the two work-ups was lower (74%) for the choice of revascularization method (i.e. PCI versus CABG).

2.4.5 Different approaches to hybrid imaging of coronary artery disease

Although increasingly utilized, the optimal strategy to use hybrid imaging of CAD in clinical practice is not very well established. The potential incremental diagnostic and prognostic information provided by the combined or “hybrid” use of multiple imaging tests should be balanced with the increased costs, time consumption, exposure to radiation and pharmacologic agents, and

patient inconvenience. Hence, sequential imaging strategies have been proposed instead of unselectively performing multimodality imaging in all patients referred to testing for CAD (Flotats et al. 2011; Saraste and Knuuti 2012). Usually this means that a second-line test is selectively performed in patients having an abnormal or equivocal result on the first-line test (Saraste and Knuuti 2012). An example of the potential utilization of selective hybrid imaging in clinical practice is given in Figure 2.

In 2006, Berman et al. proposed an approach in which symptomatic patients with an intermediate PTP of obstructive CAD and an equivocal result on coronary CTA are referred for MPI to further guide patient management (Berman et al. 2006). Later, Knuuti and Saraste in more detail described a diagnostic path in which patients with a suspicion of obstructive CAD on coronary CTA undergo non-invasive imaging of ischemia, while patients without obstructive stenoses on CTA do not undergo further testing, taking the advantage of the high NPV of coronary CTA (Knuuti and Saraste 2013). Conversely, Engbers et al. studied a large cohort of 5018 patients who first underwent stress SPECT MPI and CAC scoring (Engbers et al. 2017). If stress SPECT MPI was abnormal, additional rest SPECT MPI and coronary CTA, if feasible, were performed. The investigators found that about half of the patients could be discharged based on the stress SPECT MPI alone.

Both anatomic-first and functional-first sequential approaches may have their strengths and weaknesses related to the diagnostic accuracy and the detection of subclinical degrees of CAD, such as non-obstructive coronary atherosclerosis and coronary microvascular dysfunction. Owing to the high NPV but relatively low PPV of coronary CTA, the CTA-first approach might be a more appropriate diagnostic strategy in patients with a low–moderate PTP of obstructive CAD, while MPI-first strategy could make sense in patients with a higher PTP (Saraste and Knuuti 2012). Van Waardhuizen et al. systematically reviewed the existing literature on the cost-effectiveness of non-invasive imaging tests in symptomatic patients with suspected stable CAD (van Waardhuizen et al. 2016). Based on the evidence, they concluded that the optimal diagnostic imaging strategy for patients with a low or intermediate PTP is coronary CTA followed by stress echocardiography or SPECT MPI when necessary, while ICA is optimal for patients with a high PTP of obstructive CAD.

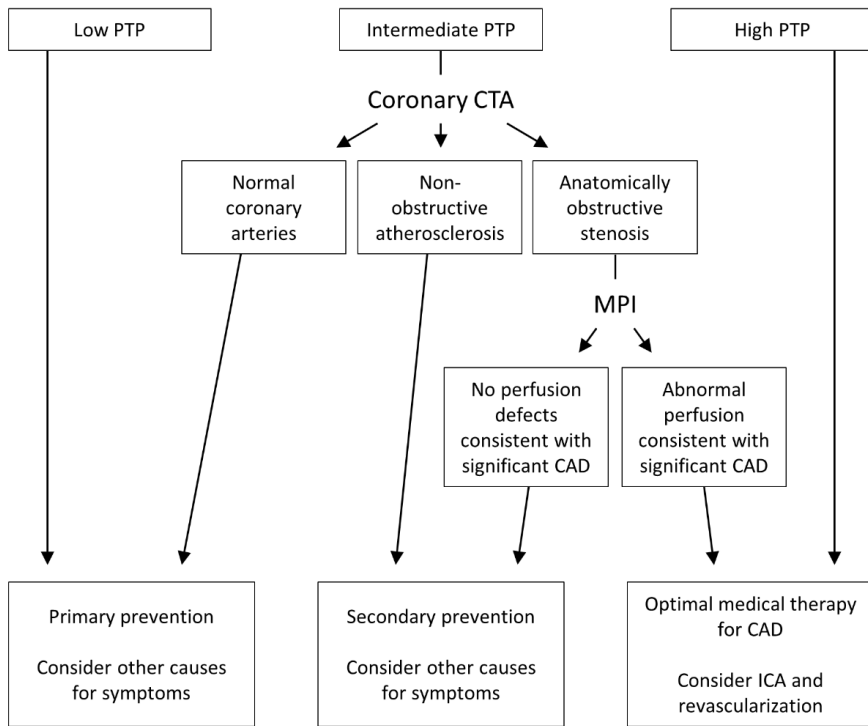


Figure 2 An example of the selective use of cardiac hybrid imaging in the diagnostic work-up of symptomatic patients with suspected obstructive coronary artery disease (CAD). The pre-test probability (PTP) of obstructive CAD can be estimated based on age, gender, and type of symptoms. Patients with intermediate PTP of obstructive CAD first undergo coronary computed tomography angiography (CTA), and only those showing an anatomically obstructive stenosis on CTA undergo further myocardial perfusion imaging (MPI). Patients having normal coronary arteries or non-obstructive coronary atherosclerosis on CTA, as well as patients having an anatomically obstructive stenosis but no corresponding perfusion defect on MPI, are targeted with preventive measures, and other causes for symptoms can be considered. An anatomical stenosis on coronary CTA and a corresponding stress perfusion defect on MPI suggest hemodynamically significant CAD. These patients should be offered with optimal medical therapy, and revascularization should be considered in case of high event risk (% ischemia LV) or persistent symptoms. CAD = coronary artery disease; CTA = computed tomography angiography; ICA = invasive coronary angiography; LV = left ventricle; MPI = myocardial perfusion imaging; PTP = pre-test probability.

2.5 Evaluation of patients with prior coronary artery disease

2.5.1 Testing strategies for symptomatic patients with prior known coronary artery disease

The previous chapters of this literature review have primarily focused on patients with suspected or recently diagnosed stable CAD. However, atherosclerosis and CAD have tendency to progress, and therefore, another challenge is to evaluate patients with prior known CAD who may have recurrent or worsening symptoms. These symptoms may appear as stable or unstable. The evaluation of unstable manifestations of CAD, such as acute myocardial infarction, usually requires invasive angiographic assessment, and is not further reviewed here.

Once the instability has been excluded, recurrent or worsening of symptoms in a patient with prior known CAD indicates the evaluation of the presence, extent, severity, and localization of inducible myocardial ischemia. The ischemia may result from the progression of atherosclerosis in native coronary arteries, but in patients with prior revascularization with PCI and/or CABG, the ischemia may also occur due to stent restenosis and/or graft stenosis or occlusion, respectively. In addition, patients with known CAD may potentially have several co-existing conditions that must be considered, such as myocardial scar due to previous infarction, LV dysfunction, presence of stents, bypass grafts, and collateral circulation, coronary microvascular dysfunction, mitral regurgitation, and cardiac arrhythmias. Both on the European and the American guidelines, either exercise ECG testing or stress imaging (with MPI or echocardiography) is recommended for the initial assessment of patients with known stable CAD and new, recurrent, or worsening symptoms, once the instability has been ruled out (Fihn et al. 2012; Montalescot et al. 2013). Repeat revascularization after CABG is a complex procedure and, if considered, usually requires invasive assessment of coronary anatomy in addition to the ischemia testing.

2.5.2 Coronary computed tomography angiography in patients with prior coronary artery disease

As previously reviewed, coronary CTA has a limited ability to assess the hemodynamic consequences of coronary stenoses. The positive predictive value is suboptimal; the specificity is deteriorated in the presence of increasing coronary calcification (Budoff et al. 2008; Meijboom, Meijs, et al. 2008; C.-C. Chen et al. 2011). Due to these factors, the use of coronary CTA for evaluation of patients with previously known obstructive CAD might be questionable (Fihn et al. 2012; Montalescot et al. 2013).

The evaluation of metallic coronary stents using coronary CTA is challenging due to blooming and beam-hardening artifacts (Wykrzykowska et al. 2010). The diagnostic accuracy and espe-

cially the NPV of CTA seem to be good in stents ≥ 3 mm in diameter, while the diagnostic accuracy is lower and the frequency of uninterpretable segments is higher among stents with < 3 mm diameter (Sheth et al. 2007; Pugliese et al. 2008; Wykrzykowska et al. 2010; Carrabba et al. 2010; Wuest et al. 2013). Coronary CTA might have a good diagnostic accuracy to detect obstruction in bioresorbable vascular scaffolds (Collet et al. 2017).

Over 90% of internal mammary artery grafts but only 50–60% of saphenous vein grafts are patent at 10 years after CABG surgery (Hillis et al. 2011). Coronary artery bypass grafts are a potential target for CTA imaging as the motion of grafts is relatively low and the diameter of venous grafts is relatively large; the evaluation of the distal anastomotic site may be more challenging (Mark et al. 2010). In addition, the metal clips that are used for the graft fixation may cause CTA image artifacts. In patients with internal mammary artery grafts, CTA imaging should cover the chest from the level of the clavicles to the diaphragm, potentially increasing the patient radiation dose (Mark et al. 2010). However, the evaluation of the patency of coronary artery bypass grafts seems to be highly accurate using CTA (Schroeder et al. 2008; Weustink et al. 2009). A sensitivity of 97% and a specificity of 95% for graft stenosis were detected in a pooled analysis, while the sensitivity and specificity for graft occlusion were 100% (Schroeder et al. 2008). Instead, the evaluation of native coronary arteries may be difficult using coronary CTA, as the patients with previous CABG usually have advanced coronary atherosclerosis, and the native vessels distal to the graft insertion tend to be small in diameter. Accordingly, the specificity is lower (around 75%) and the frequency of non-evaluable CTA findings is higher (around 20%) in the native coronary arteries of post-CABG patients (Schroeder et al. 2008). A follow-up study by Chow et al. in 250 patients demonstrated that the number of unprotected coronary territories (UCT) assessed by coronary CTA was an independent predictor of MACE in patients with prior CABG (Chow, Ahmed, et al. 2011).

2.5.3 Myocardial perfusion imaging and hybrid imaging in patients with prior coronary artery disease

Myocardial perfusion imaging (MPI) allows the assessment of the presence, extent, severity, and location of myocardial perfusion abnormalities. Rest-stress imaging permits the differentiation between reversible myocardial ischemia and myocardial infarction scars. In contrast to coronary CTA, the diagnostic accuracy of stress testing is generally similar in patients with and without known CAD (Fihn et al. 2012). The ESC guidelines on stable CAD suggest stress imaging (either nuclear, echocardiographic, or magnetic resonance) rather than exercise ECG testing for the evaluation of symptomatic patients with prior revascularization (Montalescot et al. 2013). These guidelines further suggest optimal medical therapy in previously revascularized patients showing $< 5\%$ ischemic myocardium at stress, while ICA is recommended for patients with $> 10\%$ ischemic myocardium.

Myocardial perfusion abnormalities on stress SPECT MPI seem to be prognostically important also in patients with previously known CAD (Lauer et al. 1998; Shaw et al. 2012). Moreover, non-perfusion markers such as ECG findings, wall motion abnormalities, post-stress LVEF, and transient ischemic dilation may provide prognostic information (Fihn et al. 2012). PET enables the absolute quantification of MBF, and thereby, allows the detection of global or balanced myocardial perfusion abnormalities that may be present in multivessel CAD (Kajander et al. 2011). However, the absolute quantification of MBF in an infarction scar using ^{15}O -water tracer may be problematic, at least in theory, because the blood flow is modelled in water-perfusible tissue only (Knaapen et al. 2006).

Cardiac hybrid imaging in patients with prior CAD has not been extensively studied. Theoretically, the integration of anatomy and perfusion might be helpful in the assessment of patients with previous PCI or CABG, as the current image fusion technology allows an accurate co-localization of a perfusion defect and the supplying coronary artery (Gaemperli et al. 2007; Matsuo et al. 2009). Myocardial perfusion abnormalities are known to be frequent in patients with previous CABG, even in the asymptomatic ones (Lauer et al. 1998). The information on vessel courses, stenoses, and patency of bypass grafts and stents would be potentially useful in the interpretation of these myocardial perfusion defects. A study by Kawai et al. in 204 patients with previous CABG showed that graft patency assessed by coronary CTA and myocardial ischemia detected by SPECT MPI provide incremental and complementary information on patient prognosis (Kawai et al. 2013).

3 AIMS OF THE STUDY

The aim of the present observational study is to evaluate the use of coronary CTA, PET myocardial perfusion imaging (MPI), and their combination in real-life symptomatic patients with suspected or known stable obstructive coronary artery disease (CAD). The objectives of the individual articles in this thesis are as follows:

1. To study the prognostic value of a hybrid imaging strategy with selective application of PET MPI after coronary CTA in patients with suspected CAD (Study I).
2. To evaluate how common is persistent renal dysfunction attributable to iodine contrast agent exposure in patients undergoing contrast enhanced coronary CTA for suspected CAD (Study II).
3. To validate the prognostic value of an integrated prognostic score derived from quantitative coronary CTA findings among patients with suspected CAD (Study III).
4. To study the relationship between coronary anatomy and myocardial perfusion in symptomatic patients with prior coronary artery bypass grafting using hybrid PET/CTA imaging (Study IV).

4 MATERIALS AND METHODS

4.1 General characteristics of Turku cardiac CTA registry

The materials used in the Studies I–IV of this thesis are based on Turku cardiac CTA registry that is a retrospective registry including all consecutive patients undergone cardiac CTA imaging at Turku PET Centre from 2006. Majority of the registry patients have undergone clinically indicated coronary CTA for suspected obstructive CAD (intermediate 15–85% PTP) as part of their clinical diagnostic workup. According to the local protocol, patients showing suspected obstructive CAD on coronary CTA undergo further PET myocardial perfusion imaging using ^{15}O -water tracer, usually in the same imaging session using a hybrid PET/CT scanner. For PET perfusion, stress-only imaging during adenosine-induced vasodilator stress is generally performed, but also rest images may be obtained in case of a suspected or known prior myocardial infarction. Contraindications for coronary CTA include severe renal dysfunction (eGFR <30 mL/min/1.73 m 2), a prior known severe reaction to iodine contrast media, notably irregular heart rhythm (e.g. persistent atrial fibrillation), insufficient patient co-operation or breath-hold capability, and pregnancy. In turn, contraindications for adenosine-stress PET MPI include second- or third-degree atrioventricular conduction block or sinus node disease without a functioning pacemaker, unstable bronchospastic pulmonary disease, untreated congestive heart failure, acute coronary syndrome, hypotension or uncontrolled hypertension, pregnancy, known hypersensitivity to adenosine, or any of the general contraindications for exercise stress testing including acute medical illness (Henzlova et al. 2016). Moreover, certain pharmacological agents (metformin, dipyridamole, and caffeine) may require a cessation before PET/CTA study.

Patient data have been retrospectively collected and recorded into the registry database. Information on baseline patient characteristics was manually collected from the electronic medical record system, including the study indication, referring department, age, gender, weight, height, conventional cardiovascular risk factors (previous or current smoking, prediabetes or diabetes, hypertension, dyslipidemia, and family history of CAD in first-degree relatives), symptoms (type of chest pain, dyspnea on exertion), possible previous test results (LVEF by echocardiography, ischemic ECG findings and stress capability by exercise testing, and laboratory blood test results), cardiovascular medication, prior myocardial infarction or coronary revascularization, atrial fibrillation, and presence of a cardiac pacemaker. The conventional cardiovascular risk factors were assessed based on clinically used criteria; specifically, prediabetes was defined as impaired fasting glucose (fasting plasma glucose 6.1–6.9 mmol/L), impaired glucose tolerance (2-hour plasma glucose 7.8–11.0 mmol/L in a 75 g oral glucose tolerance test), or blood hemoglobin A1c 6.0–6.4% (Canadian Diabetes Association Clinical Practice Guidelines Expert Committee, Goldenberg, and Punthakee 2013). Procedural information included the administered premedication (beta blocker, nitrate), iodine contrast volume and concentration, X-ray tube voltage, CT

dose-length product, injected PET tracer radioactivity, and heart rate and blood pressure during adenosine stress.

Each coronary CTA and PET study was originally analyzed and reported in a standardized manner for clinical purposes by at least one trained physician. The following coronary CTA parameters were recorded according to the standardized coronary artery system: presence and composition of a coronary plaque, degree of diameter luminal stenosis, presence of an image artifact, coronary dominance, and overall image quality (Leipsic et al. 2014). Total and per-vessel Agatston coronary calcium scores were recorded if available. Standardized segmental (17-segment system) and territorial (LAD, LCX, and RCA) quantitative MBF values (mL/g/min) were recorded (Cerqueira et al. 2002). In addition, perfusion in each of the three myocardial territories was graded (normal, mildly reduced, moderately reduced, or severely reduced) based on the presence of local PET perfusion defects and the individual coronary anatomy on CTA and/or hybrid images. In Studies III and IV, the imaging data were systematically re-analyzed for scientific purposes by the investigators.

Downstream referral to ICA, PCI, or CABG within 6 months after coronary CTA were also recorded, as well as laboratory blood test results and changes in medication after the PET/CTA imaging. Data on the patient characteristics, imaging findings, and downstream referral were retrospectively collected by the investigators using the local imaging database, standardized imaging reports, and patient electronic medical records. The follow-up data on all-cause mortality, cardiac mortality, MI, and UAP were collected using the registries of the Centre for Clinical Informatics of the Turku University Hospital, the Finnish National Institute for Health and Welfare, and the Statistics Finland. The adverse events were manually confirmed by the investigators using electronic medical records. The Ethics Committee of the Hospital District of Southwest Finland approved the study protocol and waived the need for an individual written informed consent. In addition, permissions to collect patient data were gained from the Turku University Hospital, the Finnish National Institute for Health and Welfare, and the Statistics Finland. The study complies with the Declaration of Helsinki.

4.2 Prognostic value of coronary CTA with selective PET perfusion imaging (Study I): Materials and methods

4.2.1 Study design and patient population in Study I

The Study I is a retrospective study including 957 consecutive symptomatic patients who had been referred to a clinically indicated coronary CTA for suspected CAD at the Turku University Hospital PET Centre during 2007–2011. The patients in the study I were identified from the Turku cardiac CTA registry. According to the local routine, patients first underwent coronary CTA. Immediately after CTA, the attending physician performed an initial evaluation of the CTA scan to

decide whether a PET perfusion study was needed to evaluate the hemodynamic significance of a coronary stenosis. If obstructive CAD was excluded by coronary CTA, no further testing was performed. In the presence of suspected obstructive CAD by CTA, a PET myocardial perfusion study using ^{15}O -water was performed during adenosine vasodilator stress. The patients had an intermediate pre-test probability (15–85%) of obstructive CAD assessed by the referring cardiologist. Patients with previous coronary revascularization or obstructive CAD documented as $>50\%$ diameter stenosis by ICA, as well as patients undergoing PET/CT to reveal the etiology of cardiomyopathy or heart failure, were not included. Fifty-two of the 957 patients were excluded due to non-diagnostic imaging results (i.e. failed CTA or PET study, or uninterpretable image quality). Forty-one patients were excluded due to failure to adhere to the local imaging protocol, i.e. PET study was not performed despite abnormal coronary CTA due to variety of reasons, such as contraindication to pharmacological stress or direct referral to invasive angiography after the CTA. As a result, the final prognostic analysis included 864 patients.

4.2.2 Data acquisition and analysis in Study I

Coronary CTA and PET scans were performed with a 64-row hybrid PET/CT scanner (GE Discovery VCT or GE D690, General Electric Medical Systems, Waukesha, Wisconsin, US). Before CTA, intravenous metoprolol (0–30 mg), if needed, was administered to achieve a target heart rate of <60 bpm. Isosorbide dinitrate aerosol (1.25 mg) or sublingual nitrate (800 μg) was also administered for coronary vasodilation. Agatston coronary artery calcium score was measured before CTA in most (78%) patients. Low-osmolal iodine contrast agents were administered during CTA, with contrast volume adjusted for body weight. The CT collimation was 64×0.625 mm, gantry rotation time 350 ms, tube current 600–750 mA, and tube voltage 100–120 kV. Prospective ECG-triggering for CTA acquisition was applied whenever feasible. A coronary CTA scan was immediately evaluated by the attending physician, and $\geq 50\%$ diameter stenosis by visual CTA analysis was used as a criterion for suspected obstructive stenosis. If indicated by the initial interpretation of CTA findings and in the absence of contraindications, dynamic quantitative PET perfusion study was carried out during adenosine vasodilator stress (140 $\mu\text{g}/\text{kg}/\text{min}$) using a hybrid PET/CT device and ^{15}O -water tracer. The patients were instructed to abstain from caffeine for 24 hours before the study. In some patients, perfusion imaging was performed in the following days or weeks due to logistic reasons or caffeine use.

The presence, extent, and severity of coronary atherosclerosis and stenoses on coronary CTA were evaluated in all patients, according to the 17-segment vessel system and using the GE ADW Workstation (General Electric, Piscataway, New Jersey, US) (Austen et al. 1975). According to the most severe CTA stenosis, the patients were first classified into those without significant CAD by CTA, and those with suspected obstructive CAD requiring further PET perfusion imaging. The PET perfusion data were quantitatively analyzed according to the standardized 17 myocardial segments using the Carimas software (Turku PET Centre, Turku, Finland) (Cerqueira et al. 2002).

Absolute myocardial stress perfusion ≤ 2.4 mL/g/min at least in 1 of the 17 myocardial segments was considered abnormal (Kajander et al. 2010). PET/CT fusion images were created, when indicated, using the GE IQfusion software (General Electric, Piscataway, New Jersey, US).

Data on coronary CTA and PET perfusion findings, as well as other patient characteristics, were retrospectively collected using the imaging database, standardized reports, and electronic medical records. The follow-up data on all-cause death, myocardial infarction (MI), and unstable angina pectoris (UAP) were recorded using the registries of the Finnish National Institute for Health and Welfare and the Centre for Clinical Informatics of the Turku University Hospital. The events identified from the registries were confirmed by investigators using electronic medical records, according to the criteria of the ESC (Hamm et al. 2011). The individual follow-up period ranged from the CTA study until the end of 2013. Information on possible early (i.e. within 6 months after CTA) invasive angiography or revascularization was collected, but these were not included as adverse events in the survival analysis.

4.2.3 Statistical methods in Study I

Continuous variables are expressed as mean \pm standard deviation (SD) or median with corresponding 25th–75th percentiles; categorical variables are shown as percentages. Independent-samples Mann–Whitney U test or Kruskal–Wallis test was used to compare continuous variables, and 2-sided Pearson chi-square test or Fisher’s exact test was used for categorical variables. Annual event rates (all-cause mortality; and the composite of mortality, MI, or UAP) were compared using Poisson regression analysis. P-values < 0.05 were considered statistically significant. Kaplan–Meier curves were created, and pooled log-rank tests conducted (Mantel–Cox). Cox’s proportional hazards model was applied to identify the predictors of adverse events; covariates with p-values ≤ 0.10 on univariable Cox’s regression analysis were included in the multivariable analysis. Specifically, the PET/CTA findings, age, gender, and other conventional cardiovascular risk factors were included in the univariable analysis; notably, coronary calcium score, exercise ECG test result, and LVEF by echocardiography were not included in the model, as not all patients underwent these test modalities. The statistical analyses were conducted with software IBM SPSS Statistics for Windows (version 22; IBM Corporation, Armonk, New York, US).

4.3 Persistent renal dysfunction after coronary computed tomography angiography (Study II): Materials and methods

4.3.1 Study design and patient population in Study II

The study II is a retrospective study including 957 consecutive symptomatic outpatients, same as in the Study I, who had undergone clinically indicated contrast enhanced coronary CTA for suspected CAD at the Turku University Hospital PET Centre during 2007–2011. The patients in the study II were identified from the Turku cardiac CTA registry, and according to the local routine practice, patients showing suspected obstructive stenosis on CTA also underwent PET MPI, if applicable. The patients had an intermediate PTP (15–85%) of obstructive CAD assessed by the referring cardiologist; patients with previous coronary revascularization or obstructive CAD documented by ICA were not included. From the cohort of 957 patients, those who had paired plasma creatinine measurements available (i.e. both before and after the coronary CTA) were selected to the analysis in the Study II (n=402).

4.3.2 Data acquisition and analysis in Study II

Non-ionic low-osmolal iodine contrast agents iohexol, iomeprol, or iobitridol were intravenously administered during coronary CTA scans. Concentration of the contrast agents was 350–400 mg of iodine per mL, and the administered contrast volume was adjusted for body weight. At the visit to the imaging center, all patients received 500 mL of intravenously administered physiological saline (NaCl 0.9%) as a 1-hour infusion during examinations. Patients considered to have an elevated risk of kidney injury per attending physician's discretion received an additional 500 mL infusion of intravenous saline before the CTA scan. Intravenous metoprolol, if needed, and short-acting nitrate were administered as in the Study I. Patients were instructed to discontinue oral metformin 24 hours before the examination and to continue it 2 days after the scan; other medications were taken as normal. The CTA scans were performed using a 64-slice multidetector CT scanner (GE Discovery VCT or GE D690, General Electric Medical Systems, Waukesha, Wisconsin, US).

Data for the Study II were retrospectively collected as part of the Turku cardiac CTA registry. According to the local protocol, patients routinely underwent testing for plasma creatinine concentration within 3 months before a coronary CTA scan, and the most recent measurement preceding the scan was defined as the pre-CTA plasma creatinine concentration in this study. Instead, plasma creatinine was not routinely assessed after the CTA. However, if plasma creatinine concentration was measured for any reason within the period from 2 weeks to 6 months after CTA, the most recent value during this period was collected and considered as the post-CTA plasma

creatinine concentration in this study. Plasma creatinine concentration was defined from the venous lithium-heparin plasma sample using the photometric enzymatic method. The eGFR was derived from the plasma creatinine concentration using the CKD-EPI equation (Levey et al. 2009). Estimated GFR values ≥ 90 (mL/min/1.73 m²) were considered normal, 60–89 mildly reduced, and 30–59 moderately reduced. All-cause mortality within 6 months after CTA was also assessed.

The intra-individual change in plasma creatinine level was assessed in patients who had both the pre-CTA and post-CTA measurements available. Patients showing a relative $\geq 25\%$ or an absolute ≥ 44.2 $\mu\text{mol/L}$ increase in plasma creatinine concentration were evaluated in more detail using electronic medical records: the individual plasma creatinine measurements, if available, were tracked for a longer time period to assess the reversibility of plasma creatinine level impairment, and plasma creatinine level was considered normalized if returning to the level lower than 25% above the baseline level in the follow-up. In addition, alternative explanations for creatinine level increase, including comorbidities and medical therapies, were evaluated. Finally, a consensus was reached by the authors to identify patients having a persistent increase in plasma creatinine level in the absence of another explanation for the increase than the contrast agent exposure during coronary CTA. The cut-off point of 25% or 44.2 $\mu\text{mol/L}$ is a commonly used definition for contrast induced nephropathy (CIN), although we applied a different time window to assess persistent renal dysfunction (Morcos, Thomsen, and Webb 1999). In addition to the creatinine concentration, the individual change in eGFR was also analyzed.

4.3.3 Statistical methods in Study II

Continuous variables are expressed as mean \pm standard deviation (SD) or median; categorical variables are expressed as percentages. To test the differences in patient characteristics between patient subgroups, the independent-samples Mann-Whitney U test was used for continuous variables, and 2-sided Pearson chi-square test or 2-sided Fisher's exact test were used for categorical variables. Related-samples Wilcoxon signed rank test was used to test median changes in creatinine level and eGFR between the paired measurements. IBM SPSS Statistics for Windows (version 22; IBM Corporation, Armonk, NY, US) was used to conduct statistical analyses. P-values < 0.05 were considered statistically significant.

4.4 Coronary computed tomography angiography -derived risk score in predicting cardiac events (Study III): Materials and methods

4.4.1 Study design and patient population in Study III

The study III is a retrospective study including 922 consecutive symptomatic patients with an intermediate PTP of obstructive CAD who had been referred to a clinically indicated coronary CTA for suspected CAD at the Turku University Hospital PET Centre during 2007–2011. The patients in the Study III were identified from the Turku cardiac CTA registry, and patients with suspected obstructive CAD on CTA also underwent PET MPI according to the local routine. Among the cohort of 922 patients, 261 had normal coronary arteries on visual CTA assessment, and in 153 patients the quantitative CTA analysis was not feasible (due to image quality, step-artefacts, or technical factors related to image acquisition or data storage). After exclusion of those patients, the final study cohort consisted of 508 patients having some degree of coronary atherosclerosis and with sufficient CTA quality, and these patients underwent quantitative CTA analysis. An individual integrated risk score was derived from the quantitative CTA findings. The prognostic value of the quantitative CTA parameters and the integrated CTA risk score was analyzed.

4.4.2 Data acquisition and analysis in Study III

Coronary CTA scans were performed with a 64-row hybrid PET/CT scanner (GE Discovery VCT or GE D690, General Electric Medical Systems, Waukesha, Wisconsin, US). Before CTA, 0–30 mg of metoprolol was intravenously administered to achieve a target heart rate of <60 bpm. Isosorbide dinitrate aerosol (1.25 mg) or sublingual nitrate (800 µg) was also administered for coronary vasodilation. Low-osmolal iodine contrast agents were administered during CTA, with contrast volume adjusted for body weight. The CT collimation was 64×0.625 mm, gantry rotation time 350 ms, tube current 600–750 mA, and voltage 100–120 kV. Prospective ECG-triggering for CTA acquisition was applied whenever feasible.

Coronary CTA data of the final study cohort were analyzed using a quantification software QAngio CT Research Edition (version 1.3.6; Medis Medical Imaging Systems, Leiden, the Netherlands), as previously described in detail (de Graaf et al. 2014). Branches of the coronary artery tree were extracted from the CTA data using an automated algorithm and automatically labelled according to the American Heart Association 17-segment model (Austen et al. 1975). Multiplanar reformations (MPR) were created based on this coronary tree, and lumen and vessel wall were automatically segmented from the MPR images. All coronary artery lesions were detected by the algorithm and confirmed by an experienced observer.

The location, stenosis severity, and plaque composition of each coronary lesion were automatically identified by the software. Lesions in the left main artery (LM), proximal LAD, proximal RCA, or proximal LCX were defined as proximal coronary artery lesions. Coronary stenosis severity was defined as any atherosclerotic plaque ($\geq 30\%$ stenosis), obstructive lesion ($\geq 50\%$ stenosis, or $\geq 30\%$ stenosis in LM), or severe lesion ($\geq 70\%$ stenosis). Coronary plaque composition was categorized as non-calcified, calcified, or partially calcified plaque using an automatic plaque characterization algorithm as previously described (de Graaf et al. 2013, 2014). Coronary artery dominance was visually assessed; chronic total occlusions were also visually identified and thereafter quantified using a dedicated algorithm.

The integrated CTA risk score was derived from the quantitative CTA findings, as previously reported (de Graaf et al. 2014). The risk score in each coronary artery segment was based on the presence and location of a plaque, stenosis severity, and plaque composition, as demonstrated in Figure 3. Each segment had a segment weight factor based on the Leaman score, and different weight factors were used for left and right dominant coronary artery trees (Leaman et al. 1981). Obstructive atherosclerotic lesions had a stenosis weight factor 1.4, while non-obstructive lesions had a weight factor of 1.0, based on a previous meta-analysis (Bamberg et al. 2011). Segments without any atherosclerotic plaque had a score of zero. Plaque weight factors were 1.2 for calcified, 1.6 for partially calcified, and 1.7 for non-calcified plaques, derived from a previous study (Gaemperli et al. 2008). Finally, the segment weight factor, stenosis weight factor, and plaque weight factor in each coronary artery segment were multiplied to get an integrated segmental score, and thereafter, the integrated segmental scores were summed to get a total per-patient CTA risk score.

The follow-up data on adverse events, including all-cause death, MI, and UAP, were recorded using the registries of the Finnish National Institute for Health and Welfare, and the Centre for Clinical Informatics of the Turku University Hospital. The events identified from the registries were confirmed by the investigators using electronic medical records, according to the criteria of the ESC (Hamm et al. 2011). The individual follow-up period ranged from the CTA study until the end of 2013. Treatment decisions after the coronary CTA were based on the clinical judgment of the referring physician.

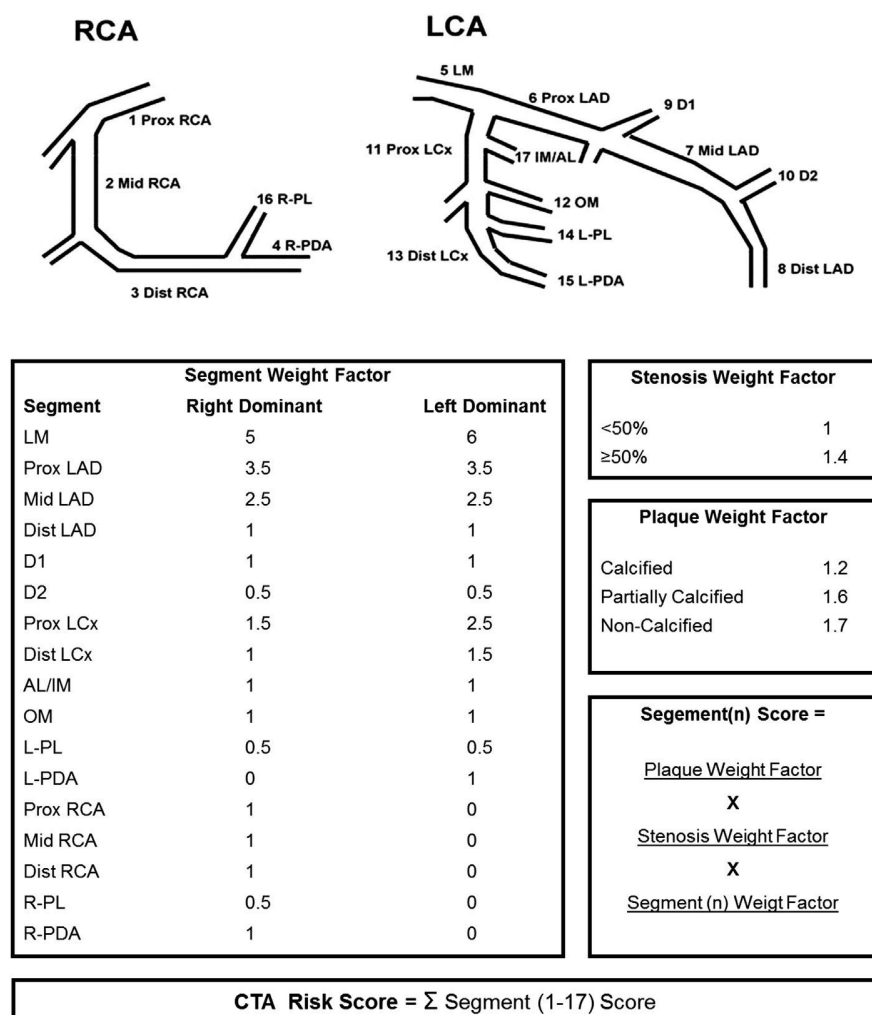


Figure 3 The CTA risk score is calculated by the summation of the individual segment scores, that are obtained by multiplying the segment weight factor, the stenosis weight factor, and the plaque weight factor. AL = anterolateral segment; CTA = computed tomography angiography; D1 = diagonal 1; D2 = diagonal 2; Dist = distal; IM = intermediate; LAD = left anterior descending artery; LCA = left coronary artery; LCx = left circumflex artery; LM = left main; L-PDA = left posterior descending artery; L-PL = left posterolateral segment; OM = obtuse marginal segment; Prox = proximal; RCA = right coronary artery; R-PDA = right posterior descending artery; R-PL = right posterolateral segment. (Originally published in de Graaf et al. *Am J Cardiol* 2014;113:1947–55. Reprinted by permission from the Elsevier.)

4.4.3 Statistical methods in Study III

Continuous variables are presented as mean \pm standard deviation (SD); 95% confidence intervals (CI) are presented in parentheses when appropriate. Normally distributed continuous variables were compared using the independent Student's T-test and non-normally distributed variables with the non-parametric Mann–Whitney U test. Categorical variables are presented as frequencies and percentages, and were compared using the Chi-square test. Baseline clinical characteristics and quantitative CTA variables were compared between patients with and without adverse events during follow-up. Based on the CTA risk score, patients were classified into lowest, middle, and highest risk score tertiles. The number of adverse events was calculated, and survival analysis was performed for the risk tertiles. Adverse event rates were estimated by the Kaplan–Meier method. Univariable and multivariable Cox proportional hazard models were used to calculate the hazard ratios (HR); variables with a p-value <0.1 in univariable analyses were included into the multivariable analysis. Two-tailed p-values <0.05 were considered statistically significant. Statistical analyses were performed using software IBM SPSS Statistics (version 22; IBM Corporation, Armonk, New York, US).

4.5 Hybrid PET/CTA imaging in patients with previous coronary artery bypass grafting (Study IV): Materials and methods

4.5.1 Study design and patient population in Study IV

The Study IV is a retrospective study of 36 consecutive clinical patients who had been referred to hybrid PET/CTA imaging due to new, recurrent, or worsening symptoms after coronary artery bypass grafting (CABG). The patients were identified from the Turku cardiac CTA registry. According to the local routine, all patients underwent both coronary CTA and stress PET MPI at the Turku University Hospital PET Centre during 2010–2017. Stress PET MPI with ^{15}O -water tracer was performed during adenosine vasodilator stress, and additionally, some patients also underwent rest PET MPI due to prior myocardial infarction. All CTA and PET studies were clinically indicated and first interpreted by the reading physician; for scientific purposes, the imaging data were systematically and uniformly re-analyzed in this study.

4.5.2 Data acquisition and analysis in Study IV

Coronary CTA and PET scans were performed with a 64-row hybrid PET/CT scanner (GE Discovery VCT or GE D690, General Electric Medical Systems, Waukesha, Wisconsin, US). Intravenous metoprolol (0–30 mg) was administered before CTA to achieve a target heart rate <60 bpm. Isosorbide dinitrate aerosol (1.25 mg) was given for coronary vasodilation. Coronary CTA

was performed using low-osmolal iodine contrast agents with contrast volume adjusted for body weight. The CT collimation was 64×0.625 mm, gantry rotation time 350 ms, tube current 600–750 mA, and tube voltage 100–120 kV. The CTA acquisition was planned to cover the chest from the level of the clavicles to the diaphragm to allow the visualization of internal mammary artery grafts. Prospective ECG-triggering for CTA acquisition was applied whenever feasible. After the CTA, a dynamic quantitative PET perfusion study was performed during adenosine vasodilator stress ($140 \mu\text{g}/\text{kg}/\text{min}$) using ^{15}O -water tracer. The patients were instructed to abstain from caffeine and discontinue oral metformin for 24 hours before the PET/CTA study.

Coronary CTA data were retrospectively analyzed on trans-axial images and multiplanar reformations using the Reformat software by GE (ADW 4.4 Workstation, General Electric Medical Systems, Waukesha, Wisconsin, US) and the 18-segment system according to the Society of Cardiovascular Computed Tomography (Leipsic et al. 2014). Each native coronary artery segment and bypass graft were assessed for interpretability, presence and type of plaque (non-calcified, predominantly calcified, mixed), and degree of stenosis (normal, $<30\%$, $30\text{--}49\%$, $50\text{--}69\%$, $\geq 70\%$, total occlusion) without information on myocardial perfusion. A diameter stenosis $\geq 50\%$ on CTA was considered significant. A native coronary segment or a bypass graft was interpreted as non-evaluable if the segment/graft was not fully covered on CTA, if there was an artifact impeding the analysis, or if the degree of stenosis could not be evaluated due to small vessel diameter (<1.5 mm).

The individual coronary artery tree on CTA was divided into three territories according to the previous studies: (1) left anterior descending artery (LAD) with diagonal branches, (2) left circumflex artery (LCX) with intermediate and marginal branches, and (3) posterior descending artery (PDA), that is an artery running in the posterior interventricular sulcus and supplied by either right coronary artery (RCA) or LCX, depending on the coronary tree dominance (Chow, Ahmed, et al. 2011). Each coronary territory was classified as grafted or non-grafted, depending on the prior CABG. A coronary territory was interpreted as unprotected if (1) there was a significant stenosis in the native artery distal to the graft anastomosis, or (2) there were significant stenoses both in a native artery and its graft, or (3) there was a significant stenosis in a non-grafted native coronary artery (Chow, Ahmed, et al. 2011). A coronary territory was designated as non-evaluable if the UCT status could not be derived due to presence of non-evaluable segments/grafts.

Stress PET perfusion data were quantitatively analyzed according to the standard 17-segment model proposed by the American Heart Association (Austen et al. 1975) using Carimas software (version 2.9, Turku PET Centre, Turku, Finland). Hybrid PET/CTA fusion images were generated from CTA data and stress PET perfusion data using the validated CardIQ Fusion software package (ADW 4.4 Workstation, General Electric Medical Systems, Waukesha, Wisconsin, US) (Gaemperli et al. 2007). Similarly as with CTA, left ventricular myocardium was divided into three territories (i.e. LAD, LCX, and PDA) according to the individual coronary tree anatomy on PET/CTA fusion images. In each territory, stress perfusion was interpreted as normal (≥ 2.3 mL/g/min), mildly reduced (≥ 2.0 and < 2.3 mL/g/min), moderately reduced (≥ 1.5 and < 2.0

mL/g/min), or severely reduced (<1.5 mL/g/min), based on the presence of perfusion defects corresponding to a size of ≥ 1 myocardial segment (Danad, Uusitalo, et al. 2014). Based on the fusion images, PET perfusion defects were further classified into two groups: (1) defects restricted to myocardial areas supplied by native branches (i.e. proximal to the graft insertion), and (2) defects involving myocardial areas supplied by a graft (i.e. distal to graft insertion).

4.5.3 Statistical methods in Study IV

Continuous variables are shown as mean \pm standard deviation (SD) or median with corresponding 25th–75th percentiles. Categorical variables are shown as percentages. Two-sided Pearson chi-square test or Fisher's exact test was used to compare categorical variables. The statistical analysis was conducted with software IBM SPSS Statistics for Windows (version 23.0, IBM Corporation, Armonk, New York, US).

5 RESULTS

5.1 Prognostic value of coronary CTA with selective PET perfusion imaging (Study I): Results

5.1.1 General patient characteristics and imaging findings in Study I

Patient basic characteristics are shown in Table 3. After exclusion of patients with non-diagnostic imaging results or non-adherence to the sequential imaging protocol, 864 patients remained in the prognostic analysis. The effective radiation dose was 8.2 ± 4.0 mSv from coronary CTA and 0.97 ± 0.11 mSv from PET perfusion imaging. The median Agatston CAC score was 26, with 25th–75th percentiles 0–255 (available for 675 patients). 23% presented with typical angina pectoris, 65% with atypical angina pectoris, non-anginal chest pain, or dyspnea on exertion, and the rest with other symptoms.

Table 3 Patient basic characteristics in Studies I–IV.

Variable	Study I	Study II	Study III	Study IV
Number of patients	n = 864	n = 402	n = 508	n = 36
Age (mean \pm SD), years	61 \pm 9	63 \pm 9	63 \pm 9	67 \pm 9
Male gender, %	45	49	54	81
Risk factors for CAD				
Current smoking, %	13	13	14	11
Previous smoking, %	20	22	n/a	36
Prediabetes, %	17	19	n/a	8
Diabetes, %	14	21	18	31
Hypertension, %	54	61	78	75
Dyslipidemia, %	62	65	73	89
Medication				
Beta blocker, %	48	55	58	86
Lipid lowering drug, %	43	51	58	92
Antiplatelet drug, %	55	60	69	75
Anticoagulant, %	6	5	n/a	25
Long-acting nitrate, %	9	11	15	36
Diuretic, %	18	25	25	39
ACE inhibitor, %	19	22	25	47
ARB, %	15	20	21	17
Calcium channel blocker, %	14	18	20	22
Antiarrhythmic agent, %	2	2	n/a	3

Abbreviations: ACE = angiotensin-converting enzyme; ARB = angiotensin receptor blocker; CAD = coronary artery disease; SD = standard deviation.

Coronary CTA alone was considered sufficient to exclude obstructive CAD in 462 patients (53% of 864) (Figure 4). In these patients, CTA was either normal (n=260) or showing non-obstructive atherosclerosis (n=202). Instead, 402 patients (47%) had coronary CTA findings suggestive of obstructive CAD, and therefore, underwent quantitative stress PET perfusion imaging. PET imaging revealed reduced myocardial perfusion in 207 (51%) patients, while 195 patients (49%) had a normal perfusion study.

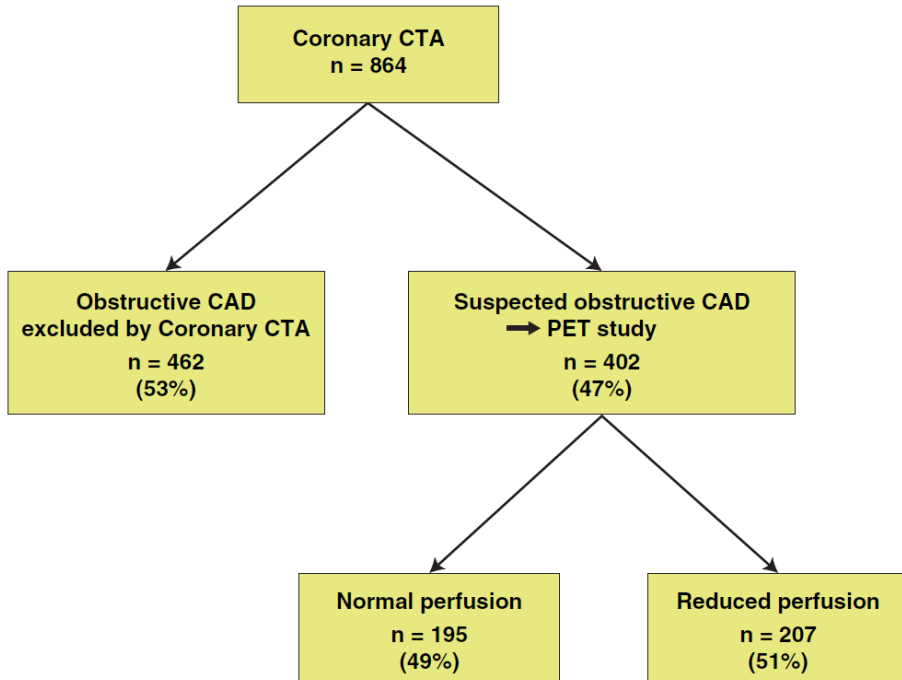


Figure 4 Hybrid imaging strategy with the selective use of PET perfusion imaging after coronary CTA. Coronary CTA alone was considered sufficient to exclude obstructive CAD in about half of the patients. The remaining patients with a suspected obstructive stenosis underwent PET perfusion imaging to study the hemodynamic significance of the stenosis. CAD = coronary artery disease; CTA = computed tomography angiography; PET = positron emission tomography. (Originally published in Maaniitty et al. *JACC Cardiovasc Imaging* 2017;10:1361–70. Reprinted by permission from the Elsevier.)

5.1.2 Prognosis in patients undergoing coronary CTA with selective PET perfusion imaging

The follow-up time was median 3.6 years (25th–75th percentile: 2.7–4.8 years), during which 31 adverse events (AE) occurred including 16 deaths, 10 MI, and 5 UAP. Two additional deaths occurred in patients with an earlier non-fatal event. The annual rate of all combined AE was 0.95% and the annual rate of all-cause mortality was 0.54%.

In patients showing normal coronary arteries on coronary CTA ($n=260$), there were 3 deaths and 1 MI; the combined annual rate of AE was 0.42% and the annual rate of all-cause mortality was 0.31% (Figure 5). In 202 patients with non-obstructive atherosclerosis, there were 3 deaths; the annual rates of AE and all-cause mortality were both 0.42%. There was no statistically significant difference in the occurrence of AE ($p=0.99$) or deaths ($p=0.71$) between patients with non-obstructive atherosclerosis and normal coronary arteries.

There were 12 deaths, 9 MI, and 5 UAP in the 402 patients who presented with suspected obstructive CAD on CTA and thus underwent subsequent PET perfusion imaging. Among these patients, the annual combined AE rate was significantly higher than in those 462 patients who had obstructive CAD excluded by CTA alone (1.50 vs. 0.42 %, $p=0.003$), but the annual mortality rates were not significantly different (0.73 vs. 0.36 %, $p=0.15$).

Out of the 402 patients with suspected CAD on coronary CTA, 207 (51%) patients had myocardial ischemia on the PET study, and among these patients there were 9 deaths, 8 MI, and 5 UAP. Instead, among patients with normal PET perfusion ($n=195$) there were only 3 deaths and 1 MI. The annual rate of AE was 5-fold in patients with abnormal perfusion compared to patients with a normal PET perfusion study (2.5 vs. 0.50 %, $p=0.004$). The annual rates of all-cause mortality in patients with reduced perfusion and normal perfusion were 1.07% and 0.38%, respectively ($p=0.12$). The AE and mortality rates were comparable between patients with suspected obstructive coronary stenosis but normal PET perfusion, and patients in whom obstructive CAD was excluded by CTA alone (0.50 vs. 0.42 %, $p=0.77$ for AEs; and 0.38 vs 0.36 %, $p=0.94$, for mortality).

None of the patients with normal CTA, 3% with non-obstructive CTA finding, 8% with normal perfusion, and 55% of patients with reduced perfusion underwent ICA within 6 months following CTA. Finally, 97 (11%) of the total 864 patients underwent revascularization within 6 months, while 42% of the patients with reduced perfusion by PET underwent early revascularization. Among the patients with reduced perfusion, there were not statistically significant differences in the annual rates of AE (2.1 vs. 2.8 %, $p=0.57$) or all-cause mortality (0.52 vs. 1.5 %, $p=0.17$) between revascularized or non-revascularized patients. Therefore, patients with or without early revascularization were pooled together for prognostic analyses.

On univariable analysis using Cox's proportional hazards model, increasing age and abnormal PET perfusion were statistically significant predictors of AE, while male gender and (pre-) diabetes were nearly significant ($p \leq 0.10$) predictors. These variables were included in the multivariable Cox regression analysis, on which increasing age (HR=1.05 per year, 95% CI: 1.00–1.10; $p=0.04$) and abnormal perfusion (HR=3.62 vs. normal CTA, 95% CI: 1.08–12.15; $p=0.04$) were found to be independent predictors of AE.

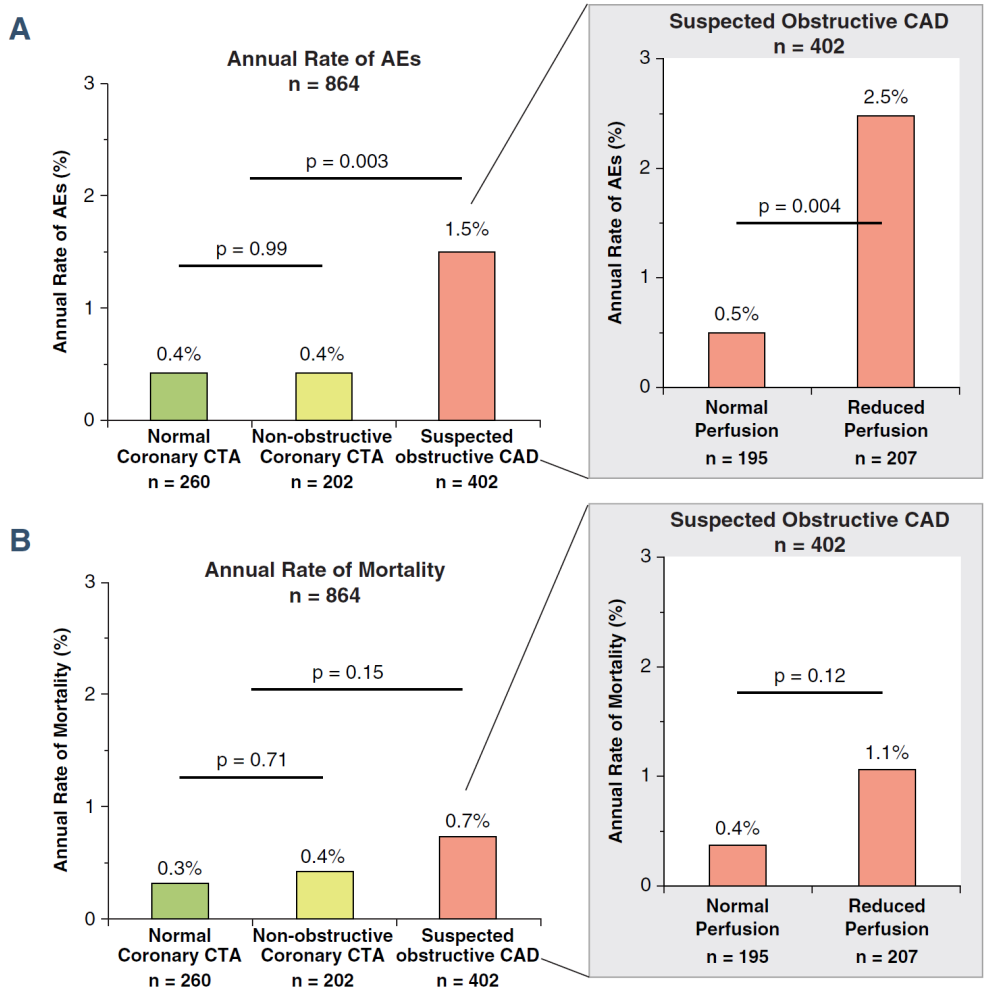


Figure 5 The annual rates of (A) adverse events and (B) all-cause mortality according to the hybrid imaging findings. AEs = adverse events; CAD = coronary artery disease; CTA = computed tomography angiography. (Originally published in Maaniitty et al. *JACC Cardiovasc Imaging* 2017;10:1361–70. Reprinted by permission from the Elsevier.)

5.2 Persistent renal dysfunction after coronary computed tomography angiography (Study II): Results

5.2.1 General patient characteristics in Study II

Patient basic characteristics are shown in Table 3. The total cohort of 957 consecutive patients undergoing coronary CTA received mean 84.8 ± 10.7 mL (ranging from 48 to 155 mL) of intravenous iodine contrast agent, and the effective radiation dose from CTA was 8.2 ± 4.0 mSv. A result of the pre-CTA plasma creatinine measurement (mean 74.8 ± 14.7 $\mu\text{mol/L}$) was available for 919 patients (96%), while paired (i.e. pre-CTA and post-CTA) creatinine measurements were found in 402 (42%) patients. The pre-CTA plasma creatinine level was comparable between the selected group of 402 patients and the rest of the patient population, but the 402 patients with paired creatinine measurements were older and had higher prevalence of diabetes, hypertension, and obstructive CAD on CTA, and were more frequently taking blood pressure-lowering, lipid-lowering, and antiplatelet medication. The 402 patients received mean 86.4 ± 10.3 mL of contrast medium, yielding mean 31.2 ± 31 grams of iodine administered. Obstructive CAD on CTA was detected in 46% of the 402 patients, while 18% underwent PCI within 6 months following CTA. Two of the 957 study patients died during the 6-month follow-up after coronary CTA, with no evidence of preceding renal dysfunction.

5.2.2 Changes in creatinine concentration and renal function after contrast agent exposure

Pre-CTA plasma creatinine concentration was measured median 6 days before the coronary CTA (ranging from 0 to 91 days), while the post-CTA level was measured median 99 days after the CTA (ranging from 15 to 184 days), yielding a median of 113 days between the two measurements. In 402 patients, the mean pre-CTA plasma creatinine concentration was 75.8 ± 16.0 $\mu\text{mol/L}$ (ranging from 37 to 142 $\mu\text{mol/L}$) and the post-CTA concentration was 75.7 ± 16.4 $\mu\text{mol/L}$ (ranging from 32 to 137 $\mu\text{mol/L}$). The mean absolute change in plasma creatinine level between pre- and post-CTA measurements was -0.14 ± 8.5 $\mu\text{mol/L}$ ($p=0.63$ for median change); the relative change in creatinine level ranged from -37% to +50%.

In 402 patients, the eGFR before CTA was 84 ± 15 (ranging from 35 to 130) mL/min/1.73 m², and the eGFR after CTA was 84 ± 15 (ranging from 37 to 135) mL/min/1.73 m². There was no significant difference in eGFR between pre- and post-CTA measurements (median change 0 mL/min/1.73 m²; $p=0.67$). According to the baseline eGFR, 37% of patients had normal, 56% had mildly reduced, and 7% had moderately reduced baseline renal function (Figure 6). The post-

CTA measured eGFR indicated normal renal function in 37%, mildly reduced in 55%, and moderately reduced renal function in 8% of patients. Both increases and decreases in individual eGFR values, compared to the baseline, were detected.

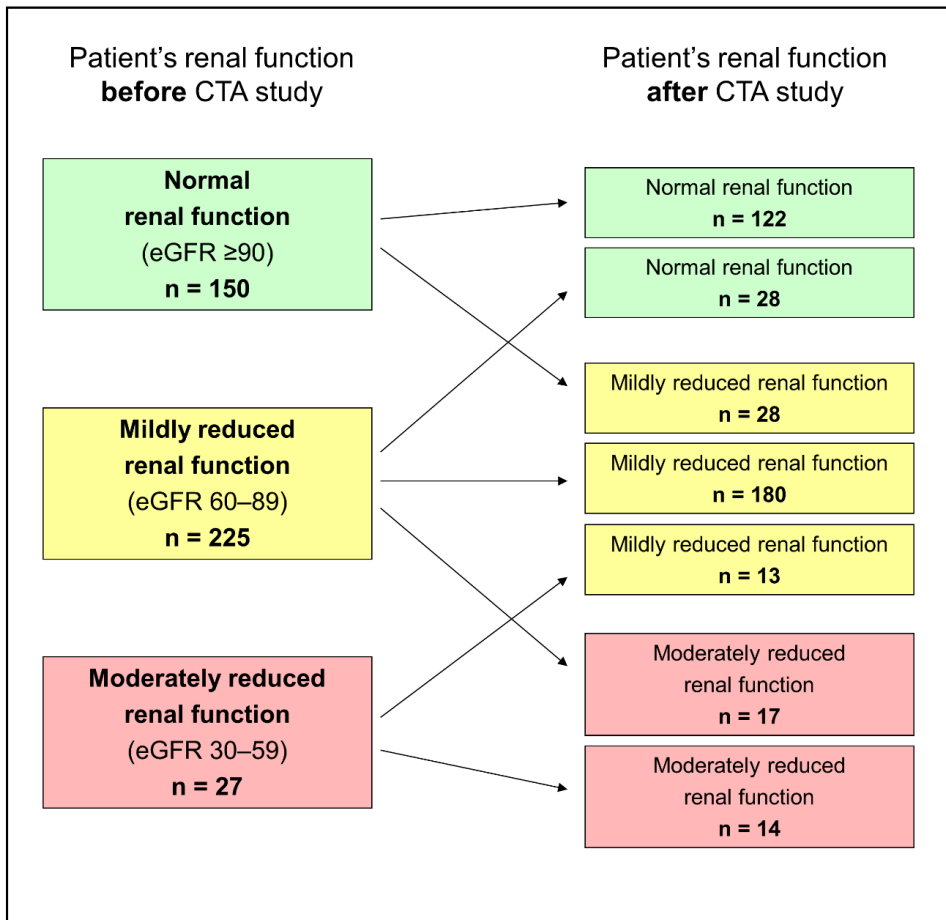


Figure 6 Distribution of patients according to the renal function (eGFR) before and after coronary CTA imaging. CTA = computed tomography angiography; eGFR = estimated glomerular filtration rate. (Originally published in Maaniitty et al. *Int J Cardiovasc Imaging* 2016;32:1567–75. Reprinted by permission from the Springer.)

5.2.3 Patients having an increase in plasma creatinine concentration after contrast agent exposure

Adapting the standard CIN definition, 14 patients (3.5% of the 402) were detected with a relative $\geq 25\%$ increase in plasma creatinine concentration between the pre-CTA and post-CTA measurements (ranging from 25% to 50%); none had an absolute increase of $\geq 44.2 \mu\text{mol/L}$. The pre-CTA creatinine level in these 14 patients was lower compared to the remaining 388 patients, while the differences in other baseline variables were statistically non-significant. In the 14 patients, the pre-CTA plasma creatinine concentration was $64.4 \pm 16.4 \mu\text{mol/L}$ (ranging from 38 to $92 \mu\text{mol/L}$) and the mean absolute increase $22.1 \pm 6.1 \mu\text{mol/L}$ (ranging from 13 to $35 \mu\text{mol/L}$). The eGFR was $93 \pm 12 \text{ mL/min/1.73 m}^2$ before CTA and $73 \pm 16 \text{ mL/min/1.73 m}^2$ after CTA, yielding a mean decrease of $20 \pm 6 \text{ mL/min/1.73 m}^2$ in eGFR. Six patients with normal eGFR before CTA had mildly reduced eGFR after the CTA, and three patients with mildly reduced eGFR before CTA had moderately reduced eGFR after the CTA study.

The medical records of the 14 patients were evaluated in more detail: in 4 patients the increase in plasma creatinine level was most likely explained by a disease or therapy not related to CIN (including multiple myeloma, heart failure, (treatment of) thyroid disease, acute kidney injury after CABG). Moreover, in 9 patients the plasma creatinine level normalized during an extended follow-up period (in a median of 311 days). Finally, only one patient (0.2% of the 402) had a persistent increase in plasma creatinine level unexplained by other factors than the contrast agent exposure. In this patient the eGFR was mildly reduced at baseline and moderately reduced after the CTA study.

5.3 Coronary computed tomography angiography -derived risk score in predicting cardiac events (Study III): Results

5.3.1 General patient characteristics in Study III

Patient basic characteristics are shown in Table 3. In the final study cohort of 508 patients, a total of 20 adverse events (AE) occurred during the follow-up of 3.6 years (25th–75th percentile: 2.7–4.8 years); 10 patients died, 5 had acute MI, and 6 had UAP (of whom 1 also died). Patients with AE were older (68 ± 8 vs. 63 ± 8 years, $p=0.008$) and had higher Agatston coronary artery calcium score (1053 ± 1205 vs. 331 ± 531 , $p=0.03$) than patients without AE. Moreover, coronary revascularization procedures within 6 months following CTA were more common in patients with AE (40% vs. 15%, $p=0.03$). Conventional cardiovascular risk factors including gender, hypertension, diabetes, dyslipidemia, obesity, smoking, and family history of CAD were comparable between patients with or without AE.

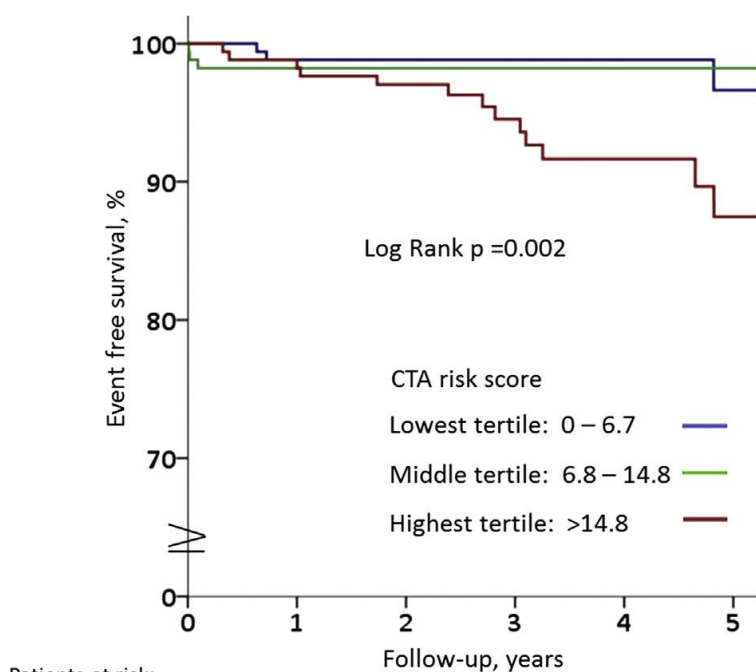
5.3.2 Association of quantitative coronary CTA characteristics with future adverse events

Compared to event-free patients, patients with AE had a higher number of any ($\geq 30\%$ stenosis) atherosclerotic plaques (5.3 ± 2.6 vs. 3.0 ± 2.2 , $p < 0.001$), obstructive ($\geq 50\%$ stenosis) plaques (3.8 ± 2.6 vs. 1.6 ± 1.7 , $p < 0.001$), severe ($\geq 70\%$ stenosis) lesions (1.9 ± 1.8 vs. 0.6 ± 1.0 , $p < 0.001$), and proximally located obstructive plaques (2.0 ± 1.5 vs. 0.8 ± 1.0 , $p < 0.001$). In addition, patients with AE more often presented with left main disease ($\geq 30\%$ stenosis) than patients without AE (40% vs. 18%, $p = 0.01$). The mean number of calcified plaques per patient was higher in patients with AE (3.7 ± 2.7 vs. 1.7 ± 1.9 , $p < 0.001$). However, the number of partially calcified or non-calcified plaques per patient were comparable between patients with and without AE (0.8 ± 1.0 vs. 0.6 ± 0.9 , $p = 0.36$; and 0.6 ± 0.8 vs. 0.5 ± 0.7 , $p = 0.37$, respectively). Univariable analyses using Cox's proportional hazards model provided similar results.

5.3.3 Prognostic value of coronary CTA -derived risk score

In the entire study population, the CTA risk score was 11.7 ± 7.8 (95% CI 4.0–10.8). The risk score was significantly higher in patients with AE compared to event-free patients (18.8 ± 9.1 vs. 11.4 ± 7.6 , $p < 0.001$; 95% CI 14.5–23.1 and 10.7–12.1, respectively). The lowest tertile of CTA risk score ranged from 0 to 6.7, the middle tertile from 6.8 to 14.8, and the highest tertile included patients with a score > 14.8 . Majority (70%) of all AE occurred in the highest tertile ($p = 0.002$); all 5 acute MI occurred in patients of the highest tertile ($p = 0.006$), while the 6 UAP were equally distributed across the three tertiles. Kaplan–Meier survival curves for CTA risk score tertiles are shown in Figure 7. Patients in the highest CTA risk score tertile had a lower event-free survival rate compared to other tertiles ($84 \pm 5\%$ vs. $97 \pm 2\%$ and $98 \pm 1\%$, $p = 0.002$).

Of the baseline patient characteristics, age (HR 1.08, 95% CI 1.02–1.14; $p = 0.005$) and male gender (HR 2.43, 95% CI 0.88–6.70; $p = 0.09$) were (nearly) significantly associated with AE in univariable Cox survival analysis, and were therefore included in multivariable Cox's survival analysis. In the multivariable analysis, the CTA risk score remained an independent predictor of future AEs after adjusting for age and gender (adjusted HR 1.09, 95% CI 1.03–1.16; $p = 0.002$).



Patients at risk:

	0	1	2	3	4	5
Lowest tertile	170	168	168	106	77	39
Middle tertile	169	166	166	103	63	31
Highest tertile	169	167	164	103	59	37

Figure 7 Kaplan–Meier curves demonstrating survival according to coronary CTA risk score tertiles. Patients in the highest risk score tertile (*red*) had significantly worse survival free from adverse events (death, myocardial infarction, or unstable angina). CTA = computed tomography angiography. (Originally published in Uusitalo et al. *J Cardiovasc Comput Tomogr* 2017;11:274–80. Reprinted by permission from the Elsevier.)

5.4 Hybrid PET/CTA imaging in patients with previous coronary artery bypass grafting (Study IV): Results

5.4.1 General patient characteristics in Study IV

Basic characteristics of the study population are shown in Table 3. Thirty-six patients with previous CABG underwent hybrid PET/CTA imaging, and each patient having three coronary territories, altogether 108 coronary territories were analyzed. Out of these, 86 (80%) territories had been previously grafted. The median time from CABG surgery to the hybrid imaging was 8.2 years (25th–75th percentile: 3.6–16.4), ranging from 0.5 to 27.8 years. 21 patients had chest pain as a

primary symptom, 7 had dyspnea, and the rest had other symptoms (e.g. exercise intolerance, arrhythmia). LVEF by echocardiography was recently measured in 30 patients, being normal ($\geq 50\%$) in 25 patients and mildly reduced (40–49%) in 5 patients. The effective radiation dose was $10.1 \text{ mSv} \pm 3.8 \text{ mSv}$ from coronary CTA and $1.0 \pm 0.09 \text{ mSv}$ from stress PET MPI.

5.4.2 Coronary CTA, PET perfusion, and hybrid imaging findings in Study IV

Of the 36 patients, 32 had right, 3 had left, and 1 had co-dominance of the coronary tree on CTA. Among all the 108 coronary territories in 36 patients (including both grafted and non-grafted), 41 (38%) territories were interpreted as protected, 48 (44%) as unprotected, and 19 (18%) as non-evaluable based on CTA.

Stress myocardial perfusion abnormalities on PET were common, as 34 of the 36 patients had any perfusion defect, and 31 patients had moderate–severe defects. Including all the 108 coronary territories, perfusion was normal in 43 (40%), mildly reduced in 11 (10%), moderately reduced in 25 (23%), and severely reduced in 29 (27%) territories. Among the 86 previously grafted territories, perfusion was normal in 34 (40%) territories.

Hybrid PET/CTA findings

The relationship between UCT status on coronary CTA and stress myocardial perfusion on PET MPI is shown in Table 4. Stress perfusion was abnormal in 12 (29%) of 41 protected territories, in 41 (85%) of 48 unprotected territories, and in 12 (63%) of 19 non-evaluable territories ($p < 0.001$).

Perfusion abnormalities were localized in relation to graft insertion based on hybrid PET/CTA images; the presence and localization of perfusion defects are demonstrated in Figure 8. Among all the 86 grafted coronary territories, stress perfusion was normal in 34 (40%) territories. The remaining territories presented with stress perfusion defects: in 12 (14%) territories the perfusion defect was restricted to myocardium supplied by native coronary branches, while in 40 (47%) territories the perfusion defect involved the myocardial area supplied by a graft (see an example in Figure 9).

The prevalence and localization of perfusion defects was significantly different when classified by CTA findings ($p < 0.001$) (Figure 8). Among the grafted protected coronary territories ($n=34$), stress perfusion was normal in 23 (68%) territories. Instead, among the grafted unprotected territories ($n=37$), stress perfusion was normal in only 5 (14%) territories, while in 29 (78%) unprotected territories there was a perfusion defect involving myocardial areas supplied by a graft. Finally, 21 (58%) of the 36 study patients presented with a matched-type PET/CTA defect, i.e. a coronary territory that was unprotected on CTA and had a co-existing perfusion defect involving the grafted myocardial areas.

Table 4 The relationship between coronary CTA and PET perfusion findings among all (i.e. grafted and non-grafted) coronary territories.

n = 36 patients	Normal perfusion	Reduced perfusion	Total	P-value
LAD				
Protected	8 (53%)	7 (47%)	15	p=0.268
Unprotected	2 (20%)	8 (80%)	10	
Non-evaluable	4 (36%)	7 (64%)	11	
Total	14 (39%)	22 (61%)	36	
LCX				
Protected	11 (85%)	2 (15%)	13	p<0.001
Unprotected	2 (11%)	16 (89%)	18	
Non-evaluable	3 (60%)	2 (40%)	5	
Total	16 (44%)	20 (56%)	36	
PDA				
Protected	10 (77%)	3 (23%)	13	p<0.001
Unprotected	3 (15%)	17 (85%)	20	
Non-evaluable	0 (0%)	3 (100%)	3	
Total	13 (36%)	23 (64%)	36	
All territories				
Protected	29 (71%)	12 (29%)	41	p<0.001
Unprotected	7 (15%)	41 (85%)	48	
Non-evaluable	7 (37%)	12 (63%)	19	
Total	43 (40%)	65 (60%)	108	

Percentages are calculated per row. P-values are calculated for the differences across the groups using the Fisher's exact test (IBM SPSS Statistics ver. 23). CTA = computed tomography angiography; LAD = left anterior descending artery; LCX = left circumflex artery; PDA = posterior descending artery; PET = positron emission tomography.

5.4.3 CTA characteristics of unprotected and non-evaluable coronary territories

Thirty-seven (43%) of the 86 grafted coronary territories were unprotected on coronary CTA: 17 territories with a significant obstruction in the bypass graft, 11 with a significant obstruction in the distal native artery, and 9 with the both. All grafted coronary territories had a significant stenosis or occlusion in the native artery proximal to a graft–coronary anastomosis.

Nineteen (18%) of the total 108 coronary territories were non-evaluable on CTA (11 LAD, 5 LCX, and 3 PDA territories). In 7 cases, this was due to too short range of scan not entirely covering the graft (usually left internal thoracic artery (LITA)–LAD graft). In 2 out of these 7 cases perfusion was mildly abnormal in the myocardial area supplied by the graft, while in the remaining 5 cases perfusion was normal. In a total of 8 cases, the non-evaluability was due to artifacts (n=6) or calcifications (n=2) in the graft–coronary anastomosis or native vessel. Only in 1 case there was an artifact in the graft impairing the interpretation. In 2 cases, there was an overall bad CTA image quality. In 1 case there was a small-diameter (2 mm) coronary stent in LCX.

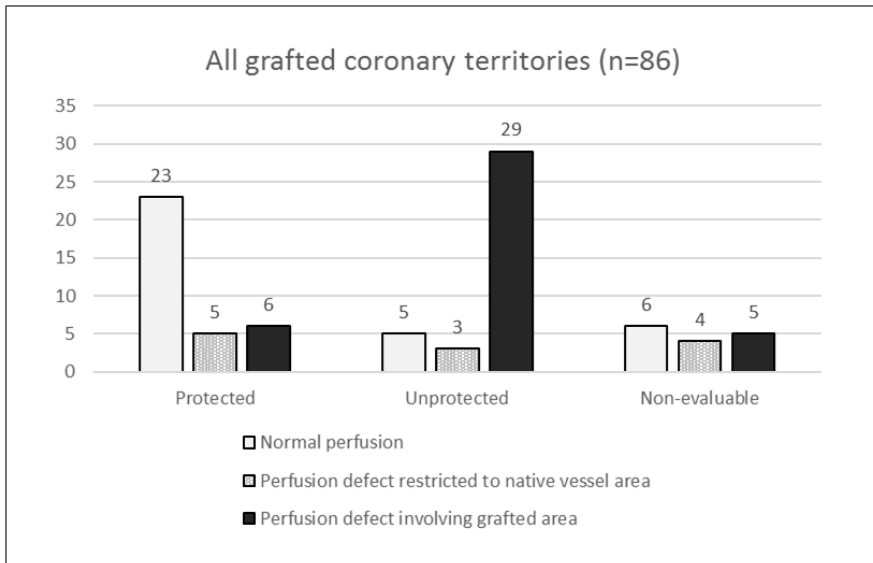


Figure 8 The presence and localization of PET perfusion abnormalities by UCT status on CTA, among grafted coronary territories. CTA = computed tomography angiography; PET = positron emission tomography; UCT = unprotected coronary territory.

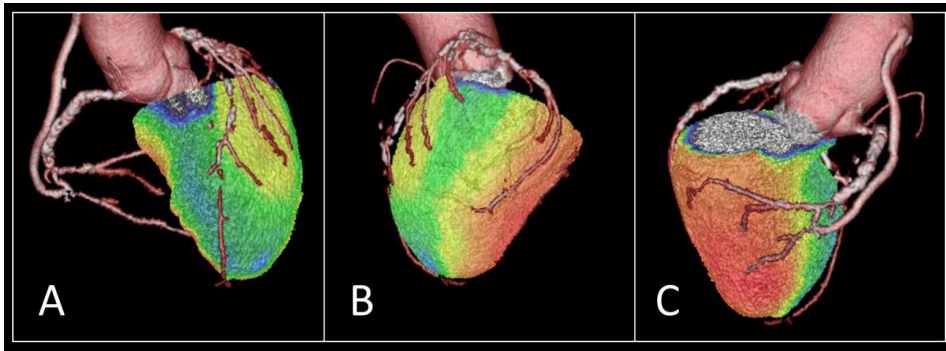


Figure 9 An example of PET/CTA hybrid imaging findings in a 64-year-old male. **A)** The native LAD and the LITA-LAD graft are occluded, and the stress perfusion is severely reduced (*blue*) in this area. The first diagonal branch appears with a 50–70% stenosis co-localizing with mildly abnormal perfusion (*yellow*). **B)** The IM branch appears with an obstructive (>70%) stenosis co-localizing with moderately reduced (*green*) perfusion. The proximal LCX shows an obstructive stenosis (>70%) on CTA, and the Aorta-LPL graft is occluded. However, stress perfusion in the LPL area is preserved as normal. **C)** Native RCA is occluded, but the patent Aorta-RCA graft maintains normal perfusion (*red*) in the inferior left ventricular wall. CTA = computed tomography angiography; IM = intermediate; LAD = left anterior descending artery; LCX = left circumflex artery; LITA = left internal thoracic artery; LPL = left posterolateral; PET = positron emission tomography; RCA = right coronary artery.

6 DISCUSSION

6.1 Prognostic value of coronary CTA with selective PET perfusion imaging: Discussion

The results of the Study I show that the hybrid imaging approach with sequential use of coronary CTA followed by selective application of PET perfusion imaging can accurately identify patients with low and high risk of death or adverse cardiac events. Obstructive CAD could be excluded by coronary CTA alone in about half of the patients with suspected CAD, and these patients had a good outcome. Among the patients with suspected obstructive CAD on CTA, about half had normal myocardial perfusion by PET imaging, and this was still associated with a low adverse event rate comparable to those patients without significant CAD on coronary CTA. Instead, patients with significant CAD on CTA and abnormally low perfusion by PET had a 5-fold adverse event rate compared to the patients with normal PET perfusion. Our findings are in an agreement with the previous studies showing that the presence, extent, and severity of myocardial ischemia on MPI are associated with poor prognosis while patients normal MPI findings have a low risk for adverse events (K. Brown 1991; Hachamovitch et al. 1998; Shaw and Iskandrian 2004; Herzog et al. 2009; Dorbala et al. 2013). The results of the Study I also agree with the previous studies indicating an excellent prognosis in patients with normal coronary CTA (Min et al. 2011; Chow, Small, et al. 2011; Hadamitzky, Täubert, et al. 2013). The study I demonstrates that the risk stratification of patients with suspected obstructive CAD is feasible and safe using the sequential hybrid imaging approach with selective application of PET perfusion imaging after coronary CTA.

Previous studies have shown incremental prognostic value of anatomic CTA findings and SPECT perfusion findings (van Werkhoven et al. 2009; Pazhenkottil, Nkoulou, Ghadri, Herzog, Buechel, et al. 2011). In those studies, all patients underwent both anatomical and perfusion imaging. The local routine practice with the selective application of PET MPI after coronary CTA at Turku PET Centre is based on the high NPV of coronary CTA shown in previous studies (Schroeder et al. 2008; Knuuti and Saraste 2013; Montalescot et al. 2013). The Study I provides a real-life evidence suggesting that MPI can be safely avoided in about half of the patients referred to imaging for suspected obstructive CAD and having an intermediate PTP. The outcome was excellent in patients who had obstructive CAD ruled-out by coronary CTA alone. An alternative approach for sequential imaging would be to start with MPI and selectively proceed to coronary CTA, as was done in a study by Engbers et al. (Engbers et al. 2017). An advantage of CTA-first approach is the detection of non-obstructive coronary atherosclerosis, while coronary microvascular dysfunction could be theoretically missed using this strategy. However, the optimal strategy of using cardiac hybrid imaging in clinical practice still remains unknown, and when comparing different non-invasive modalities and their combinations, different aspects such as diagnostic accuracy, prognostic value, effects on downstream testing, radiation dose to patient, and costs should be considered.

The Study I has some limitations. The study was retrospective and observational in design, and some information was not available. However, the registries in Finland are highly reliable and complete (Sund 2012). All-cause mortality, rather than cardiovascular mortality, was used as an endpoint to avoid verification bias. Due to the relatively low number of adverse events, more detailed prognostic analyses on CTA or PET characteristics were not reasonable. Moreover, coronary calcium score was not measured for all patients, and therefore, was not included in the multivariable Cox's regression model. Each imaging study was analyzed and reported for clinical purposes principally by (only) one trained physician. However, the interobserver agreement has previously appeared good for the presence or absence of obstructive CAD on coronary CTA (Williams et al. 2015). Moreover, the intra- and interobserver differences have been small for the quantification of myocardial perfusion using the Carimas software and ^{15}O -water tracer (Nesterov et al. 2009). Some patients had a non-diagnostic coronary CTA scan, majority of whom underwent further PET perfusion study to exclude significant CAD; there were also some non-diagnostic MPI scans in the study cohort. Four percent of the study cohort did not adhere to the sequential imaging protocol due to a variety of reasons, such as a contraindication to vasodilator stress or direct referral to ICA.

6.2 Persistent renal dysfunction after coronary computed tomography angiography: Discussion

The results of the Study II indicate that persistent renal dysfunction attributable to iodine contrast agent exposure is a rare and benign phenomenon and occurs in 0.2% of typical patients referred to coronary CTA for suspected stable obstructive CAD. Most of the observed increases in plasma creatinine levels either normalized during the follow-up or were primarily explained by other causes.

Previously, two large meta-analyses have reported 5–6% overall incidences of CIN after intravenous contrast enhanced CT (Kooiman et al. 2012; Moos et al. 2013). Relatively few studies have reported the incidence of CIN after coronary CTA, and the reported incidences have varied between 0% and 10% (El-Hajjar et al. 2008; Yoshikawa et al. 2011; Pedersen et al. 2014; Li et al. 2015). Instead, a high incidence of CIN up to 15% has been reported in patients undergoing PCI (McCullough et al. 2006). However, stable patients referred to coronary CTA represent a relative different population than unselected patients undergoing PCI. The observed low incidence of persistent renal dysfunction in the Study II is in agreement with relatively favorable baseline clinical characteristics of these patients, as they were mostly outpatients with suspected stable CAD, and the baseline eGFR was ≥ 60 mL/min/1.73 m² in 93% of patients. The low incidence of renal dysfunction may be partly explained by the fact that, in contrast to most of the previous studies, we applied later time points of creatinine measurements to detect persistent renal dysfunction. The aim was to distinguish true persistent increase in plasma creatinine level from transient fluctuation. However, the low incidence of persistent renal dysfunction in our study is in agreement with

low 1.1% incidence of persistent renal dysfunction after contrast enhanced CT reported by Kooiman et al., and 0.3% incidence after coronary CTA reported by Pedersen et al. (Kooiman et al. 2012; Pedersen et al. 2014).

The study II demonstrated that increases and decreases in eGFR were equally common after contrast agent exposure in patients undergoing coronary CTA. This reflects a problem in the current criteria for CIN, as these criteria focus only on those patients showing an increase in creatinine concentration after the contrast agent exposure (Morcos, Thomsen, and Webb 1999). Newhouse et al. demonstrated that a $\geq 25\%$ change (either increase or decrease) in serum creatinine concentration during 5 consecutive days occurred in over half of the 32,161 patients not receiving iodine contrast media, and a $\geq 25\%$ increase in creatinine level was observed in 27% of the patients (Newhouse et al. 2008). Relatively few studies have compared the incidence of CIN after contrast enhanced CT to that among control subjects not receiving contrast agents, and these studies have reported no or minor effects of contrast agent exposure on the subsequent risk of meeting the CIN criteria (Katzberg and Newhouse 2010; J. S. McDonald et al. 2013). Therefore, increases in creatinine concentration after contrast agent exposure may reflect transient physiological fluctuation and “regression to the mean” phenomenon rather than true kidney injury. This is supported by the finding that the 14 patients showing a $\geq 25\%$ increase in plasma creatinine concentration in the Study II had significantly lower pre-CTA creatinine levels than the other patients. Moreover, factors such as diseases and medications may have effects on plasma creatinine concentration, and therefore, we conducted a more detailed analysis of the 14 patients showing a creatinine increase. We found that in most of these patients the plasma creatinine concentration either normalized in the follow-up, or the increase in creatinine was primarily explained by a co-existing disease or therapeutic intervention other than contrast enhanced coronary CTA.

The Study II has several limitations. The study was retrospective and observational in design, and there was no control group not receiving contrast agents. Plasma creatinine concentration was not routinely measured after coronary CTA, and the time points for the measurements were not standardized. Creatinine measurements within two weeks following a coronary CTA scan were not included for analysis, and therefore, we can only assess persistent but not transient acute renal dysfunction. The study cohort represents real-life patients undergoing coronary CTA for suspected CAD, and the impact of possible use of preventive tools for CIN cannot be assessed as these were not recorded. Unfortunately, the individual volume of intravenous fluid administered was not retrospectively accessible, and therefore, cannot be considered in the analysis. There was no patient with pre-existing severe renal dysfunction (i.e. eGFR < 30) in the study cohort, as this is a contraindication for coronary CTA. Furthermore, patients with relatively low eGFR values may have been referred to other testing modalities rather than contrast enhanced coronary CTA. We aimed to evaluate potential etiologies for the increase in plasma creatinine level, but finally, we cannot certainly prove their causal relationships.

6.3 Coronary computed tomography angiography -derived risk score in predicting cardiac events: Discussion

The results of the Study III demonstrate that the risk score derived from quantitative coronary CTA findings predicts future adverse events. The risk score is obtained using an automated quantification software, and integrates the extent of coronary atherosclerosis, the location and composition of a plaque, and the severity of stenosis. The CTA quantification of coronary atherosclerosis using this software has been previously cross-correlated with intravascular ultrasound virtual histology (IVUS-VH) (de Graaf et al. 2013). Moreover, the CTA risk score derived from the quantitative CTA parameters has been previously evaluated in a smaller patient cohort (de Graaf et al. 2014), and the results of the Study III are largely in agreement with the previous study.

The extent of coronary atherosclerosis is an important prognostic marker, and the number of obstructive coronary arteries is associated with an increasing rate of future adverse events (Min et al. 2011). Furthermore, extensive non-obstructive coronary atherosclerosis is associated with an impaired survival (Ostrom et al. 2008; Bittencourt et al. 2014). Similarly, the number of atherosclerotic coronary plaques was associated with future adverse events in the Study III. Moreover, previous studies have reported the prognostic significance of proximally located coronary lesions (Pundziute et al. 2007; Min et al. 2007). Accordingly, the number of proximal obstructive lesions was reported to have an univariable hazard ratio of 2.10 for adverse events in the Study III.

Previous studies have suggested that CTA-determined composition of a coronary artery plaque may be related to the subsequent adverse event risk (Gaemperli et al. 2008; Otsuka et al. 2014). In the study III, the number of calcified coronary plaques per patient was statistically significantly associated with an increased risk for adverse events, while the numbers of non-calcified or partially calcified plaques were not. This may be partly related to insufficient statistical power due to the low prevalence of non-calcified or partially calcified plaques, and the low incidence of adverse events. Moreover, the automated quantification software does not recognize high-risk plaque features such as positive remodeling, spotty calcification, or a napkin-ring sign (Otsuka et al. 2014; Maurovich-Horvat et al. 2014). Finally, the constitution of medical therapy, possibly triggered by the CTA findings, may have stabilized the plaques prone to rupture.

As shown in previous studies and in the Study III, multiple CTA parameters provide independent information on patient's outcome (Pundziute et al. 2007; Min et al. 2007, 2011; Ostrom et al. 2008; Gaemperli et al. 2008; Bittencourt et al. 2014; Otsuka et al. 2014; Maurovich-Horvat et al. 2014). The aim of CTA-derived prognostic scores is to integrate the effects of different CTA parameters into a single prognostic risk score. The hypothesis is that risk scores derived from individual CTA findings would provide a better estimate of patient's prognosis than risk scores that are based on conventional cardiovascular risk factors alone (e.g. the European SCORE charts) (Conroy et al. 2003). The CTA risk score in the Study III well predicted outcome, as all patients with an acute MI and majority (70%) of patients with death during follow-up were classified into the highest CTA risk score tertile. However, the CTA risk score was not associated with UAP.

Importantly, the CTA risk score provided independent prognostic information after adjustment for baseline patient characteristics. Previous studies have demonstrated a good prognostic value of simpler CTA risk scores, including segment-involvement score (i.e. the number of coronary segments with plaque, irrespective of the degree of stenosis) and segment-stenosis score (integrating the number and severity of coronary stenoses) (Min et al. 2011; Andreini et al. 2012). More recently, a CTA-adapted Leaman score (CT-LeSc) was introduced, integrating the extent of coronary atherosclerosis, stenosis severity, and plaque location and composition, largely in the same way as the CTA risk score in the Study III (de Araújo Gonçalves et al. 2013). This CTA-adapted Leaman score seems to be a prognostic marker independent on the stenosis severity (Mushtaq et al. 2015; Andreini et al. 2017). On the contrary to the CTA-adapted Leaman score, the CTA risk score in the Study III was based on the automated software quantification of coronary CTA findings.

The Study III has some limitations. An automated quantification of coronary atherosclerosis was not feasible in some patients due to technical factors or inadequate image quality. Also, patients with normal CTA scans were excluded as they were assumed to have a CTA risk score of zero. The number of adverse events was relatively low as the study cohort represents a population with a generally favorable outcome. All-cause mortality instead of cardiac mortality was used as an endpoint to avoid verification bias. The weight factors for plaque composition in the CTA risk score were based on a single previous study in a relatively small patient cohort (Gaemperli et al. 2008). The previous study comparing the automated quantitative CTA measurements with intravascular ultrasound virtual histology found good correlations between the two modalities for the volumes of plaques with different compositions, but the quantitative CTA significantly overestimated the plaque volumes compared to the intravascular ultrasound virtual histology (de Graaf et al. 2013). Furthermore, the current CTA risk score does not take into account some less-established CTA markers of plaque vulnerability (Otsuka et al. 2014; Maurovich-Horvat et al. 2014).

6.4 Hybrid PET/CTA imaging in patients with previous coronary artery bypass grafting: Discussion

The results of the Study IV suggest that hybrid PET/CTA imaging of symptomatic patients with previous CABG is feasible, providing an integrative assessment of native-bypass coronary anatomy and myocardial perfusion. Based on the literature, 50–60% of saphenous vein grafts are patent at 10 years after CABG, while the patency rate is higher for internal mammary artery grafts (Hillis et al. 2011). Previous studies have shown the high accuracy of coronary CTA in detection of graft stenosis or occlusion (Schroeder et al. 2008; Weustink et al. 2009). However, the per-patient accuracy in post-CABG patients may be limited due to calcifications and borderline stenoses in native coronary arteries and artifacts caused by surgical metal clips, and the specificity of CTA is lower in the evaluation of native arteries of these patients (Schroeder et al. 2008). Accordingly, in the Study IV only 67% of normally-perfused territories were “protected” on CTA,

reflecting the relatively low specificity of CTA. Moreover, 18% of territories were interpreted as non-evaluable based on CTA.

Myocardial perfusion imaging (MPI) provides information on the presence, extent, severity, and reversibility of perfusion abnormalities, and therefore, on the functional significance of a coronary or graft stenosis. Stress perfusion defects were commonly detected in the Study IV, that is in line with the known high sensitivity of quantitative PET MPI. The high prevalence of perfusion abnormalities emphasizes the need for their proper interpretation. We hypothesized that non-invasive anatomical information provided by coronary CTA would be useful for the interpretation of the perfusion defects, as the defects can be assigned to a supplying graft or coronary artery using hybrid images. The hybrid imaging approach appears justifiable, as the individual coronary anatomy may be especially complex after CABG surgery. In addition, potential culprit-lesions may be detectable on coronary CTA.

In the study IV, stress perfusion defects were more common among unprotected coronary territories than in protected territories, but the agreement was not perfect. Perfusion abnormalities were frequent in protected coronary territories also, and on the other hand, not all unprotected territories were ischemic. These findings suggest complementary roles of anatomic and functional imaging, as demonstrated by the following examples: First, perfusion abnormalities that are restricted to myocardial areas supplied by native coronary branches may be caused by obstructive atherosclerosis in native coronary branches proximal to the graft insertion, that may not be accessible by invasive procedures. Second, abnormal perfusion in the absence of obstructive stenosis might be explained by a microvascular mechanism. Third, normal perfusion in the presence of an anatomically obstructive stenosis may be maintained by an adequate collateral circulation, or may reflect the limited PPV of coronary CTA. In all these example cases, invasive coronary procedures could be potentially avoided based on the non-invasive hybrid imaging findings.

In the Study IV, LITA grafts were not entirely covered by coronary CTA in a significant proportion of patients. Moreover, image artifacts and calcifications also led to non-evaluable CTA findings. These problems should be minimized by appropriate patient preparation and image acquisition. However, the perfusion findings may provide valuable information in the case of non-diagnostic CTA quality.

The Study IV has several limitations. The imaging data were retrospectively analyzed for scientific purposes, and therefore, the actual downstream referral and patient management after PET/CTA hybrid imaging cannot be reliably assessed. There is no gold standard, as ICA was not performed in all patients. Majority of the patients had undergone stress-only perfusion imaging, and therefore, only hyperemic perfusion data were included in the analysis. Theoretically, the quantification of myocardial blood flow in an infarction scar may be inaccurate using ^{15}O -water tracer, as the flow is modelled in water-perfusible tissue only (Knaapen et al. 2006). There might have been selection bias due to the availability of other modalities (e.g. SPECT MPI, stress echocardiography) for the evaluation of patients with previous CABG at the Turku University Hospi-

tal. Finally, the Study IV evaluates the feasibility and findings of cardiac hybrid PET/CTA imaging after CABG; future studies are needed to evaluate the utility of hybrid imaging findings to guide downstream referral and patient management.

6.5 Future study directions on coronary CTA and PET MPI

The studies I–IV in this thesis are retrospective in design, i.e. they are “looking back”. The results of these studies strengthen the clinical utility of the investigated imaging approaches, such as selective application of MPI after coronary CTA, coronary CTA-derived prognostic scores, and renal safety of iodine contrast media. Potentially, the results encourage for a more widespread utilization of non-invasive imaging modalities in other medical centers also. Finally, we take a short look to the potential future visions and research topics in the area of non-invasive cardiac imaging.

Novel fluorine-18-labeled PET perfusion tracers will probably make quantitative MPI more widely available, as the production of these tracers does not require an on-site cyclotron (Packard et al. 2014). The development and validation of models for MBF quantification using ^{18}F -labeled tracers requires more research. Similarly, the reduction in patient effective radiation dose facilitates the clinical use of coronary CTA (Stocker et al. 2018).

Anatomical and functional imaging seem to provide complementary information on CAD. In the Study I, we demonstrated the clinical use and prognostic value of a hybrid imaging strategy with selective application of PET MPI after coronary CTA. This approach takes advantage of the high negative predictive value of coronary CTA, while the limited specificity of CTA is compensated by the selective use of PET perfusion imaging and subsequent fusion of CTA and PET imaging data. It would be another option, for example, to perform MPI first, or to unselectively use both anatomical and functional imaging modalities. Importantly, it should be noted that not all patients need real hybrid imaging combining two different imaging modalities, as was demonstrated in the Study I, since a single modality may be sufficient for exclusion or detection of the disease. A prerequisite for the safe use of sequential hybrid imaging strategies in detection of hemodynamically significant CAD is that the first-line test has an enough high sensitivity, as is the case with e.g. coronary CTA and quantitative PET MPI. The utilization of cardiac hybrid or combined imaging varies in different medical centers, and no strategy has been shown to be obviously superior to the others. Furthermore, the best imaging approach may differ based on patient characteristics and pre-test probability of obstructive CAD. Comparative studies would be needed to establish the optimal use of hybrid imaging for suspected obstructive CAD in different patient groups.

Previous studies have suggested that coronary revascularization in stable CAD may be superior to medical therapy alone in terms of ischemia reduction and patient outcome if the myocardial ischemia is moderate or severe (Hachamovitch et al. 2003; Shaw et al. 2008). However, large

prospective randomized trials would be needed to study the interaction between non-invasive imaging findings, choice of treatment strategy, and prognosis. Hopefully, the ongoing ISCHEMIA trial will shed light on this issue (Phillips et al. 2013).

The high sensitivity of non-invasive imaging modalities such as coronary CTA and quantitative PET MPI enables the detection of non-obstructive coronary atherosclerosis and coronary microvascular dysfunction. Large-scale studies would be needed to assess the prognostic implications of these findings, as well as to establish the optimal use of medical therapy to improve prognosis in the presence of these “subclinical” manifestations of coronary disease. Currently, machine learning and artificial intelligence are increasingly utilized in medicine and research. The application of these techniques to the analysis and interpretation of non-invasive imaging data might improve the risk stratification and reveal novel, yet unidentified patterns of disease carrying a high adverse event risk.

The evaluation and management of a patient with prior CABG and new, recurrent, or worsening symptoms pose a clinical challenge. In the Study IV, we investigated the feasibility of hybrid PET/CTA imaging in the assessment of this patient group. Prospective larger-scale studies are needed to validate the accuracy of non-invasive imaging after CABG and to assess its effects on downstream referral and patient management.

7 CONCLUSIONS

The major findings and conclusions of the Studies I–IV are as follows:

- I** In symptomatic patients with suspected stable CAD, coronary CTA alone is sufficient for exclusion of significant CAD in about half (53%) of the patients, and these patients have a good outcome. Even in the presence of suspected obstructive CAD on CTA, about half (49%) have normal myocardial PET perfusion, and this is associated with a low adverse event risk comparable to the patients with obstructive CAD excluded by CTA. Instead, patients with abnormal perfusion have a significantly worse outcome. A hybrid imaging approach with selective application of PET perfusion imaging when coronary CTA is suggestive of obstructive CAD, is a safe strategy to identify patients without significant ischemic CAD.
- II** Persistent renal dysfunction attributable to iodine contrast agent exposure is rare (0.2%) in stable patients referred to coronary CTA for suspected CAD. Fluctuations in plasma creatinine concentration occur frequently, possibly related to a variety of physiological and pathological conditions.
- III** The comprehensive risk score integrating quantitative coronary CTA parameters of atherosclerotic burden and plaque severity, location, and composition, permits adverse event risk stratification in patients with suspected stable CAD.
- IV** Hybrid PET/CTA imaging provides an integrative assessment of native–bypass coronary anatomy and myocardial perfusion in symptomatic patients with previous CABG. Even in protected coronary territories perfusion abnormalities are frequent, and correspondingly, not all unprotected territories are ischemic. The fusion of coronary CTA and PET MPI data allows co-localization of a myocardial perfusion defect with the supplying coronary artery and potential culprit-lesions.

ACKNOWLEDGEMENTS

This research was conducted at Turku PET Centre during 2012–2018 as part of the Academy of Finland Centre of Excellence in Cardiovascular and Metabolic Disease. The research was conducted in the Department of Clinical Physiology and Nuclear Medicine and the Doctoral Programme in Clinical Research of the University of Turku, Turku, Finland. The research is based on diagnostic imaging studies performed in the Department of Clinical Physiology, Nuclear Medicine and PET of the Turku University Hospital. Collaboration was done with the Heart Center of the Turku University Hospital and the Department of Cardiology of the Leiden University Medical Center, Leiden, the Netherlands.

I am grateful to docent Antti Loimaala for serving as the opponent in the public defense of my PhD thesis. I want to thank professor Riemer Slart and professor Jari Laukkanen for reviewing my thesis. I am very grateful to my supervisors professor Juhani Knuuti and associate professor Antti Saraste for all their effort in my PhD process, as well as for professional mentoring in cardiovascular imaging.

I want to thank the sources of funding, including the Finnish Cardiac Society, the Foundation of Ida Montin, the Finnish Foundation for Cardiovascular Research, the Turku University Foundation, and the Doctoral Programme in Clinical Research and the Faculty of Medicine Postgraduate Education Unit of the University of Turku.

I want to express my gratitude towards physicians at the Department of Clinical Physiology, Nuclear Medicine and PET and the Heart Center of the Turku University Hospital who have mentored me in the field of cardiovascular imaging and other medical investigations. I am thankful to professor Juhani Airaksinen and research coordinator Tuija Vasankari for collaboration with the Heart Center. I want to thank information technology experts, medical physicists, and biostatisticians for their help when struggling with technical and statistical issues. I want to also thank other personnel of the Turku PET Centre, and importantly, the investigators of the cardiovascular research group in the Turku PET Centre for support and company.

I am grateful to the co-authors of the scientific articles included in this thesis. I want to thank docent Heikki Ukkonen and doctor Samuli Jaakkola for collaboration. I want to express plentiful thanks to docent Maija Mäki and docent Sami Kajander not only for the research collaboration but also for their patience and guidance in the analysis of diagnostic cardiac studies. I am grateful to professor Jeroen Bax and his research group in Leiden for collaboration. I want to warmly thank doctor Valterri Uusitalo for collaboration and company during my PhD process. I am very thankful to doctor Iida Stenström for collaboration and for her remarkable role in establishing the Turku cardiac CTA registry. I want to warmly thank study coordinator Heli Louhi for her help and company. I want to also thank Esa Harjulahti for his effort.

I am thankful to my friends for discussions and company. I am grateful to my grandparents and other close people for all kinds of support provided. I want to thank my sisters Elina and Eveliina for company (and for all those delicious meals served after long working days). I am very grateful to my parents Taina and Timo Maaniitty for all types of support and for making this PhD thesis possible at all.

Finally, I want to warmly thank Rebekka Saarijärvi for all her love and support in my life.

Pori, 24th April 2018



Teemu Maaniitty

REFERENCES

1. Abbara S, Blanke P, Maroules CD, Cheezum M, Choi AD, Han BK, Marwan M, Naoum C, Norgaard BL, Rubinshtein R, Schoenhagen P, Villines T, Leipsic J. SCCT guidelines for the performance and acquisition of coronary computed tomographic angiography: A report of the society of Cardiovascular Computed Tomography Guidelines Committee: Endorsed by the North American Society for Cardiovascular Imaging (NASCI). *J Cardiovasc Comput Tomogr* 2016;10:435–449.
2. Agatston AS, Janowitz WR, Hildner FJ, Zusmer NR, Viamonte M, Detrano R. Quantification of coronary artery calcium using ultrafast computed tomography. *J Am Coll Cardiol* 1990;15:827–832.
3. Alluri K, Joshi PH, Henry TS, Blumenthal RS, Nasir K, Blaha MJ. Scoring of coronary artery calcium scans: history, assumptions, current limitations, and future directions. *Atherosclerosis* 2015;239:109–117.
4. Anagnostopoulos C, Almonacid A, Fakhri G El, Curillova Z, Sitek A, Roughton M, Dorbala S, Popma JJ, Di Carli MF. Quantitative relationship between coronary vasodilator reserve assessed by 82Rb PET imaging and coronary artery stenosis severity. *Eur J Nucl Med Mol Imaging* 2008;35:1593–1601.
5. Anderson KM, Wilson PW, Odell PM, Kannel WB. An updated coronary risk profile. A statement for health professionals. *Circulation* 1991;83:356–362.
6. Andreini D, Pontone G, Mushtaq S, Bartorelli AL, Bertella E, Antonioli L, Formenti A, Cortinovis S, Veglia F, Annoni A, Agostoni P, Montorsi P, Ballerini G, Fiorentini C, Pepi M. A long-term prognostic value of coronary CT angiography in suspected coronary artery disease. *JACC Cardiovasc Imaging* 2012;5:690–701.
7. Andreini D, Pontone G, Mushtaq S, Gransar H, Conte E, Bartorelli AL, Pepi M, Opolski MP, ó Hartaigh B, Berman DS, Budoff MJ, Achenbach S, Al-Mallah M, Cademartiri F, Callister TQ, Chang HJ, Chinnaiyan K, Chow BJW, Cury R, Delago A, Hadamitzky M, Hausleiter J, Feuchtner G, Kim YJ, Kaufmann PA, Leipsic J, Lin FY, Maffei E, Raff G, Shaw LJ, et al. Long-term prognostic impact of CT-Leaman score in patients with non-obstructive CAD: Results from the Coronary CT Angiography Evaluation For Clinical Outcomes International Multicenter (CONFIRM) study. *Int J Cardiol* 2017;231:18–25.
8. Ashley EA, Myers J, Froelicher V. Exercise testing in clinical medicine. *Lancet* 2000;356:1592–1597.
9. Austen WG, Edwards JE, Frye RL, Gensini GG, Gott VL, Griffith LS, McGoan DC, Murphy ML, Roe BB. A reporting system on patients evaluated for coronary artery disease. Report of the Ad Hoc Committee for Grading of Coronary Artery Disease, Council on Cardiovascular Surgery, American Heart Association. *Circulation* 1975;51:5–40.
10. Baigent C, Blackwell L, Emberson J, Holland L, Reith C, Bhala N, Peto R, Barnes E, Keech A, Simes J, Collins R. Efficacy and safety of more intensive lowering of LDL cholesterol: A meta-analysis of data from 170 000 participants in 26 randomised trials. *Lancet* 2010;376:1670–1681.
11. Bamberg F, Sommer WH, Hoffmann V, Achenbach S, Nikolaou K, Conen D, Reiser MF, Hoffmann U, Becker CR. Meta-analysis and systematic review of the long-term predictive value of assessment of coronary atherosclerosis by contrast-enhanced coronary computed tomography angiography. *J Am Coll Cardiol* 2011;57:2426–2436.
12. Bateman TM, Heller G V., McGhie AI, Friedman JD, Case JA, Bryngelson JR, Hertenstein GK, Moutray KL, Reid K, Cullom SJ. Diagnostic accuracy of rest/stress ECG-gated Rb-82 myocardial perfusion PET: Comparison with ECG-gated Tc-99m sestamibi SPECT. *J Nucl Cardiol* 2006;13:24–33.
13. Bech GJW, De Bruyne B, Pijls NHJ, Muinck ED de, Hoortje JCA, Escaned J, Stella PR, Boersma E, Bartunek J, Koolen JJ, Wijns W. Fractional Flow Reserve to Determine the Appropriateness of Angioplasty in Moderate Coronary Stenosis. *Circulation*

- 2001;103:2928–2934.
14. Berger JS, Brown DL, Becker RC. Low-Dose Aspirin in Patients with Stable Cardiovascular Disease: A Meta-analysis. *Am J Med* 2008;121:43–49.
 15. Berman DS, Hachamovitch R, Shaw LJ, Friedman JD, Hayes SW, Thomson LEJ, Fieno DS, Germano G, Wong ND, Kang X, Rozanski A. Roles of nuclear cardiology, cardiac computed tomography, and cardiac magnetic resonance: Noninvasive risk stratification and a conceptual framework for the selection of noninvasive imaging tests in patients with known or suspected coronary artery disease. *J Nucl Med* 2006;47:1107–1118.
 16. Berman DS, Maddahi J, Tamarappoo BK, Czernin J, Taillefer R, Udelson JE, Gibson CM, Devine M, Lazewatsky J, Bhat G, Washburn D. Phase II safety and clinical comparison with single-photon emission computed tomography myocardial perfusion imaging for detection of coronary artery disease: Flurpiridaz F 18 positron emission tomography. *J Am Coll Cardiol* 2013;61:469–477.
 17. Berti V, Sciagrà R, Neglia D, Pietilä M, Scholte AJ, Nekolla S, Rouzet F, Pupi A, Knuuti J. Segmental quantitative myocardial perfusion with PET for the detection of significant coronary artery disease in patients with stable angina. *Eur J Nucl Med Mol Imaging* 2016;43:1522–1529.
 18. Bischoff B, Hein F, Meyer T, Krebs M, Hadamitzky M, Martinoff S, Schömig A, Hausleiter J. Comparison of sequential and helical scanning for radiation dose and image quality: Results of the Prospective Multicenter Study on Radiation Dose Estimates of Cardiac CT Angiography (PROTECTION) I Study. *AJR Am J Roentgenol* 2010;194:1495–1499.
 19. Bittencourt MS, Hulten E, Ghoshhajra B, O’Leary D, Christman MP, Montana P, Truong QA, Steigner M, Murthy VL, Rybicki FJ, Nasir K, Gowdak LHW, Hainer J, Brady TJ, Di Carli MF, Hoffmann U, Abbara S, Blankstein R. Prognostic value of nonobstructive and obstructive coronary artery disease detected by coronary computed tomography angiography to identify cardiovascular events. *Circ Cardiovasc Imaging* 2014;7:282–291.
 20. Boden WE, O’Rourke RA, Teo KK, Hartigan PM, Maron DJ, Kostuk WJ, Knudtson M, Dada M, Casperson P, Harris CL, Chaitman BR, Shaw L, Gosselin G, Nawaz S, Title LM, Gau G, Blaustein AS, Booth DC, Bates ER, Spertus JA, Berman DS, Mancini GBJ, Weintraub WS. Optimal Medical Therapy with or without PCI for Stable Coronary Disease. *N Engl J Med* 2007;356:1503–1516.
 21. Boersma E. Does time matter? A pooled analysis of randomized clinical trials comparing primary percutaneous coronary intervention and in-hospital fibrinolysis in acute myocardial infarction patients. *Eur Heart J* 2006;27:779–788.
 22. Brown JR, DeVries JT, Piper WD, Robb JF, Hearne MJ, Lee PM Ver, Kellet MA, Watkins MW, Ryan TJ, Silver MT, Ross CS, MacKenzie TA, O’Connor GT, Malenka DJ. Serious renal dysfunction after percutaneous coronary interventions can be predicted. *Am Heart J* 2008;155:260–266.
 23. Brown JR, Malenka DJ, DeVries JT, Robb JF, Jayne JE, Friedman BJ, Hettleman BD, Niles NW, Kaplan A V., Schoolwerth AC, Thompson CA. Transient and persistent renal dysfunction are predictors of survival after percutaneous coronary intervention: Insights from the Dartmouth Dynamic Registry. *Catheter Cardiovasc Interv* 2008;72:347–354.
 24. Brown K. Prognostic value of thallium-201 myocardial perfusion imaging. A diagnostic tool comes of age. *Circulation* 1991;83:363–381.
 25. Budoff MJ, Dowe D, Jollis JG, Gitter M, Sutherland J, Halamert E, Scherer M, Bellinger R, Martin A, Benton R, Delago A, Min JK. Diagnostic performance of 64-multidetector row coronary computed tomographic angiography for evaluation of coronary artery stenosis in individuals without known coronary artery disease: results from the prospective multicenter ACCURACY trial. *J Am Coll Cardiol* 2008;52:1724–1732.
 26. Canadian Diabetes Association Clinical Practice Guidelines Expert Committee R, Goldenberg R, Punthakee Z. Definition, classification and diagnosis of diabetes, prediabetes and metabolic syndrome. *Can J diabetes* 2013;37 Suppl 1:S8–11.

27. Carrabba N, Schuijff JD, de Graaf FR, Parodi G, Maffei E, Valenti R, Palumbo A, Weustink AC, Mollet NR, Accetta G, Cademartiri F, Antoniucci D, Bax JJ. Diagnostic accuracy of 64-slice computed tomography coronary angiography for the detection of in-stent restenosis: A meta-analysis. *J Nucl Cardiol* 2010;17:470–478.
28. Castelli WP, Garrison RJ, Wilson PW, Abbott RD, Kalousdian S, Kannel WB. Incidence of coronary heart disease and lipoprotein cholesterol levels. The Framingham Study. *JAMA* 1986;256:2835–2838.
29. Cavalcante R, Onuma Y, Sotomi Y, Collet C, Thomsen B, Rogers C, Zeng Y, Tenekecioglu E, Asano T, Miyasaki Y, Abdelghani M, Morel M-A, Serruys PW. Non-invasive Heart Team assessment of multivessel coronary disease with coronary computed tomography angiography based on SYNTAX score II treatment recommendations: design and rationale of the randomised SYNTAX III Revolution trial. *EuroIntervention* 2017;12:2001–2008.
30. Cerqueira MD, Weissman NJ, Dilsizian V, Jacobs AK, Kaul S, Laskey WK, Pennell DJ, Rumberger JA, Ryan T, Verani MS, American Heart Association Writing Group on Myocardial Segmentation and Registration for Cardiac Imaging. Standardized myocardial segmentation and nomenclature for tomographic imaging of the heart. A statement for healthcare professionals from the Cardiac Imaging Committee of the Council on Clinical Cardiology of the American Heart Association. *Circulation* 2002;105:539–542.
31. Chen C-C, Chen C-C, Hsieh I-C, Liu Y-C, Liu C-Y, Chan T, Wen M-S, Wan Y-L. The effect of calcium score on the diagnostic accuracy of coronary computed tomography angiography. *Int J Cardiovasc Imaging* 2011;27 Suppl 1:37–42.
32. Chen MY, Rochitte CE, Arbab-Zadeh A, Dewey M, George RT, Miller JM, Niinuma H, Yoshioka K, Kitagawa K, Sakuma H, Laham R, Vavere AL, Cerci RJ, Mehra VC, Nomura C, Kofoed KF, Jinzaki M, Kuribayashi S, Scholte AJ, Laule M, Tan SY, Hoe J, Paul N, Rybicki FJ, Brinker JA, Arai AE, Matheson MB, Cox C, Clouse ME, Di Carli MF, et al. Prognostic Value of Combined CT Angiography and Myocardial Perfusion Imaging versus Invasive Coronary Angiography and Nuclear Stress Perfusion Imaging in the Prediction of Major Adverse Cardiovascular Events: The CORE320 Multicenter Study. *Radiology* 2017;284:55–65.
33. Chow BJW, Ahmed O, Small G, Alghamdi A-A, Yam Y, Chen L, Wells GA. Prognostic Value of CT Angiography in Coronary Bypass Patients. *JACC Cardiovasc Imaging* 2011;4:496–502.
34. Chow BJW, Small G, Yam Y, Chen L, Achenbach S, Al-Mallah M, Berman DS, Budoff MJ, Cademartiri F, Callister TQ, Chang H-J, Cheng V, Chinnaiyan KM, Delago A, Dunning A, Hadamitzky M, Hausleiter J, Kaufmann P, Lin F, Maffei E, Raff GL, Shaw LJ, Villines TC, Min JK. Incremental Prognostic Value of Cardiac Computed Tomography in Coronary Artery Disease Using CONFIRM: CoroNary Computed Tomography Angiography Evaluation for Clinical Outcomes: An International Multicenter Registry. *Circ Cardiovasc Imaging* 2011;4:463–472.
35. Collet C, Chevalier B, Cequier A, Fajadet J, Dominici M, Helqvist S, Boven AJ Van, Dudek D, McClean D, Almeida M, Piek JJ, Tenekecioglu E, Bartorelli A, Windecker S, Serruys PW, Onuma Y. Diagnostic Accuracy of Coronary CT Angiography for the Evaluation of Bioresorbable Vascular Scaffolds. *JACC Cardiovasc Imaging* 2017 Jul 13 [Epub ahead of print]; <http://dx.doi.org/10.1016/j.jcmg.2017.04.013>.
36. Conroy RM, Pyörälä K, Fitzgerald AP, Sans S, Menotti A, Backer G De, Bacquer D De, Ducimetière P, Jousilahti P, Keil U, Njølstad I, Oganov RG, Thomsen T, Tunstall-Pedoe H, Tverdal A, Wedel H, Whincup P, Witheimsen L, Graham IM. Estimation of ten-year risk of fatal cardiovascular disease in Europe: The SCORE project. *Eur Heart J* 2003;24:987–1003.
37. Crea F, Camici PG, Merz CNB. Coronary microvascular dysfunction: An update. *Eur Heart J* 2014;35:1101–1111.
38. D'Agostino RB, Vasan RS, Pencina MJ, Wolf PA, Cobain M, Massaro JM, Kannel WB. General cardiovascular risk profile for use in primary care: The Framingham heart study. *Circulation* 2008;117:743–753.

39. Danad I, Raijmakers PG, Appelman YE, Harms HJ, Haan S de, Oever MLP van den, Heymans MW, Tulevski II, Kuijk C van, Hoekstra OS, Lammertsma AA, Lubberink M, Rossum AC van, Knaapen P. Hybrid Imaging Using Quantitative H215O PET and CT-Based Coronary Angiography for the Detection of Coronary Artery Disease. *J Nucl Med* 2013;54:55–63.
40. Danad I, Raijmakers PG, Harms HJ, Kuijk C Van, Royen N Van, Diamant M, Lammertsma AA, Lubberink M, Rossum AC Van, Knaapen P. Effect of cardiac hybrid 15O-water PET/CT imaging on downstream referral for invasive coronary angiography and revascularization rate. *Eur Heart J Cardiovasc Imaging* 2014;15:170–179.
41. Danad I, Szymonifka J, Twisk JWR, Norgaard BL, Zarins CK, Knaapen P, Min JK. Diagnostic performance of cardiac imaging methods to diagnose ischaemia-causing coronary artery disease when directly compared with fractional flow reserve as a reference standard: A meta-analysis. *Eur Heart J* 2017;38:991–998.
42. Danad I, Uusitalo V, Kero T, Saraste A, Raijmakers PG, Lammertsma AA, Heymans MW, Kajander SA, Pietilä M, James S, Sörensen J, Knaapen P, Knuuti J. Quantitative assessment of myocardial perfusion in the detection of significant coronary artery disease: Cutoff values and diagnostic accuracy of quantitative [15O]H2O PET imaging. *J Am Coll Cardiol* 2014;64:1464–1475.
43. de Araújo Gonçalves P, Garcia-Garcia HM, Dores H, Carvalho MS, Sousa PJ, Marques H, Ferreira A, Cardim N, Teles RC, Raposo L, Gabriel HM, Almeida MS, Aleixo A, Carmo MM, Machado FP, Mendes M. Coronary computed tomography angiography-Adapted Leaman score as a tool to noninvasively quantify total coronary atherosclerotic burden. *Int J Cardiovasc Imaging* 2013;29:1575–1584.
44. De Bruyne B, Fearon WF, Pijls NHJ, Barbato E, Tonino P, Piroth Z, Jagic N, Möbius-Winkler S, Rioufol G, Witt N, Kala P, MacCarthy P, Engström T, Oldroyd K, Mavromatis K, Manoharan G, Verlee P, Frobert O, Curzen N, Johnson JB, Limacher A, Nüesch E, Jüni P. Fractional Flow Reserve-Guided PCI for Stable Coronary Artery Disease. *N Engl J Med* 2014;371:1208–1217.
45. De Bruyne B, Hersbach F, Pijls NH, Bartunek J, Bech JW, Heyndrickx GR, Gould KL, Wijns W. Abnormal epicardial coronary resistance in patients with diffuse atherosclerosis but ‘Normal’ coronary angiography. *Circulation* 2001;104:2401–2406.
46. De Bruyne B, Pijls NHJ, Kalesan B, Barbato E, Tonino PAL, Piroth Z, Jagic N, Möbius-Winkler S, Rioufol G, Witt N, Kala P, MacCarthy P, Engström T, Oldroyd KG, Mavromatis K, Manoharan G, Verlee P, Frobert O, Curzen N, Johnson JB, Jüni P, Fearon WF, Fearon WF, FAME 2 Trial Investigators. Fractional Flow Reserve-Guided PCI versus Medical Therapy in Stable Coronary Disease. *N Engl J Med* 2012;367:991–1001.
47. de Graaf MA, Broersen A, Ahmed W, Kitslaar PH, Dijkstra J, Kroft LJ, Delgado V, Bax JJ, Reiber JHC, Scholte AJ. Feasibility of an Automated Quantitative Computed Tomography Angiography-Derived Risk Score for Risk Stratification of Patients With Suspected Coronary Artery Disease. *Am J Cardiol* 2014;113:1947–1955.
48. de Graaf MA, Broersen A, Kitslaar PH, Roos CJ, Dijkstra J, Lelieveldt BPF, Jukema JW, Schalij MJ, Delgado V, Bax JJ, Reiber JHC, Scholte AJ. Automatic quantification and characterization of coronary atherosclerosis with computed tomography coronary angiography: Cross-correlation with intravascular ultrasound virtual histology. *Int J Cardiovasc Imaging* 2013;29:1177–1190.
49. Deb S, Wijesundera HC, Ko DT, Tsubota H, Hill S, Femes SE. Coronary artery bypass graft surgery vs percutaneous interventions in coronary revascularization: A systematic review. *JAMA* 2013;310:2086–2095.
50. deKemp RA, Renaud JM, Klein R, Beanlands RSB. Radionuclide Tracers for Myocardial Perfusion Imaging and Blood Flow Quantification. *Cardiol Clin* 2016;34:37–46.
51. Deseive S, Pugliese F, Meave A, Alexanderson E, Martinoff S, Hadamitzky M, Massberg S, Hausleiter J. Image quality and radiation dose of a prospectively electrocardiography-triggered high-pitch data acquisition strategy for coronary CT angiography: The multicenter, randomized

- PROTECTION IV study. *J Cardiovasc Comput Tomogr* 2015;9:278–285.
52. Dharampal AS, Papadopoulou SL, Rossi A, Meijboom WB, Weustink A, Dijkshoorn M, Nieman K, Boersma EH, Feijter PJ de, Krestin GP. Diagnostic performance of computed tomography coronary angiography to detect and exclude left main and/or three-vessel coronary artery disease. *Eur Radiol* 2013;23:2934–2943.
53. Di Carli M, Czernin J, Hoh CK, Gerbaudo VH, Brunken RC, Huang SC, Phelps ME, Schelbert HR. Relation among stenosis severity, myocardial blood flow, and flow reserve in patients with coronary artery disease. *Circulation* 1995;91:1944–1951.
54. Di Carli M, Dorbala S, Curillova Z, Kwong RJ, Goldhaber SZ, Rybicki FJ, Hachamovitch R. Relationship between CT coronary angiography and stress perfusion imaging in patients with suspected ischemic heart disease assessed by integrated PET-CT imaging. *J Nucl Cardiol* 2007;14:799–809.
55. Di Carli M, Murthy V. Cardiac PET/CT for the evaluation of known or suspected coronary artery disease. *Radiographics* 2011;31:1239–1254.
56. Dorbala S, Di Carli MF, Beanlands RS, Merhige ME, Williams BA, Veledar E, Chow BJW, Min JK, Pencina MJ, Berman DS, Shaw LJ. Prognostic value of stress myocardial perfusion positron emission tomography: Results from a multicenter observational registry. *J Am Coll Cardiol* 2013;61:176–184.
57. Dorbala S, Hachamovitch R, Curillova Z, Thomas D, Vangala D, Kwong RY, Di Carli MF. Incremental Prognostic Value of Gated Rb-82 Positron Emission Tomography Myocardial Perfusion Imaging Over Clinical Variables and Rest LVEF. *JACC Cardiovasc Imaging* 2009;2:846–854.
58. Einstein AJ. Radiation risk from coronary artery disease imaging: how do different diagnostic tests compare? *Heart* 2008;94:1519–1521.
59. El-Hajjar M, Bashir I, Khan M, Min J, Torosoff M, DeLago A. Incidence of Contrast-Induced Nephropathy in Patients With Chronic Renal Insufficiency Undergoing Multidetector Computed Tomographic Angiography Treated With Preventive Measures. *Am J Cardiol* 2008;102:353–356.
60. Emond M, Mock MB, Davis KB, Fisher LD, Holmes DR, Chaitman BR, Kaiser GC, Alderman E, Killip T. Long-term survival of medically treated patients in the Coronary Artery Surgery Study (CASS) Registry. *Circulation* 1994;90:2645–2657.
61. Engbers EM, Timmer JR, Ottervanger JP, Mouden M, Knollema S, Jager PL. Prognostic Value of Coronary Artery Calcium Scoring in Addition to Single-Photon Emission Computed Tomographic Myocardial Perfusion Imaging in Symptomatic Patients. *Circ Cardiovasc Imaging* 2016;9:e003966.
62. Engbers EM, Timmer JR, Ottervanger JP, Mouden M, Oostdijk AHJ, Knollema S, Jager PL. Sequential SPECT/CT imaging for detection of coronary artery disease in a large cohort: evaluation of the need for additional imaging and radiation exposure. *J Nucl Cardiol* 2017;24:212–223.
63. Fiechter M, Ghadri JR, Gebhard C, Fuchs TA, Pazhenkottil AP, Nkoulou RN, Herzog BA, Wyss CA, Gaemperli O, Kaufmann PA. Diagnostic Value of ¹³N-Ammonia Myocardial Perfusion PET: Added Value of Myocardial Flow Reserve. *J Nucl Med* 2012;53:1230–1234.
64. Fihn SD, Blankenship JC, Alexander KP, Bittl JA, Byrne JG, Fletcher BJ, Fonarow GC, Lange RA, Levine GN, Maddox TM, Naidu SS, Ohman EM, Smith PK. 2014 ACC/AHA/AATS/PCNA/SCAI/STS focused update of the guideline for the diagnosis and management of patients with stable ischemic heart disease. *Circulation* 2014;130:1749–1767.
65. Fihn SD, Gardin JM, Abrams J, Berra K, Blankenship JC, Dallas AP, Douglas PS, Foody JM, Gerber TC, Hinderliter AL, King SB, Kligfield PD, Krumholz HM, Kwong RYK, Lim MJ, Linderbaum JA, MacK MJ, Munger MA, Prager RL, Sabik JF, Shaw LJ, Sikkema JD, Smith CR, Smith SC, Spertus JA, Williams S V. 2012 ACCF/AHA/ACP/AATS/PCNA/SCAI/STS guideline for the diagnosis and management of patients with stable ischemic heart disease. *J Am Coll Cardiol* 2012;60:e44–c164.

66. Flotats A, Knuuti J, Gutberlet M, Marcassa C, Bengel FM, Kaufmann PA, Rees MR, Hesse B. Hybrid cardiac imaging: SPECT/CT and PET/CT. A joint position statement by the European Association of Nuclear Medicine (EANM), the European Society of Cardiac Radiology (ESCR) and the European Council of Nuclear Cardiology (ECNC). *Eur J Nucl Med Mol Imaging* 2011;38:201–212.
67. Fox KAA, Clayton TC, Damman P, Pocock SJ, Winter RJ de, Tijssen JGP, Lagerqvist B, Wallentin L. Long-Term Outcome of a Routine Versus Selective Invasive Strategy in Patients With Non-ST-Segment Elevation Acute Coronary Syndrome. A Meta-Analysis of Individual Patient Data. *J Am Coll Cardiol* 2010;55:2435–2445.
68. Frishman WH, Glasser S, Stone P, Deedwania PC, Johnson M, Fakouhi TD. Comparison of controlled-onset, extended-release verapamil with amlodipine and amlodipine plus atenolol on exercise performance and ambulatory ischemia in patients with chronic stable angina pectoris. *Am J Cardiol* 1999;83:507–514.
69. Gaemperli O, Bengel FM, Kaufmann PA. Cardiac hybrid imaging. *Eur Heart J* 2011;32:2100–2108.
70. Gaemperli O, Schepis T, Kalff V, Namdar M, Valenta I, Stefani L, Desbiolles L, Leschka S, Husmann L, Alkadhi H, Kaufmann PA. Validation of a new cardiac image fusion software for three-dimensional integration of myocardial perfusion SPECT and stand-alone 64-slice CT angiography. *Eur J Nucl Med Mol Imaging* 2007;34:1097–1106.
71. Gaemperli O, Valenta I, Schepis T, Husmann L, Scheffel H, Desbiolles L, Leschka S, Alkadhi H, Kaufmann PA. Coronary 64-slice CT angiography predicts outcome in patients with known or suspected coronary artery disease. *Eur Radiol* 2008;18:1162–1173.
72. Geleijnse ML, Elhendy A, Fioretti PM, Roelandt JRTC. Dobutamine stress myocardial perfusion imaging. *J Am Coll Cardiol* 2000;36:2017–2027.
73. Genders TSS, Steyerberg EW, Alkadhi H, Leschka S, Desbiolles L, Nieman K, Galema TW, Meijboom WB, Mollet NR, Feyter PJ De, Cademartiri F, Maffei E, Dewey M, Zimmermann E, Laule M, Pugliese F, Barbagallo R, Sinitsyn V, Bogaert J, Goetschalckx K, Schoepf UJ, Rowe GW, Schuijf JD, Bax JJ, de Graaf FR, Knuuti J, Kajander S, Mieghem CAG Van, Meijls MFL, Cramer MJ, et al. A clinical prediction rule for the diagnosis of coronary artery disease: Validation, updating, and extension. *Eur Heart J* 2011;32:1316–1330.
74. Ghadri JR, Fiechter M, Fuchs TA, Scherrer A, Stehli J, Gebhard C, Kläser B, Gaemperli O, Lüscher TF, Templin C, Kaufmann PA. Registry for the Evaluation of the PROgnostic value of a novel integrated imaging approach combining Single Photon Emission Computed Tomography with coronary calcification imaging (REPROSPECT). *Eur Heart J Cardiovasc Imaging* 2013;14:374–380.
75. Goff DCJ, Lloyd-Jones DM, Bennett G, Coady S, D'Agostino RB, Gibbons R, Greenland P, Lackland DT, Levy D, O'Donnell CJ, Robinson JG, Schwartz JS, Shero ST, Smith SC, Sorlie P, Stone NJ, Wilson PWF, Jordan HS, Nevo L, Wnek J, Anderson JL, Halperin JL, Albert NM, Bozkurt B, Brindis RG, Curtis LH, DeMets D, Hochman JS, Kovacs RJ, Ohman EM, et al. 2013 ACC/AHA Guideline on the Assessment of Cardiovascular Risk. *Circulation* 2014;129:S49–S73.
76. Gould KL, Johnson NP. Physiologic severity of diffuse coronary artery disease hidden high risk. *Circulation* 2015;131:4–6.
77. Gowd BMP, Heller G V., Parker MW. Stress-only SPECT myocardial perfusion imaging: A review. *J Nucl Cardiol* 2014;21:1200–1212.
78. Groves AM, Speechly-Dick ME, Kayani I, Pugliese F, Endozo R, McEwan J, Menezes LJ, Habib SB, Prvulovich E, Ell PJ. First experience of combined cardiac PET/64-detector CT angiography with invasive angiographic validation. *Eur J Nucl Med Mol Imaging* 2009;36:2027–2033.
79. Hachamovitch R, Berman DS, Shaw LJ, Kiat H, Cohen I, Cabico JA, Friedman J, Diamond GA. Incremental prognostic value of myocardial perfusion single photon emission computed tomography for the prediction of cardiac death: differential stratification for risk of cardiac death and myocardial infarction. *Circulation* 1998;97:535–543.
80. Hachamovitch R, Hayes SW, Friedman JD,

- Cohen I, Berman DS. Comparison of the short-term survival benefit associated with revascularization compared with medical therapy in patients with no prior coronary artery disease undergoing stress myocardial perfusion single photon emission computed tomography. *Circulation* 2003;107:2900–2906.
81. Hachamovitch R, Rozanski A, Shaw LJ, Stone GW, Thomson LEJ, Friedman JD, Hayes SW, Cohen I, Germano G, Berman DS. Impact of ischaemia and scar on the therapeutic benefit derived from myocardial revascularization vs. medical therapy among patients undergoing stress-rest myocardial perfusion scintigraphy. *Eur Heart J* 2011;32:1012–1024.
82. Hadamitzky M, Achenbach S, Al-Mallah M, Berman D, Budoff M, Cademartiri F, Callister T, Chang HJ, Cheng V, Chinnaiyan K, Chow BJW, Cury R, Delago A, Dunning A, Feuchtner G, Gomez M, Kaufmann P, Kim YJ, Leipsic J, Lin FY, Maffei E, Min JK, Raff G, Shaw LJ, Villines TC, Hausleiter J. Optimized prognostic score for coronary computed tomographic angiography: Results from the CONFIRM registry. *J Am Coll Cardiol* 2013;62:468–476.
83. Hadamitzky M, Freißmuth B, Meyer T, Hein F, Kastrati A, Martinoff S, Schömig A, Hausleiter J. Prognostic Value of Coronary Computed Tomographic Angiography for Prediction of Cardiac Events in Patients With Suspected Coronary Artery Disease. *JACC Cardiovasc Imaging* 2009;2:404–411.
84. Hadamitzky M, Täubert S, Deseive S, Byrne RA, Martinoff S, Schömig A, Hausleiter J. Prognostic value of coronary computed tomography angiography during 5 years of follow-up in patients with suspected coronary artery disease. *Eur Heart J* 2013;34:3277–3285.
85. Hajjiri MM, Leavitt MB, Zheng H, Spooner AE, Fischman AJ, Gewirtz H. Comparison of Positron Emission Tomography Measurement of Adenosine-Stimulated Absolute Myocardial Blood Flow Versus Relative Myocardial Tracer Content for Physiological Assessment of Coronary Artery Stenosis Severity and Location. *JACC Cardiovasc Imaging* 2009;2:751–758.
86. Hamm CW, Bassand J-P, Agewall S, Bax J, Boersma E, Bueno H, Caso P, Dudek D, Gielen S, Huber K, Ohman M, Petric MC, Sonntag F, Uva MS, Storey RF, Wijns W, Zahger D, ESC Committee for Practice Guidelines JJ, Auricchio A, Baumgartner H, Ceconi C, Dean V, Deaton C, Fagard R, Funck-Brentano C, Hasdai D, Hoes A, Knuuti J, Kolh P, McDonagh T, et al. ESC Guidelines for the management of acute coronary syndromes in patients presenting without persistent ST-segment elevation. *Eur Heart J* 2011;32:2999–3054.
87. Hausleiter J, Martinoff S, Hadamitzky M, Martuscelli E, Pschierer I, Feuchtner GM, Cataln-Sanz P, Czermak B, Meyer TS, Hein F, Bischoff B, Kuse M, Schmig A, Achenbach S. Image Quality and Radiation Exposure with a Low Tube Voltage Protocol for Coronary CT Angiography: Results of the PROTECTION II Trial. *JACC Cardiovasc Imaging* 2010;3:1113–1123.
88. Hausleiter J, Meyer TS, Martuscelli E, Spagnolo P, Yamamoto H, Carrascosa P, Anger T, Lehmkuhl L, Alkadhi H, Martinoff S, Hadamitzky M, Hein F, Bischoff B, Kuse M, Schömig A, Achenbach S. Image quality and radiation exposure with prospectively ECG-triggered axial scanning for coronary CT angiography: The multicenter, multivendor, randomized PROTECTION-III study. *JACC Cardiovasc Imaging* 2012;5:484–493.
89. Hecht H, Blaha MJ, Berman DS, Nasir K, Budoff M, Leipsic J, Blankstein R, Narula J, Rumberger J, Shaw LJ. Clinical indications for coronary artery calcium scoring in asymptomatic patients: Expert consensus statement from the Society of Cardiovascular Computed Tomography. *J Cardiovasc Comput Tomogr* 2017;11:157–168.
90. Heidenreich PA, McDonald KM, Hastie T, Fadel B, Hagan V, Lee BK, Hlatky MA. Meta-analysis of trials comparing beta-blockers, calcium antagonists, and nitrates for stable angina. *JAMA* 1999;281:1927–1936.
91. Henzlova MJ, Duvall WL, Einstein AJ, Travin MI, Verberne HJ. ASNC imaging guidelines for SPECT nuclear cardiology procedures: Stress, protocols, and tracers. *J Nucl Cardiol* 2016;23:606–639.
92. Herzog BA, Husman L, Valenta I, Gaemperli O, Siegrist PT, Tay FM, Burkhard N, Wyss CA, Kaufmann PA. Long-Term Prognostic Value of ¹³N-Ammonia

- Myocardial Perfusion Positron Emission Tomography. Added Value of Coronary Flow Reserve. *J Am Coll Cardiol* 2009;54:150–156.
93. Higgins JP, Williams G, Nagel JS, Higgins JA. Left bundle-branch block artifact on single photon emission computed tomography with technetium Tc 99m (Tc-99m) agents: Mechanisms and a method to decrease false-positive interpretations. *Am Heart J* 2006;152:619–626.
 94. Hillis LD, Smith PK, Anderson JL, Bittl JA, Bridges CR, Byrne JG, Cigarroa JE, DiSesa VJ, Hiratzka LF, Hutter AM, Jessen ME, Keeley EC, Lahey SJ, Lange RA, London MJ, Mack MJ, Patel MR, Puskas JD, Sabik JF, Selnes O, Shahian DM, Trost JC, Winniford MD. 2011 ACCF/AHA Guideline for Coronary Artery Bypass Graft Surgery: A Report of the American College of Cardiology Foundation/American Heart Association Task Force on Practice Guidelines. *Circulation* 2011;124:e652–e735.
 95. Hjelm Dahl P, Eriksson S V., Held C, Forslund L, Näsman P, Rehnqvist N. Favourable long term prognosis in stable angina pectoris: An extended follow up of the angina prognosis study in Stockholm (APSIS). *Heart* 2006;92:177–182.
 96. Hou Z, Lu B, Gao Y, Jiang S, Wang Y, Li W, Budoff MJ. Prognostic Value of Coronary CT Angiography and Calcium Score for Major Adverse Cardiac Events in Outpatients. *JACC Cardiovasc Imaging* 2012;5:990–999.
 97. Hsu B, Chen FC, Wu TC, Huang WS, Hou PN, Chen CC, Hung GU. Quantitation of myocardial blood flow and myocardial flow reserve with ^{99m}Tc-sestamibi dynamic SPECT/CT to enhance detection of coronary artery disease. *Eur J Nucl Med Mol Imaging* 2014;41:2294–2306.
 98. Huang J-Y, Huang C-K, Yen R-F, Wu H-Y, Tu Y-K, Cheng M-F, Lu C-C, Tzen K-Y, Chien K-L, Wu Y-W. Diagnostic Performance of Attenuation-Corrected Myocardial Perfusion Imaging for Coronary Artery Disease: A Systematic Review and Meta-Analysis. *J Nucl Med* 2016;57:1893–1898.
 99. Huisman MC, Higuchi T, Reder S, Nekolla SG, Poethko T, Wester H-J, Ziegler SI, Casebier DS, Robinson SP, Schwaiger M. Initial Characterization of an 18F-Labeled Myocardial Perfusion Tracer. *J Nucl Med* 2008;49:630–636.
 100. Hulten EA, Carbonaro S, Petrillo SP, Mitchell JD, Villines TC. Prognostic value of cardiac computed tomography angiography: A systematic review and meta-analysis. *J Am Coll Cardiol* 2011;57:1237–1247.
 101. Hulten EA, Pickett C, Bittencourt MS, Villines TC, Petrillo S, Di Carli MF, Blankstein R. Outcomes after coronary computed tomography angiography in the emergency department: A systematic review and meta-analysis of randomized, controlled trials. *J Am Coll Cardiol* 2013;61:880–892.
 102. Jaarsma C, Leiner T, Bekkers SC, Crijns HJ, Wildberger JE, Nagel E, Nelemans PJ, Schalla S. Diagnostic performance of noninvasive myocardial perfusion imaging using single-photon emission computed tomography, cardiac magnetic resonance, and positron emission tomography imaging for the detection of obstructive coronary artery disease: A meta-anal. *J Am Coll Cardiol* 2012;59:1719–1728.
 103. Javadi MS, Lautamäki R, Merrill J, Voicu C, Epley W, McBride G, Bengel FM. Definition of vascular territories on myocardial perfusion images by integration with true coronary anatomy: a hybrid PET/CT analysis. *J Nucl Med* 2010;51:198–203.
 104. Jespersen L, Hvelplund A, Abildstrøm SZ, Pedersen F, Galatius S, Madsen JK, Jørgensen E, Kelbæk H, Prescott E. Stable angina pectoris with no obstructive coronary artery disease is associated with increased risks of major adverse cardiovascular events. *Eur Heart J* 2012;33:734–744.
 105. Johnson NP, Tóth GG, Lai D, Zhu H, Açar G, Agostoni P, Appelman Y, Arslan F, Barbato E, Chen SL, Serafino L Di, Domínguez-Franco AJ, Dupouy P, Esen AM, Esen ÖB, Hamilos M, Iwasaki K, Jensen LO, Jiménez-Navarro MF, Katritsis DG, Kocaman SA, Koo BK, López-Palop R, Lorin JD, Miller LH, Muller O, Nam CW, Oud N, Puymirat E, Rieber J, et al. Prognostic value of fractional flow reserve: Linking physiologic severity to clinical outcomes. *J Am Coll Cardiol* 2014;64:1641–1654.
 106. Juonala M, Viikari JSA, Laitinen T, Marniemi J, Helenius H, Rönnemaa T,

- Raitakari OT. Interrelations between brachial endothelial function and carotid intima-media thickness in young adults: the cardiovascular risk in young Finns study. *Circulation* 2004;110:2918–2923.
107. Kajander S, Joutsiniemi E, Saraste M, Pietilä M, Ukkonen H, Saraste A, Sipilä HT, Teräs M, Mäki M, Airaksinen J, Hartiala J, Knuuti J. Cardiac positron emission tomography/computed tomography imaging accurately detects anatomically and functionally significant coronary artery disease. *Circulation* 2010;122:603–613.
108. Kajander S, Joutsiniemi E, Saraste M, Pietilä M, Ukkonen H, Saraste A, Sipilä H, Teräs M, Mäki M, Airaksinen J, Hartiala J, Knuuti J. Clinical value of absolute quantification of myocardial perfusion with ¹⁵O-water in coronary artery disease. *Circ Cardiovasc Imaging* 2011;4:678–684.
109. Kajander S, Ukkonen H, Sipilä H, Teräs M, Knuuti J. Low radiation dose imaging of myocardial perfusion and coronary angiography with a hybrid PET/CT scanner. *Clin Physiol Funct Imaging* 2009;29:81–88.
110. Katzberg RW, Lamba R. Contrast-Induced Nephropathy after Intravenous Administration: Fact or Fiction? *Radiol Clin North Am* 2009;47:789–800.
111. Katzberg RW, Newhouse JH. Intravenous contrast medium-induced nephrotoxicity: is the medical risk really as great as we have come to believe? *Radiology* 2010;256:21–28.
112. Kaufmann PA. Cardiac hybrid imaging: State-of-the-art. *Ann Nucl Med* 2009;23:325–331.
113. Kawai H, Sarai M, Motoyama S, Ito H, Takada K, Harigaya H, Takahashi H, Hashimoto S, Takagi Y, Ando M, Anno H, Ishii J, Murohara T, Ozaki Y. A combination of anatomical and functional evaluations improves the prediction of cardiac event in patients with coronary artery bypass. *BMJ Open* 2013;3:e003474.
114. Kitta Y, Obata J, Nakamura T, Hirano M, Kodama Y, Fujioka D, Saito Y, Kawabata K, Sano K, Kobayashi T, Yano T, Nakamura K, Kugiyama K. Persistent Impairment of Endothelial Vasomotor Function Has a Negative Impact on Outcome in Patients With Coronary Artery Disease. *J Am Coll Cardiol* 2009;53:323–330.
115. Knaapen P, Bondarenko O, Beek AM, Götte MJW, Boellaard R, Weerdt AP van der, Visser CA, Rossum AC van, Lammertsma AA, Visser FC. Impact of scar on water-perfusible tissue index in chronic ischemic heart disease: Evaluation with PET and contrast-enhanced MRI. *Mol Imaging Biol* 2006;8:245–251.
116. Knuuti J, Kajander S, Mäki M, Ukkonen H. Quantification of myocardial blood flow will reform the detection of CAD. *J Nucl Cardiol* 2009;16:497–506.
117. Knuuti J, Saraste A. Combined functional and anatomical imaging for the detection and guiding the therapy of coronary artery disease. *Eur Heart J* 2013;34:1954–1957.
118. Koh KK. Effects of statins on vascular wall: vasomotor function, inflammation, and plaque stability. *Cardiovasc Res* 2000;47:648–657.
119. Kondo T, Kumamaru KK, Fujimoto S, Matsutani H, Sano T, Takase S, Rybicki FJ. Prospective ECG-gated coronary 320-MDCT angiography with absolute acquisition delay strategy for patients with persistent atrial fibrillation. *AJR Am J Roentgenol* 2013;201:1197–1203.
120. Kooiman J, Pasha SM, Zondag W, Sijpkens YWJ, Molen AJ Van Der, Huisman M V., Dekkers OM. Meta-analysis: Serum creatinine changes following contrast enhanced CT imaging. *Eur J Radiol* 2012;81:2554–2561.
121. Ladenheim ML, Pollock BH, Rozanski A, Berman DS, Staniloff HM, Forrester JS, Diamond GA. Extent and severity of myocardial hypoperfusion as predictors of prognosis in patients with suspected coronary artery disease. *J Am Coll Cardiol* 1986;7:464–471.
122. Lauer MS, Lytle B, Pashkow F, Snader CE, Marwick TH. Prediction of death and myocardial infarction by screening with exercise-thallium testing after coronary-artery-bypass grafting. *Lancet* 1998;351:615–622.
123. Leaman DM, Brower RW, Meester GT, Serruys P, Brand M van den. Coronary artery atherosclerosis: severity of the disease,

- severity of angina pectoris and compromised left ventricular function. *Circulation* 1981;63:285–299.
124. Lee H, Yoon YE, Park J-B, Kim H-L, Park HE, Lee S-P, Kim H-K, Choi S-Y, Kim Y-J, Cho G-Y, Zo J-H, Sohn D-W. The Incremental Prognostic Value of Cardiac Computed Tomography in Comparison with Single-Photon Emission Computed Tomography in Patients with Suspected Coronary Artery Disease. *PLoS One* 2016;11:e0160188.
 125. Lee JM, Kim CH, Koo B-K, Hwang D, Park J, Zhang J, Tong Y, Jeon K-H, Bang J-I, Suh M, Paeng JC, Cheon GJ, Na S-H, Ahn J-M, Park S-J, Kim H-S. Integrated Myocardial Perfusion Imaging Diagnostics Improve Detection of Functionally Significant Coronary Artery Stenosis by ¹³N-ammonia Positron Emission Tomography. *Circ Cardiovasc Imaging* 2016;9:e004768.
 126. Leipsic J, Abbara S, Achenbach S, Cury R, Earls JP, Mancini GJ, Nieman K, Pontone G, Raff GL. SCCT guidelines for the interpretation and reporting of coronary CT angiography: a report of the Society of Cardiovascular Computed Tomography Guidelines Committee. *J Cardiovasc Comput Tomogr* 2014;8:342–358.
 127. Levey AS, Stevens LA, Schmid CH, Zhang YL, Castro AF, Feldman HI, Kusek JW, Eggers P, Lente F Van, Greene T, Coresh J, CKD-EPI (Chronic Kidney Disease Epidemiology Collaboration). A new equation to estimate glomerular filtration rate. *Ann Intern Med* 2009;150:604–612.
 128. Li S, Tang X, Peng L, Luo Y, Zhao Y, Chen L, Dong R, Zhu J, Chen Y, Liu J. A head-to-head comparison of homocysteine and cystatin C as pre-procedure predictors for contrast-induced nephropathy in patients undergoing coronary computed tomography angiography. *Clin Chim Acta* 2015;444:86–91.
 129. Libby P. Mechanisms of acute coronary syndromes and their implications for therapy. *N Engl J Med* 2013;368:2004–2013.
 130. Liga R, Vontobel J, Rovai D, Marinelli M, Caselli C, Pietila M, Teresinska A, Aguadé-Bruix S, Pizzi MN, Todiere G, Gimelli A, Chiappino D, Marraccini P, Schroeder S, Drosch T, Poddighe R, Casolo G, Anagnostopoulos C, Pugliese F, Rouzet F, Guludec D Le, Cappelli F, Valente S, Gensini GF, Zawaideh C, Capitanio S, Sambuceti G, Marsico F, Filardi PP, Fernández-Golfín C, et al. Multicentre multi-device hybrid imaging study of coronary artery disease: Results from the Evaluation of INtegrated Cardiac Imaging for the Detection and Characterization of Ischaemic Heart Disease (EVINCI) hybrid imaging population. *Eur Heart J Cardiovasc Imaging* 2016;17:951–960.
 131. Lima RSL, Watson DD, Goode AR, Siadaty MS, Ragosta M, Beller GA, Samady H. Incremental value of combined perfusion and function over perfusion alone by gated SPECT myocardial perfusion imaging for detection of severe three-vessel coronary artery disease. *J Am Coll Cardiol* 2003;42:64–70.
 132. Mahajan N, Polavaram L, Vankayala H, Ference B, Wang Y, Ager J, Kovach J, Afonso L. Diagnostic accuracy of myocardial perfusion imaging and stress echocardiography for the diagnosis of left main and triple vessel coronary artery disease: a comparative meta-analysis. *Heart* 2010;96:956–966.
 133. Mark DB, Berman DS, Budoff MJ, Carr JJ, Gerber TC, Hecht HS, Hlatky MA, Hodgson JMB, Lauer MS, Miller JM, Morin RL, Mukherjee D, Poon M, Rubin GD, Schwartz RS. ACCF/ACR/AHA/NASCI/SAIP/SCAI/SCCT 2010 Expert Consensus Document on Coronary Computed Tomographic Angiography. A Report of the American College of Cardiology Foundation Task Force on Expert Consensus Documents. *J Am Coll Cardiol* 2010;55:2663–2699.
 134. Marwan M, Achenbach S, Korosoglou G, Schermund A, Schneider S, Bruder O, Hausleiter J, Schroeder S, Barth S, Kerber S, Leber A, Moshage W, Senges J. German cardiac CT registry: indications, procedural data and clinical consequences in 7061 patients undergoing cardiac computed tomography. *Int J Cardiovasc Imaging* 2017 Dec 1 [Epub ahead of print]; <http://dx.doi.org/10.1007/s10554-017-1282-0>.
 135. Matsuo S, Nakajima K, Akhter N, Wakabayashi H, Taki J, Okuda K, Kinuya S. Clinical usefulness of novel cardiac MDCT/SPECT fusion image. *Ann Nucl Med*

- 2009;23:579–586.
136. Maurovich-Horvat P, Ferencik M, Voros S, Merkely B, Hoffmann U. Comprehensive plaque assessment by coronary CT angiography. *Nat Rev Cardiol* 2014;11:390–402.
137. Mc Ardle BA, Dowsley TF, Dekemp RA, Wells GA, Beanlands RS. Does rubidium-82 PET have superior accuracy to SPECT perfusion imaging for the diagnosis of obstructive coronary disease?: A systematic review and meta-analysis. *J Am Coll Cardiol* 2012;60:1828–1837.
138. McCullough PA, Adam A, Becker CR, Davidson C, Lameire N, Stacul F, Tumlin J, CIN Consensus Working Panel. Epidemiology and prognostic implications of contrast-induced nephropathy. *Am J Cardiol* 2006;98:5K–13K.
139. McCullough PA, Sandberg KR. Epidemiology of contrast-induced nephropathy. *Rev Cardiovasc Med* 2003;4 Suppl 5:S3-9.
140. McDonald JS, McDonald RJ, Comin J, Williamson EE, Katzberg RW, Murad MH, Kallmes DF. Frequency of acute kidney injury following intravenous contrast medium administration: a systematic review and meta-analysis. *Radiology* 2013;267:119–128.
141. McDonald RJ, McDonald JS, Bida JP, Carter RE, Fleming CJ, Misra S, Williamson EE, Kallmes DF. Intravenous Contrast Material–induced Nephropathy: Causal or Coincident Phenomenon? *Radiology* 2013;267:106–118.
142. Meijboom WB, Meijs MFL, Schuijf JD, Cramer MJ, Mollet NR, Mieghem CAG van, Nieman K, van Werkhoven JM, Pundziute G, Weustink AC, Vos AM de, Pugliese F, Rensing B, Jukema JW, Bax JJ, Prokop M, Doevendans PA, Hunink MGM, Krestin GP, Feyter PJ de. Diagnostic Accuracy of 64-Slice Computed Tomography Coronary Angiography. A Prospective, Multicenter, Multivendor Study. *J Am Coll Cardiol* 2008;52:2135–2144.
143. Meijboom WB, Mieghem CAG van, Mollet NR, Pugliese F, Weustink AC, Pelt N van, Cademartiri F, Nieman K, Boersma E, Jaegere P de, Krestin GP, Feyter PJ de. 64-Slice Computed Tomography Coronary Angiography in Patients With High, Intermediate, or Low Pretest Probability of Significant Coronary Artery Disease. *J Am Coll Cardiol* 2007;50:1469–1475.
144. Meijboom WB, Mieghem CAG van, Pelt N van, Weustink A, Pugliese F, Mollet NR, Boersma E, Regar E, Geuns RJ van, Jaegere PJ de, Serruys PW, Krestin GP, Feyter PJ de. Comprehensive Assessment of Coronary Artery Stenoses. Computed Tomography Coronary Angiography Versus Conventional Coronary Angiography and Correlation With Fractional Flow Reserve in Patients With Stable Angina. *J Am Coll Cardiol* 2008;52:636–643.
145. Min JK, Dunning A, Lin FY, Achenbach S, Al-Mallah M, Budoff MJ, Cademartiri F, Callister TQ, Chang H-J, Cheng V, Chinnaiyan K, Chow BJW, Delago A, Hadamitzky M, Hausleiter J, Kaufmann P, Maffei E, Raff G, Shaw LJ, Villines T, Berman DS, CONFIRM Investigators. Age- and sex-related differences in all-cause mortality risk based on coronary computed tomography angiography findings results from the International Multicenter CONFIRM (Coronary CT Angiography Evaluation for Clinical Outcomes: An International Multicenter). *J Am Coll Cardiol* 2011;58:849–860.
146. Min JK, Shaw LJ, Devereux RB, Okin PM, Weinsaft JW, Russo DJ, Lippolis NJ, Berman DS, Callister TQ. Prognostic Value of Multidetector Coronary Computed Tomographic Angiography for Prediction of All-Cause Mortality. *J Am Coll Cardiol* 2007;50:1161–1170.
147. Montalescot G, Sechtem U, Achenbach S, Andreotti F, Arden C, Budaj A, Bugiardini R, Crea F, Cuisset T, Mario C Di, Ferreira JR, Gersh BJ, Gitt AK, Hulot JS, Marx N, Opie LH, Pfisterer M, Prescott E, Ruschitzka F, Sabaté M, Senior R, Taggart DP, Wall EE Van Der, Vrints CJM, Zamorano JL, Baumgartner H, Bax JJ, Bueno H, Dean V, Deaton C, et al. 2013 ESC guidelines on the management of stable coronary artery disease. *Eur Heart J* 2013;34:2949–3003.
148. Moos SI, Vemde DNH Van, Stoker J, Bipat S. Contrast induced nephropathy in patients undergoing intravenous (IV) contrast enhanced computed tomography (CECT) and the relationship with risk factors: A meta-analysis. *Eur J Radiol* 2013;82:e387–e399.

149. Morcos SK, Thomsen HS, Webb JA. Contrast-media-induced nephrotoxicity: a consensus report. Contrast Media Safety Committee, European Society of Urogenital Radiology (ESUR). *Eur Radiol* 1999;9:1602–1613.
150. Motoyama S, Sarai M, Harigaya H, Anno H, Inoue K, Hara T, Naruse H, Ishii J, Hishida H, Wong ND, Virmani R, Kondo T, Ozaki Y, Narula J. Computed Tomographic Angiography Characteristics of Atherosclerotic Plaques Subsequently Resulting in Acute Coronary Syndrome. *J Am Coll Cardiol* 2009;54:49–57.
151. Murthy VL, Naya M, Foster CR, Hainer J, Gaber M, Di Carli G, Blankstein R, Dorbala S, Sitek A, Pencina MJ, Di Carli MF. Improved cardiac risk assessment with noninvasive measures of coronary flow reserve. *Circulation* 2011;124:2215–2224.
152. Mushtaq S, de Araujo Gonçalves P, Garcia-Garcia HM, Pontone G, Bartorelli AL, Bertella E, Campos CM, Pepi M, Serruys PW, Andreini D. Long-term prognostic effect of coronary atherosclerotic burden: validation of the computed tomography-Leaman score. *Circ Cardiovasc Imaging* 2015;8:e002332.
153. Muzik O, Duvernoy C, Beanlands RSB, Sawada S, Dayanikli F, Wolfe ER, Schwaiger M. Assessment of diagnostic performance of quantitative flow measurements in normal subjects and patients with angiographically documented coronary artery disease by means of nitrogen-13 ammonia and positron emission tomography. *J Am Coll Cardiol* 1998;31:534–540.
154. Myers RH, Kiely DK, Cupples LA, Kannel WB. Parental history is an independent risk factor for coronary artery disease: the Framingham Study. *Am Heart J* 1990;120:963–969.
155. Nakashima Y, Fujii H, Sumiyoshi S, Wight TN, Sueishi K. Early human atherosclerosis: accumulation of lipid and proteoglycans in intimal thickenings followed by macrophage infiltration. *Arterioscler Thromb Vasc Biol* 2007;27:1159–1165.
156. Nakazato R, Arsanjani R, Achenbach S, Gransar H, Cheng VY, Dunning A, Lin FY, Al-Mallah M, Budoff MJ, Callister TQ, Chang HJ, Cademartiri F, Chinnaiyan K, Chow BJW, Delago A, Hadamitzky M, Hausleiter J, Kaufmann P, Raff G, Shaw LJ, Villines T, Cury RC, Feuchtnner G, Kim YJ, Leipsic J, Berman DS, Min JK. Age-related risk of major adverse cardiac event risk and coronary artery disease extent and severity by coronary CT angiography: Results from 15 187 patients from the international multisite CONFIRM study. *Eur Heart J Cardiovasc Imaging* 2014;15:586–594.
157. Namdar M, Hany TF, Koepfli P, Siegrist PT, Burger C, Wyss CA, Luscher TF, Schulthess GK von, Kaufmann PA. Integrated PET/CT for the assessment of coronary artery disease: a feasibility study. *J Nucl Med* 2005;46:930–935.
158. Nesterov SV, Han C, Mäki M, Kajander S, Naum AG, Helenius H, Lisinen I, Ukkonen H, Pietilä M, Joutsiniemi E, Knuuti J. Myocardial perfusion quantitation with ¹⁵O-labelled water PET: High reproducibility of the new cardiac analysis software (Carimas™). *Eur J Nucl Med Mol Imaging* 2009;36:1594–1602.
159. Newhouse JH, Kho D, Rao QA, Starren J. Frequency of serum creatinine changes in the absence of iodinated contrast material: Implications for studies of contrast nephrotoxicity. *AJR Am J Roentgenol* 2008;191:376–382.
160. Nissen L, Winther S, Westra J, Ejlersen JA, Isaksen C, Rossi A, Holm NR, Urbonaviciene G, Gormsen LC, Madsen LH, Christiansen EH, Maeng M, Knudsen LL, Frost L, Brix L, Bøtker HE, Petersen SE, Bøttcher M. Diagnosing coronary artery disease after a positive coronary computed tomography angiography: the Dan-NICAD open label, parallel, head to head, randomized controlled diagnostic accuracy trial of cardiovascular magnetic resonance and myocardial perfusion s. *Eur Heart J Cardiovasc Imaging* 2018;19:369–377.
161. Nordström J, Kero T, Harms HJ, Widström C, Flachskampf FA, Sörensen J, Lubberink M. Calculation of left ventricular volumes and ejection fraction from dynamic cardiac-gated ¹⁵O-water PET/CT: 5D-PET. *EJNMMI Phys* 2017;4:26.
162. Nørgaard BL, Leipsic J, Gaur S, Seneviratne S, Ko BS, Ito H, Jensen JM, Mauri L, De Bruyne B, Bezerra H, Osawa K, Marwan M, Naber C, Erglis A, Park S-J, Christiansen EH, Kaltoft A, Lassen JF, Bøtker HE, Achenbach

- S, NXT Trial Study Group. Diagnostic Performance of Noninvasive Fractional Flow Reserve Derived From Coronary Computed Tomography Angiography in Suspected Coronary Artery Disease. *J Am Coll Cardiol* 2014;63:1145–1155.
163. O'Rourke RA, Brundage BH, Froelicher VF, Greenland P, Grundy SM, Hachamovitch R, Pohost GM, Shaw LJ, Weintraub WS, Winters WL, Forrester JS, Douglas PS, Faxon DP, Fisher JD, Gregoratos G, Hochman JS, Hutter AM, Kaul S, Wolk MJ. American College of Cardiology/American Heart Association Expert Consensus document on electron-beam computed tomography for the diagnosis and prognosis of coronary artery disease. *Circulation* 2000;102:126–140.
164. Oesterle A, Laufs U, Liao JK. Pleiotropic Effects of Statins on the Cardiovascular System. *Circ Res* 2017;120:229–243.
165. Ostrom MP, Gopal A, Ahmadi N, Nasir K, Yang E, Kakadiaris I, Flores F, Mao SS, Budoff MJ. Mortality Incidence and the Severity of Coronary Atherosclerosis Assessed by Computed Tomography Angiography. *J Am Coll Cardiol* 2008;52:1335–1343.
166. Otsuka K, Fukuda S, Tanaka A, Nakanishi K, Taguchi H, Yoshiyama M, Shimada K, Yoshikawa J. Prognosis of vulnerable plaque on computed tomographic coronary angiography with normal myocardial perfusion image. *Eur Heart J Cardiovasc Imaging* 2014;15:332–340.
167. Packard RRS, Huang S-C, Dahlbom M, Czernin J, Maddahi J. Absolute Quantitation of Myocardial Blood Flow in Human Subjects With or Without Myocardial Ischemia Using Dynamic Flurpiridaz F 18 PET. *J Nucl Med* 2014;55:1438–1444.
168. Paech DC, Weston AR. A systematic review of the clinical effectiveness of 64-slice or higher computed tomography angiography as an alternative to invasive coronary angiography in the investigation of suspected coronary artery disease. *BMC Cardiovasc Disord* 2011;11:32.
169. Parker MW, Iskandar A, Limone B, Perugini A, Kim H, Jones C, Calamari B, Coleman CI, Heller G V. Diagnostic accuracy of cardiac positron emission tomography versus single photon emission computed tomography for coronary artery disease: A bivariate meta-analysis. *Circ Cardiovasc Imaging* 2012;5:700–707.
170. Pazhenkottil AP, Nkoulou RN, Ghadri J-R, Herzog B a, Küest SM, Husmann L, Wolfrum M, Goetti R, Buechel RR, Gaemperli O, Lüscher TF, Kaufmann P a. Impact of cardiac hybrid single-photon emission computed tomography/computed tomography imaging on choice of treatment strategy in coronary artery disease. *Eur Heart J* 2011;32:2824–2829.
171. Pazhenkottil AP, Nkoulou RN, Ghadri J-R, Herzog BA, Buechel RR, Kuest SM, Wolfrum M, Fiechter M, Husmann L, Gaemperli O, Kaufmann PA. Prognostic value of cardiac hybrid imaging integrating single-photon emission computed tomography with coronary computed tomography angiography. *Eur Heart J* 2011;32:1465–1471.
172. Pedersen C, Thomsen CF, Hosbond SE, Thomassen A, Mickley H, Diederichsen ACP. Coronary computed tomography angiography-Tolerability of β -blockers and contrast media, and temporal changes in radiation dose. *Scand Cardiovasc J* 2014;48:271–277.
173. Phillips LM, Hachamovitch R, Berman DS, Iskandrian AE, Min JK, Picard MH, Kwong RY, Friedrich MG, Scherrer-Crosbie M, Hayes SW, Sharir T, Gosselin G, Mazzanti M, Senior R, Beanlands R, Smanio P, Goyal A, Al-Mallah M, Reynolds H, Stone GW, Maron DJ, Shaw LJ. Lessons learned from MPI and physiologic testing in randomized trials of stable ischemic heart disease: COURAGE, BARI 2D, FAME, and ISCHEMIA. *J Nucl Cardiol* 2013;20:969–975.
174. Pijls NH, Gelder B Van, Voort P Van der, Peels K, Bracke FA, Bonnier HJ, Gamal MI el. Fractional flow reserve. A useful index to evaluate the influence of an epicardial coronary stenosis on myocardial blood flow. *Circulation* 1995;92:3183–3193.
175. Pijls NH, Schaardenburgh P van, Manoharan G, Boersma E, Bech J-W, van't Veer M, Bär F, Hoorntje J, Koolen J, Wijns W, De Bruyne B. Percutaneous Coronary Intervention of Functionally Nonsignificant Stenosis. *J Am Coll Cardiol* 2007;49:2105–2111.

176. Pomikowski P, Voors AA, Anker SD, Bueno H, Cleland JGF, Coats AJS, Falk V, González-Juanatey JR, Harjola VP, Jankowska EA, Jessup M, Linde C, Nihoyannopoulos P, Parissis JT, Pieske B, Riley JP, Rosano GMC, Ruilope LM, Ruschitzka F, Rutten FH, Meer P Van Der. 2016 ESC Guidelines for the diagnosis and treatment of acute and chronic heart failure. *Eur Heart J* 2016;37:2129–2200.
177. Pugliese F, Weustink a C, Mieghem C Van, Alberghina F, Otsuka M, Meijboom WB, Pelt N van, Mollet NR, Cademartiri F, Krestin GP, Hunink MGM, Feyter PJ de. Dual source coronary computed tomography angiography for detecting in-stent restenosis. *Heart* 2008;94:848–854.
178. Pundziute G, Schuijf JD, Jukema JW, Boersma E, Roos A de, Wall EE van der, Bax JJ. Prognostic Value of Multislice Computed Tomography Coronary Angiography in Patients With Known or Suspected Coronary Artery Disease. *J Am Coll Cardiol* 2007;49:62–70.
179. Renker M, Baumann S, Rier J, Ebersberger U, Fuller SR, Batalis NI, Schoepf UJ, Chiaramida SA. Imaging coronary artery disease and the myocardial ischemic cascade: Clinical principles and scope. *Radiol Clin North Am* 2015;53:261–269.
180. Rihal CS, Textor SC, Grill DE, Berger PB, Ting HH, Best PJ, Singh M, Bell MR, Barsness GW, Mathew V, Garratt KN, Holmes DR. Incidence and prognostic importance of acute renal failure after percutaneous coronary intervention. *Circulation* 2002;105:2259–2264.
181. Rispler S, Keidar Z, Ghersin E, Roguin A, Soil A, Dragu R, Litmanovich D, Frenkel A, Aronson D, Engel A, Beyar R, Israel O. Integrated Single-Photon Emission Computed Tomography and Computed Tomography Coronary Angiography for the Assessment of Hemodynamically Significant Coronary Artery Lesions. *J Am Coll Cardiol* 2007;49:1059–1067.
182. Rudnick M, Feldman H. Contrast-induced nephropathy: What are the true clinical consequences? *Clin J Am Soc Nephrol* 2008;3:263–272.
183. Santana CA, Garcia E V, Faber TL, Sirineni GKR, Esteves FP, Sanyal R, Halkar R, Ornelas M, Verdes L, Lerakis S, Ramos JJ, Aguadé-Bruix S, Cuéllar H, Candell-Riera J, Raggi P. Diagnostic performance of fusion of myocardial perfusion imaging (MPI) and computed tomography coronary angiography. *J Nucl Cardiol* 2009;16:201–211.
184. Saraste A, Kajander S, Han C, Nesterov SV, Knuuti J. PET: Is myocardial flow quantification a clinical reality? *J Nucl Cardiol* 2012;19:1044–1059.
185. Saraste A, Knuuti J. Cardiac PET, CT, and MR: What are the advantages of hybrid imaging? *Curr Cardiol Rep* 2012;14:24–31.
186. Sato A, Hiroe M, Tamura M, Ohigashi H, Nozato T, Hikita H, Takahashi A, Aonuma K, Isobe M. Quantitative measures of coronary stenosis severity by 64-Slice CT angiography and relation to physiologic significance of perfusion in nonobese patients: comparison with stress myocardial perfusion imaging. *J Nucl Med* 2008;49:564–572.
187. Sato A, Nozato T, Hikita H, Miyazaki S, Takahashi Y, Kuwahara T, Takahashi A, Hiroe M, Aonuma K. Incremental value of combining 64-slice computed tomography angiography with stress nuclear myocardial perfusion imaging to improve noninvasive detection of coronary artery disease. *J Nucl Cardiol* 2010;17:19–26.
188. Schaap J, Groot JAH de, Nieman K, Meijboom WB, Boekholdt SM, Kauling RM, Post MC, Heyden JA Van der, Kroon TL de, Rensing BJWM, Moons KGM, Verzijlbergen JF. Added value of hybrid myocardial perfusion SPECT and CT coronary angiography in the diagnosis of coronary artery disease. *Eur Heart J Cardiovasc Imaging* 2014;15:1281–1288.
189. Schaap J, Groot JAH De, Nieman K, Meijboom WB, Boekholdt SM, Post MC, Heyden JAS Van Der, Kroon TL De, Rensing BJWM, Moons KGM, Verzijlbergen JF. Hybrid myocardial perfusion SPECT/CT coronary angiography and invasive coronary angiography in patients with stable angina pectoris lead to similar treatment decisions. *Heart* 2013;99:188–194.
190. Schenker MP, Dorbala S, Hong ECT, Rybicki FJ, Hachamovitch R, Kwong RY, Di Carli MF. Interrelation of coronary calcification, myocardial ischemia, and outcomes in patients with intermediate likelihood of

- coronary artery disease: A combined positron emission tomography/computed tomography study. *Circulation* 2008;117:1693–1700.
191. Schinkel AFL, Bax JJ, Geleijnse ML, Boersma E, Elhendy A, Roelandt JRTC, Poldermans D. Noninvasive evaluation of ischaemic heart disease: Myocardial perfusion imaging or stress echocardiography? *Eur Heart J* 2003;24:789–800.
192. Schroeder S, Achenbach S, Bengel F, Burgstahler C, Cademartiri F, Feyter P de, George R, Kaufmann P, Kopp AF, Knuuti J, Ropers D, Schuijf J, Tops LF, Bax JJ. Cardiac computed tomography: indications, applications, limitations, and training requirements. *Eur Heart J* 2008;29:531–556.
193. Senthamizhchelvan S, Bravo PE, Esaia C, Lodge M a, Merrill J, Hobbs RF, Sgouros G, Bengel FM. Human Biodistribution and Radiation Dosimetry of ⁸²Rb. *J Nucl Med* 2010;51:1592–1599.
194. Shaw LJ, Berman DS, Maron DJ, Mancini GBJ, Hayes SW, Hartigan PM, Weintraub WS, O'Rourke RA, Dada M, Spertus JA, Chaitman BR, Friedman J, Slomka P, Heller G V., Germano G, Gosselin G, Berger P, Kostuk WJ, Schwartz RG, Knudtson M, Veledar E, Bates ER, McCallister B, Teo KK, Boden WE. Optimal medical therapy with or without percutaneous coronary intervention to reduce ischemic burden: results from the Clinical Outcomes Utilizing Revascularization and Aggressive Drug Evaluation (COURAGE) trial nuclear substudy. *Circulation* 2008;117:1283–1291.
195. Shaw LJ, Cerqueira MD, Brooks MM, Althouse AD, Sansing V V, Beller GA, Pop-Busui R, Taillefer R, Chaitman BR, Gibbons RJ, Heo J, Iskandrian AE. Impact of left ventricular function and the extent of ischemia and scar by stress myocardial perfusion imaging on prognosis and therapeutic risk reduction in diabetic patients with coronary artery disease. *J Nucl Cardiol* 2012;19:658–669.
196. Shaw LJ, Iskandrian AE. Prognostic value of gated myocardial perfusion SPECT. *J Nucl Cardiol* 2004;11:171–185.
197. Shaw LJ, Raggi P, Schisterman E, Berman DS, Callister TQ. Prognostic Value of Cardiac Risk Factors and Coronary Artery Calcium Screening for All-Cause Mortality. *Radiology* 2003;228:826–833.
198. Sheth T, Dodd JD, Hoffmann U, Abbara S, Finn A, Gold HK, Brady TJ, Cury RC. Coronary stent assessability by 64 slice multi-detector computed tomography. *Catheter Cardiovasc Interv* 2007;69:933–938.
199. Sianos G, Morel M-A, Kappetein AP, Morice M-C, Colombo A, Dawkins K, Brand M van den, Dyck N Van, Russell ME, Mohr FW, Serruys PW. The SYNTAX Score: an angiographic tool grading the complexity of coronary artery disease. *EuroIntervention* 2005;1:219–227.
200. Simoons ML, Windecker S. Chronic stable coronary artery disease: Drugs vs. revascularization. *Eur Heart J* 2010;31:530–541.
201. Slomka PJ, Dey D, Duvall WL, Henzlova MJ, Berman DS, Germano G. Advances in nuclear cardiac instrumentation with a view towards reduced radiation exposure. *Curr Cardiol Rep* 2012;14:208–216.
202. Stacul F, Molen AJ Van Der, Reimer P, Webb JAW, Thomsen HS, Morcos SK, Almén T, Aspelin P, Bellin MF, Clement O, Heinz-Peer G. Contrast induced nephropathy: Updated ESUR Contrast Media Safety Committee guidelines. *Eur Radiol* 2011;21:2527–2541.
203. Stocker TJ, Deseive S, Chen M, Leipsic J, Hadamitzky M, Rubinshtein R, Grove EL, Fang X-M, Lesser J, Maurovich-Horvat P, Marques H, Andreini D, Tabbalat R, Kang J-W, Eckert J, Dickson P, Forsdahl SH, Lambrechtsen J, Cury RC, Hausleiter J. Rationale and design of the worldwide prospective multicenter registry on radiation dose estimates of cardiac CT angiography in daily practice in 2017 (PROTECTION VI). *J Cardiovasc Comput Tomogr* 2018;12:81–85.
204. Sund R. Quality of the Finnish Hospital Discharge Register: a systematic review. *Scand J Public Health* 2012;40:505–515.
205. Takx RAP, Suchá D, Park J, Leiner T, Hoffmann U. Sublingual Nitroglycerin Administration in Coronary Computed Tomography Angiography: a Systematic Review. *Eur Radiol* 2015;25:3536–3542.
206. Taqueti VR, Hachamovitch R, Murthy VL,

- Naya M, Foster CR, Hainer J, Dorbala S, Blankstein R, Di Carli MF. Global coronary flow reserve is associated with adverse cardiovascular events independently of luminal angiographic severity and modifies the effect of early revascularization. *Circulation* 2015;131:19–27.
207. Taqueti VR. Myocardial perfusion imaging in extreme obesity: Leveraging modern technologies to meet a modern challenge. *J Nucl Cardiol* 2017 Jun 19 [Epub ahead of print]; <http://dx.doi.org/10.1007/s12350-017-0956-2>.
208. Thomassen A, Petersen H, Johansen A, Braad P-E, Diederichsen ACP, Mickley H, Jensen LO, Gerke O, Simonsen JA, Thyssen P, Høiland-Carlsen PF. Quantitative myocardial perfusion by O-15-water PET: individualized vs. standardized vascular territories. *Eur Heart J Cardiovasc Imaging* 2015;16:970–976.
209. Thompson PL. Should β -blockers still be routine after myocardial infarction? *Curr Opin Cardiol* 2013;28:399–404.
210. Tonino PAL, De Bruyne B, Pijls NHJ, Siebert U, Ikeno F, 't Veer M van, Klauss V, Manoharan G, Engström T, Oldroyd KG, Lee PN Ver, MacCarthy PA, Fearon WF, FAME Study Investigators. Fractional Flow Reserve versus Angiography for Guiding Percutaneous Coronary Intervention. *N Engl J Med* 2009;360:213–224.
211. Tumlin J, Stacul F, Adam A, Becker CR, Davidson C, Lameire N, McCullough PA, CIN Consensus Working Panel. Pathophysiology of contrast-induced nephropathy. *Am J Cardiol* 2006;98:14K–20K.
212. Uren NG, Melin JA, De Bruyne B, Wijns W, Baudhuin T, Camici PG. Relation between myocardial blood flow and the severity of coronary-artery stenosis. *N Engl J Med* 1994;330:1782–1788.
213. Valenta I, Dilsizian V, Quercioli A, Ruddy TD, Schindler TH. Quantitative PET/CT measures of myocardial flow reserve and atherosclerosis for cardiac risk assessment and predicting adverse patient outcomes. *Curr Cardiol Rep* 2013;15:344.
214. van Waardhuizen CN, Khanji MY, Genders TSS, Ferket BS, Fleischmann KE, Hunink MGM, Petersen SE. Comparative cost-effectiveness of non-invasive imaging tests in patients presenting with chronic stable chest pain with suspected coronary artery disease: a systematic review. *Eur Heart J Qual Care Clin Outcomes* 2016;2:245–260.
215. van Werkhoven JM, Heijnenbroek MW, Schuijff JD, Jukema JW, Wall EE van der, Schreur JHM, Bax JJ. Combined non-invasive anatomical and functional assessment with MSCT and MRI for the detection of significant coronary artery disease in patients with an intermediate pre-test likelihood. *Heart* 2010;96:425–431.
216. van Werkhoven JM, Schuijff JD, Gaemperli O, Jukema JW, Boersma E, Wijns W, Stolzmann P, Alkadhi H, Valenta I, Stokkel MPM, Kroft LJ, Roos A de, Pundziute G, Scholte A, Wall EE van der, Kaufmann PA, Bax JJ. Prognostic Value of Multislice Computed Tomography and Gated Single-Photon Emission Computed Tomography in Patients With Suspected Coronary Artery Disease. *J Am Coll Cardiol* 2009;53:623–632.
217. Weintraub WS, Spertus JA, Kolm P, Maron DJ, Zhang Z, Jurkovic Z, Zhang W, Hartigan PM, Lewis C, Veledar E, Bowen J, Dunbar SB, Deaton C, Kaufman S, O'Rourke RA, Goeree R, Barnett PG, Teo KK, Boden WE, COURAGE Trial Research Group, Mancini GBJ. Effect of PCI on quality of life in patients with stable coronary disease. *N Engl J Med* 2008;359:677–687.
218. Weisbord SD, Mor MK, Resnick AL, Hartwig KC, Palevsky PM, Fine MJ. Incidence and outcomes of contrast-induced AKI following computed tomography. *Clin J Am Soc Nephrol* 2008;3:1274–1281.
219. Weustink AC, Nieman K, Pugliese F, Mollet NR, Meijboom BW, Mieghem C van, Kate GJ ten, Cademartiri F, Krestin GP, Feyter PJ de. Diagnostic Accuracy of Computed Tomography Angiography in Patients After Bypass Grafting. Comparison With Invasive Coronary Angiography. *JACC Cardiovasc Imaging* 2009;2:816–824.
220. Williams MC, Golay SK, Hunter A, Weir-McCall JR, Mlynska L, Dweck MR, Uren NG, Reid JH, Lewis SC, Berry C, Beek EJR van, Roditi G, Newby DE, Mirsadraee S. Observer variability in the assessment of CT coronary angiography and coronary artery

- calcium score: substudy of the Scottish Computed Tomography of the HEART (SCOT-HEART) trial. *Open Heart* 2015;2:e000234.
221. Williams MC, Hunter A, Shah ASV, Assi V, Lewis S, Smith J, Berry C, Boon NA, Clark E, Flather M, Forbes J, McLean S, Roditi G, Beek EJR Van, Timmis AD, Newby DE. Use of Coronary Computed Tomographic Angiography to Guide Management of Patients with Coronary Disease. *J Am Coll Cardiol* 2016;67:1759–1768.
222. Windecker S, Kolh P, Alfonso F, Collet JP, Cremer J, Falk V, Filippatos G, Hamm C, Head SJ, Juni P, Kappetein AP, Kastrati A, Knuuti J, Landmesser U, Laufer G, Neumann FJ, Richter DJ, Schauerte P, Uva MS, Stefanini GG, Taggart DP, Torracca L, Valgimigli M, Wijns W, Witkowski A, Baumgartner H, Bax JJ, Bueno H, Dean V, Deaton C, et al. 2014 ESC/EACTS Guidelines on myocardial revascularization. *Eur Heart J* 2014;35:2541–2619.
223. Wong PCY, Li Z, Guo J, Zhang A. Pathophysiology of contrast-induced nephropathy. *Int J Cardiol* 2012;158:186–192.
224. Wuest W, May MS, Scharf M, Layritz C, Eisentopf J, Ropers D, Pflederer T, Uder M, Achenbach S, Lell MM. Stent evaluation in low-dose coronary CT angiography: Effect of different iterative reconstruction settings. *J Cardiovasc Comput Tomogr* 2013;7:319–325.
225. Wykrzykowska JJ, Arbab-Zadeh A, Godoy G, Miller JM, Lin S, Vavere A, Paul N, Niinuma H, Hoe J, Brinker J, Khosa F, Sarwar S, Lima J, Clouse ME. Assessment of in-stent restenosis using 64-MDCT: analysis of the CORE-64 Multicenter International Trial. *AJR Am J Roentgenol* 2010;194:85–92.
226. Yoshikawa D, Isobe S, Sato K, Ohashi T, Fujiwara Y, Ohyama H, Ishii H, Murohara T. Importance of oral fluid intake after coronary computed tomography angiography: An observational study. *Eur J Radiol* 2011;77:118–122.
227. Yoshinaga K, Katoh C, Manabe O, Klein R, Naya M, Sakakibara M, Yamada S, deKemp RA, Tsutsui H, Tamaki N. Incremental Diagnostic Value of Regional Myocardial Blood Flow Quantification Over Relative Perfusion Imaging With Generator-Produced Rubidium-82 PET. *Circ J* 2011;75:2628–2634.
228. Zimmermann FM, Ferrara A, Johnson NP, Nunen LX van, Escaned J, Albertsson P, Erbel R, Legrand V, Gwon H-C, Remkes WS, Stella PR, Schaardenburgh P van, Bech GJW, De Bruyne B, Pijls NHJ. Deferral vs. performance of percutaneous coronary intervention of functionally non-significant coronary stenosis: 15-year follow-up of the DEFER trial. *Eur Heart J* 2015;36:3182–3188.

Annales Universitatis Turkuensis



Turun yliopisto
University of Turku

ISBN 978-951-29-7245-6 (PRINT)
ISBN 978-951-29-7246-3 (PDF)
ISSN 0355-9483 (PRINT) | ISSN 2343-3213 (PDF)